



ฤทธิ์ของสารสกัดหัวข้าวเย็น (*Dioscorea membranacea* Pierre)

ที่มีต่อหนูแรทที่ถูกเหนี่ยวนำให้เกิดมะเร็งตับ

EFFECTS OF HUA-KHAO-YEN EXTRACT (*DIOSCOREA MEMBRANACEA* PIERRE)

IN HEPATOCELLULAR CARCINOMA-INDUCED RAT

VICHUNUNT KERDPUT

ฤทธิ์ของสารสกัดหัวข้าวเย็น (*Dioscorea membranacea* Pierre)
ที่มีต่อหนูแรทที่ถูกเหนี่ยวนำให้เกิดมะเร็งตับ



ปริญญานิพนธ์นี้เป็นส่วนหนึ่งของการศึกษาตามหลักสูตร
ปรัชญาดุษฎีบัณฑิต สาขาวิชาชีวภาพการแพทย์
คณะแพทยศาสตร์ มหาวิทยาลัยศรีนครินทรวิโรฒ
ปีการศึกษา 2562
ลิขสิทธิ์ของมหาวิทยาลัยศรีนครินทรวิโรฒ

EFFECTS OF HUA-KHAO-YEN EXTRACT (*DIOSCOREA MEMBRANACEA*
PIERRE)
IN HEPATOCELLULAR CARCINOMA-INDUCED RAT



VICHUNUNT KERDPUT

A Dissertation Submitted in partial Fulfillment of Requirements
for DOCTOR OF PHILOSOPHY (Biomedical Sciences)
Faculty of Medicine Srinakharinwirot University

2019

Copyright of Srinakharinwirot University

THE DISSERTATION TITLED

EFFECTS OF HUA-KHAO-YEN EXTRACT (*DIOSCOREA MEMBRANACEA* PIERRE)
IN HEPATOCELLULAR CARCINOMA-INDUCED RAT

BY

VICHUNUNT KERDPUT

HAS BEEN APPROVED BY THE GRADUATE SCHOOL IN PARTIAL FULFILLMENT OF
THE REQUIREMENTS FOR THE DOCTOR OF PHILOSOPHY IN BIOMEDICAL
SCIENCES

AT SRINAKHARINWIROT UNIVERSITY

Dean of Graduate School

.....
(Assoc. Prof. Dr. Chatchai Ekpanyaskul, MD.)
.....

ORAL DEFENSE COMMITTEE

..... Major-advisor

(Assoc. Prof. Wisuit Pradidarcheep, Ph.D.)

..... Co-advisor

(Assoc. Prof. Arunporn Itharat, Ph.D.)

..... Co-advisor

(Sittiruk Roytrakul, Ph.D.)

..... Chair

(Prof. Wouter H Lamers, M.D., Ph.D.)

..... Committee

(Asst. Prof. Wanlaya Tanechpongamb,
Ph.D.)

..... Committee

(Asst. Prof. Yamaratee Jaisin, Ph.D.)

Title	EFFECTS OF HUA-KHAO-YEN EXTRACT (<i>DIOSCOREA MEMBRANACEA</i> PIERRE) IN HEPATOCELLULAR CARCINOMA-INDUCED RAT
Author	VICHUNUNT KERDPUT
Degree	DOCTOR OF PHILOSOPHY
Academic Year	2019
Thesis Advisor	Associate Professor Wisuit Pradidarcheep , Ph.D.

Hepatocellular carcinoma (HCC) is the most common liver cancer in adults. The lack of effective treatment for HCC is still problematic and leads to a high mortality rate. Sorafenib (SF) is an orally administered drug currently approved to treat advanced HCC patients. However, it mediates many of the side effects. Owing to the common usage of the rhizomes of Hua-Khao-Yen, *Dioscorea membranacea* Pierre (DM), a medicinal herbal plant, is an alternative medicine for treatment of various cancers in Thailand. Therefore, the present study aimed to demonstrate the anticancer effect of the DM extract in HCC-bearing rats. In this study, such anti-cancer properties of DM extract were demonstrated through the gross morphology, histopathology, and liver enzymes aspects. In addition the mechanisms of DM for treatment of HCC were explored by using a proteomics assay and quantitative real-time PCR. The six groups of rats were set: (1) control rats; (2) control rats receiving DM extract at 40 mg/kg; (3) HCC rats; (4) HCC rats receiving DM extract at 4 mg/kg; (5) HCC rats receiving DM extract at 40 mg/kg, and (6) HCC rats receiving SF at 30 mg/kg. It was found that the HCC-bearing rats were present macroscopically with various sizes of hepatic nodules and microscopically with thick hepatic cell cords, or pseudoglandular patterns together with abnormal scaffolds of reticulin stain. The HCC rats with DM treatment showed significantly decreased cancer areas and reticulin expression compared with the untreated group. Even though treatment of HCC rats with SF yielded the lowest cancer areas, it also caused a rising level of liver enzymes and a low level of albumin in serum. With proteomics analysis the mechanisms of DM extract were shown to exert via inhibiting proteins involved in proliferation and angiogenesis pathways. In DM-treated HCC rats down-regulation of PDGFRA, VEGFR1, and MSK2 proteins were detected in comparison to HCC rats without any treatment, suggesting less cancer cell proliferation and less neovascularization. The HCC-bearing rats treated with DM extract also caused the up-regulation of a tumor suppressor, NEMO protein, in the liver. Moreover, HCC-bearing rats treated with DM extract caused a higher expression of BIK and DIABLO proteins but a lower expression of PARP1 compared with the non-treated HCC rats indicating the apoptotic effects of the extract. The alteration of the related-gene expressions revealed by quantitative real-time PCR were in similar trend of changes in the protein profile. Last but not least, the HCC rats treated with DM showed a decrease in malondialdehyde (MDA) level, suggesting lower lipid peroxidation compared to the nontreated HCC group. The findings suggest that DM extract could reduce cancer in HCC-induced rats. It has an antioxidant effect and exerts an anti-cancer effect on HCC-induced rats through VEGF/PDGF, and the apoptosis signaling pathway.

Keyword : Hepatocellular carcinoma, Proteomics, *Dioscorea membranacea*, Traditional medicine, Hua-Khao-Yen

ACKNOWLEDGEMENTS

Firstly, I would like to express my sincere gratitude to my advisor, Associate Professor Dr. Wisuit Pradidarcheep for the continuous support of my Ph.D. study and related research, for his patience, motivation, and immense knowledge. His guidance helped me in all the time of research and writing of this thesis. I could not have imagined having a better advisor and mentor for my Ph.D. life.

Besides my advisor, I would like to thank the rest of my co-advisor, Associate Professor Dr. Arunporn Itharat, and Dr. Sittiruk Roytrakul, for their insightful comments and encouragement, but also for the hard question which incited me to widen my research from various perspectives including traditional medicine and proteomics. I would like to express my sincere gratitude to Dr. Suriya Pongsawat for his advice on histopathological knowledge.

My sincere thanks also go to Professor Dr. Wouter H Lamers and Assistant Professor Dr. Yip George, who provided me an opportunity to research aboard, and who gave access to the laboratory and research facilities. I am very grateful to their invaluable support, immense knowledge, and guidance during research. I am very thankful to Professor Dr. Wouter De Jonge for giving me the opportunity to work in the Tytgat Institute for Liver and Intestinal Research, Academic Medical Center, University of Amsterdam, Amsterdam, The Netherlands. I would like to acknowledge everyone in his lab for all the help and every concern during my stay in the Netherlands. I wish to express my sincere gratitude to Dr. Wei Xuan for his very kind teaching me several molecular techniques in the Department of Anatomy, Yong Loo Lin School of Medicine, National University of Singapore, Singapore. My warm thanks to everyone in the GPRO221 proteomics lab group at Genome Institute, National Center for Genetic Engineering and Biotechnology (BIOTEC), Pathum Thani, Thailand, for providing proteomics suggestions and big warm friendship.

I would like to thank everyone in the Biomedical Sciences Program, Srinakharinwirot University, and everyone in the Anatomy Department, especially Dr. Wisuit's advisees, for generous assistance and giving me a warm and friendly working

environment. Without their precious support, it would not be possible to conduct this research. I am also indebted to all the animals that sacrificed themselves in this study. Moreover, I also would like to thank the Royal Golden Jubilee Ph.D. program from the Thailand Research Fund and the grants from the Faculty of Medicine and The Graduate School, Srinakharinwirot University, for financial support throughout my study.

Most especially to my family, without them, none of this would be possible. I would like to thank my family, who always believe in me, for their love, patience, and support throughout my life. Thank you also to my sister, my sister's boyfriend, and all of my best friends, who help me with every possibility whenever I needed it.



VICHUNUNT KERDPUT

TABLE OF CONTENTS

	Page
ABSTRACT	D
ACKNOWLEDGEMENTS.....	E
TABLE OF CONTENTS.....	G
LIST OF TABLES.....	L
LIST OF FIGURES	M
CHAPTER 1 INTRODUCTION	1
Conceptual framework.....	4
CHAPTER 2 REVIEW OF THE LITERATURE.....	5
1. The liver.....	5
1.1 Gross structure of human liver.....	5
1.2 Rat liver.....	7
1.2.1 Liver anatomy.....	7
1.2.2 Liver lobes.....	7
1.3 Liver histology.....	10
1.3.1 Liver cell types	10
1.3.1.1 Hepatocytes.....	11
1.3.1.2 Kupffer cells.....	13
1.3.1.3 Space of Disse.....	14
1.3.2 Liver lobules	16
1.3.2.1 Classic liver lobule.....	16
1.3.2.2 Portal lobule	17

1.3.2.3 Hepatic acinus.....	17
1.3.3. Biliary system	20
1.4 Liver function	21
2. Hepatocellular carcinoma (HCC)	22
2.1 Risk factors for development of HCC.....	22
2.2 Signs and symptoms.....	23
2.3 Laboratory findings	24
2.3.1 Liver function test.....	24
2.3.2 Tumor markers	25
2.4 HCC staging.....	26
2.5 Pathological analysis of HCC.....	29
2.6 Treatment of HCC.....	32
2.6.1 Sorafenib.....	33
2.7 Induction of HCC.....	34
2.7.1 Carcinogenesis	34
2.7.2 Chemically induced models	38
2.7.2.1 Dinitrosodiethylamine (DEN)	39
2.7.2.2 Thioacetamide (TAA).....	41
2.8. Molecular pathogenesis of HCC	43
2.8.1 PI3K/AKT/MTOR pathway.....	43
2.8.2 RAS/RAF/MEK/ERK pathway	45
2.8.3 Wnt/Beta-catenin pathway.....	48
2.8.4 Angiogenesis	49

2.8.5 Apoptotic pathway	50
2.9. Proteomics study in HCC	52
3. <i>Dioscorea membranacea</i> (DM)	55
3.1 General description of <i>Dioscorea membranacea</i>	55
3.2 Chemical compounds	56
3.3 The extract properties	57
3.3.1 Anti-cancer property	57
3.3.2 Anti-oxidant and anti-inflammatory properties	58
3.3.3 Anti-allergic property	59
3.3.4 Anti-HIV property.....	60
3.3.5 Toxicity	60
CHAPTER 3 MATERIALS AND METHODS	61
1. Chemicals and reagents	61
2. Plant extract	61
3. Experimental animals.....	61
4. Experimental designs	62
5. Methods	64
5.1 Gross examination of the liver	64
5.2 Histopathological studies.....	64
5.3 Proteomics study	65
5.3.1 Protein extraction.....	65
5.3.2 Analysis of protein profiles by LC-MS/MS.....	65
5.3.3 Analysis of peptide pattern by MALDI-TOF MS	67

5.4 Real-time PCR	68
5.4.1 Real-time quantitative PCR	68
5.4.2 RNA extraction and qualification	68
5.4.3 Reverse transcription	68
5.4.4 Real time quantitative PCR.....	69
5.5 Liver function tests	70
5.6 MDA assay	70
6. Statistical analysis	71
CHAPTER 4 RESULTS.....	72
1. The rat body weight and liver weight ratio	72
2. Gross structure and histopathology of the rat liver	74
3. Protein pathway profiles.....	79
3.1 The proteins associated with proliferation, angiogenesis, and apoptosis in STITCH database.....	79
3.2 The up-and down-regulation proteins in treatment group compared to HCC	82
3.3 Peptide pattern from MALDITOF/MS	84
4. qPCR analysis	87
5. The liver enzyme and liver function test	89
5.1 The liver enzyme	89
5.2 The liver function test	90
6. MDA assay	91
CHAPTER 5 DISCUSSION AND CONCLUSION.....	92
REFERENCES.....	96

VITA 110



LIST OF TABLES

	Page
Table 1 Experimental animal groups.	63
Table 2 Primers for qPCR.....	69
Table 3 PrimePCR primers designed for SYBR® Green gene expression	70
Table 4 The liver weight relative to body weight ratio.	73
Table 5 The differentially expressed of proteins among six groups	83



LIST OF FIGURES

	Page
Figure 1 Conceptual framework.....	4
Figure 2 The human liver.....	6
Figure 3 Anatomy of rat liver and human liver	9
Figure 4 The spatial relationship among the different cell types of the liver	10
Figure 5 A hepatocyte	13
Figure 6 Schematic structure of the liver	15
Figure 7 Histological structure of a liver lobule.....	17
Figure 8 Schematic drawing of the territories of the classic liver lobules, hepatic acini, and portal lobules.....	19
Figure 9 The BCLC staging system	28
Figure 10 Macroscopic aspects of Hepatocellular carcinoma	30
Figure 11 Growth patterns of progressed hepatocellular carcinoma	32
Figure 12 Different stages of carcinogenesis	35
Figure 13 Mechanism-based liver injury of thioacetamide.....	43
Figure 14 The RAF/MEK/ERK and the PI3K/AKT/mTOR signaling pathways	47
Figure 15 The Alterations in the expression or functions of death receptor pathways and apoptosis regulatory proteins in HCC cells	52
Figure 16 Plants called Hua-Khao-Yen; <i>Dioscorea membranacea</i>	56
Figure 17 Chemical structures of compounds 1–9 isolated from <i>Dioscorea</i> <i>membranacea</i>	57
Figure 18 Procedure and timeframe for induction of hepatocellular carcinoma (HCC) and treatment in rat.....	63

Figure 19 Assessment criteria for cancer area.....	65
Figure 20 Graph illustrating the body weight from week 0 to week 16	72
Figure 21 Photograph illustrating the gross examination and histology of the rat livers. 75	
Figure 22 The light micrograph of histopathology in HCC rat.....	76
Figure 23 Light micrographs of the liver sections of reticulin staining.	77
Figure 24 Diagram showing the surface of the reticulin areas per section (A) and relative cancer area (B) in rat liver tissues	78
Figure 25 The association network of proteins, chemical, and drug analyzed by using STITCH 4.0.	81
Figure 26 The heat map of 7 differentially expressed of proteins among six groups.....	82
Figure 27 Overview of MALDI-TOF/TOF mass signals of 1,000–15,000 Da from liver tissues of the six animal groups.....	85
Figure 28 Overview of MALDI-TOF/TOF mass signals of 1,000–10,000 Da from serum of the six animal groups.	86
Figure 29 Diagram showing the relative gene expression of <i>Pdgfra</i> , <i>Flt1</i> , <i>Rps6ka4</i> , <i>Bik</i> , <i>Diablo</i> , and <i>Parp1</i> by real-time PCR.....	88
Figure 30 Diagram showing the serum liver enzyme levels.	89
Figure 31 Diagram showing the albumin and total protein levels.	90
Figure 32 Photograph illustrating the MDA level in the rat liver	91

CHAPTER 1

INTRODUCTION

Hepatocellular carcinoma (HCC) is a liver cancer which is most common in adults. HCC is the fifth most frequent cause of cancer-related deaths in males and is the third most frequent cause of cancer-related deaths worldwide.⁽¹⁾ The mortality rate of HCC is high because of the lack of effective treatment options.⁽²⁾

Molecular biomarkers associated with HCC have been found. These include genes involved in the regulation of the cell cycle, apoptosis, DNA repair, and cell-cycle checkpoints. In addition, developmental and oncogenic pathways with activation of Wnt/beta-catenin, RAS/RAF, PI3K/Akt/mTOR, and angiogenesis are involved.⁽³⁻⁶⁾ Further investigations of biomarkers as well as studies on HCC classification are ongoing. Several studies of the HCC transcriptome have been performed for decades.⁽⁷⁾ Protein expression profiles of cancers obtained by proteomic studies could also provide useful information regarding cancer classification, aid in the establishment of diagnostic markers, and allow for the selection of target therapeutic candidates.⁽⁸⁾ Proteomics is a tool to examine expression profiles at the protein level and may help to establish a molecular definition of the benign and cancer states of each patient and contribute to the discovery of diagnostic markers and therapeutic targets.⁽⁹⁾

Therapy for HCC is currently disappointing. It is thus of great importance to identify novel HCC markers for early detection of the disease and tumor-specific proteins as potential therapeutic targets.⁽⁷⁾ At the present, the standard therapy for HCC is removal of the tumor by surgery or liver transplantation. For treatment of HCC, sorafenib (Nexavar; Bayer Pharmaceuticals) is the first and only p.o. administered drug currently approved to treat advanced HCC patients.^(10, 11) Sorafenib, a multikinase inhibitor, is a small molecule that inhibits tumor cell proliferation and tumor angiogenesis in a wide range of tumor models.⁽¹²⁾ However, apart from side effects, tumors quickly develop resistance against the drug.⁽¹⁰⁾ Moreover, the drug is very costly.

Nowadays, many researches investigate the effect of medicinal plants as a potential source of drugs against HCC. Cytotoxicity screening models provide important data to help select plant extracts with potential anti-cancer properties.⁽¹³⁾ In Thailand, the rhizomes of *Dioscorea membranacea* Pierre (DM) are commonly used as ingredients in Thai traditional medicine drug formulations for alternative treatment of cancer.⁽¹⁴⁾ DM is known in Thai as Hua-Khao-Yen. It has been used as common ingredient in the treatment of inflammatory diseases, arthritis, lymphopathy, dermatopathy, venereal diseases, leprosy, and cancers. Hua-Khao-Yen extract is available as drug in traditional drug stores across Thailand.⁽¹⁵⁾ DM extract exhibits a high cytotoxic activity against several cancer cell lines, including breast, lung, colon, and liver cancers.^(15, 16) but is less toxic in normal cells. Moreover, the extract has anti-inflammatory, anti-allergic, and antioxidant properties.⁽¹⁷⁻¹⁹⁾ Our preliminary *in vivo* study has investigated the efficacy of DM extract for treatment in HCC-induced rats and has established that treatment with DM extract decreases the number of hepatic nodules in rats with HCC. The main aim of this study is to explore the mechanism by which DM extract exerts its positive effect on HCC by using a proteomics assay and real-time PCR. In addition, the proteomics technique may help us to understand the disease mechanism, uncover effective diagnostic markers, and develop therapeutic targets against HCC.⁽²⁰⁾

This study aims to determine whether DM extract has any potentially anti-cancer effect in the HCC rats through the following aspects:

1. Gross structure and histopathology of the liver
 - 1.1 changes in gross morphology of the liver
 - 1.2 changes in the size of hepatic nodules and histopathology of the cancer cells in the liver tissue by hematoxylin and eosin staining
2. Protein fingerprints and protein profiles.
 - 2.1 determine the identity of differentially expressed proteins in HCC by LC-MS/MS analysis.

2.2 determine changes in protein composition of the liver by MALDI-TOF mass spectrometry analysis.

3. Gene expression

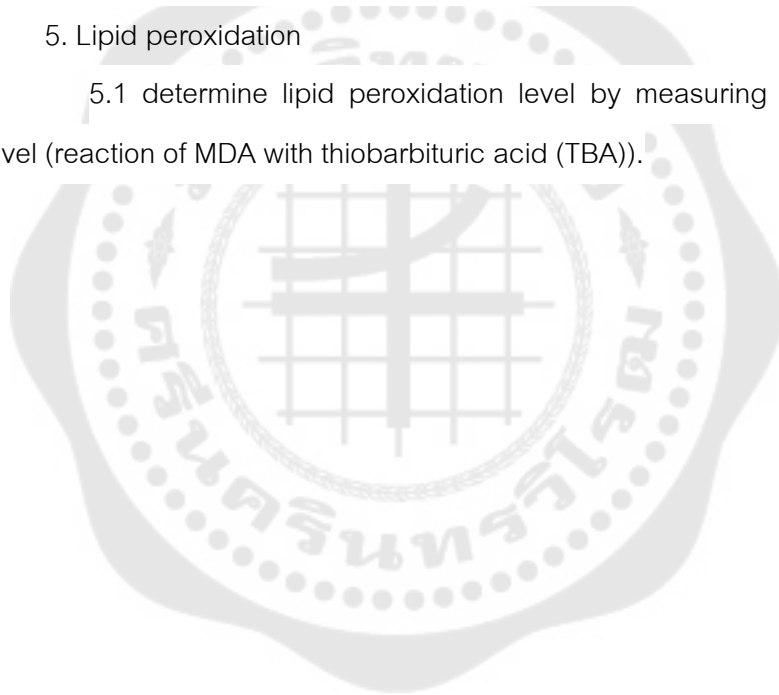
3.1 determine the expression of genes associated with HCC by real-time PCR.

4. Liver enzymes

4.1 assess liver functions by measuring the plasma levels of liver enzymes (alanine aminotransferase (ALT), alkaline phosphatase (ALP), aspartate aminotransferase (AST), γ -glutamyltransferase (GGT)), total proteins, and albumin

5. Lipid peroxidation

5.1 determine lipid peroxidation level by measuring malondialdehyde (MDA) level (reaction of MDA with thiobarbituric acid (TBA)).



Conceptual framework

In this study, the molecular markers of cancer will be identified in rat liver at the level of protein and gene expression. Understanding cell signaling molecules which are involved in HCC treatment will help to elucidate the functional role of *D. membranacea* extract in inhibiting cancer in liver and will prove the function of Hua-Khoa-Yen, a Thai traditional medicine drug, to cure HCC.

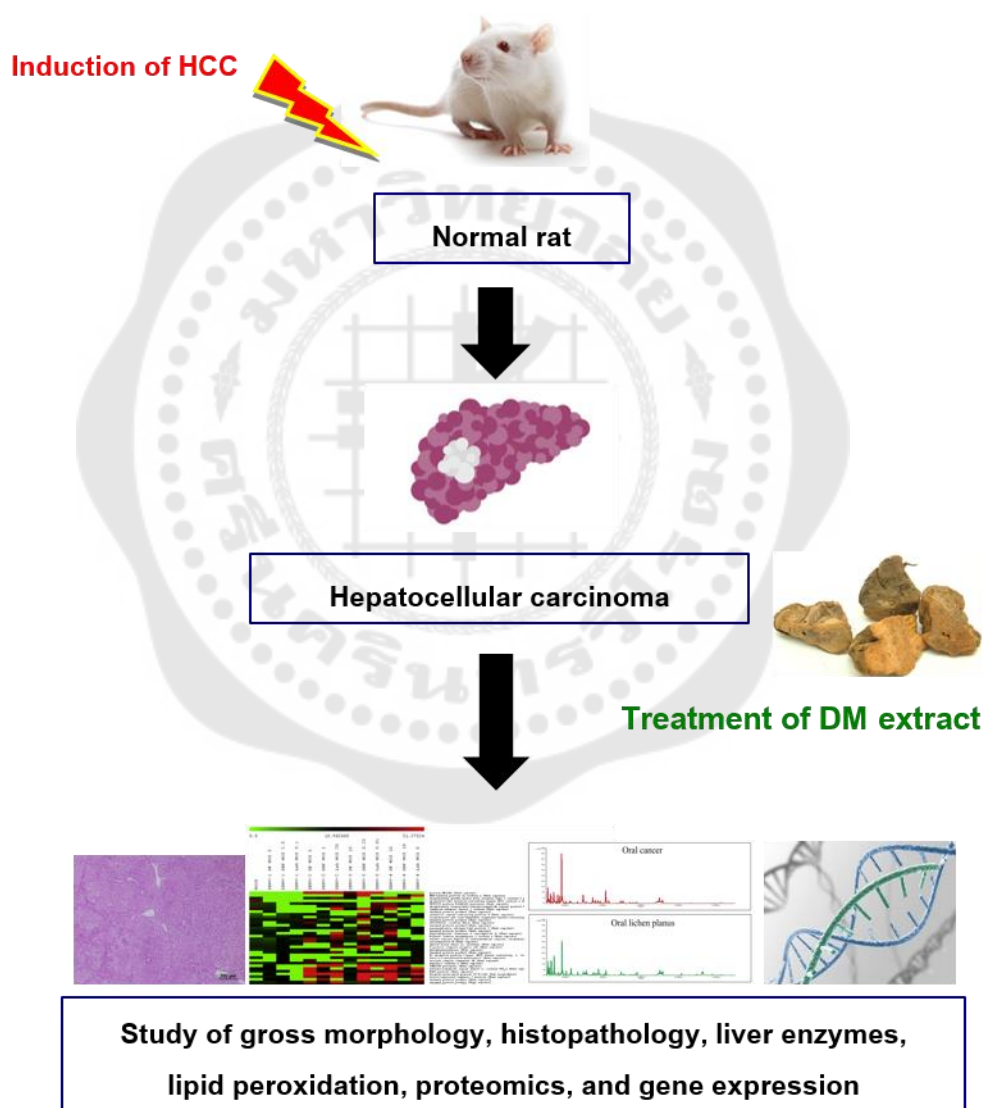


Figure 1 Conceptual framework

CHAPTER 2

REVIEW OF THE LITERATURE

1. The liver

The liver is the largest internal organ of the human body. The adult human liver normally weighs around 1.0- 2.5 kilograms. It is found in the upper-right part of the abdomen and beneath the diaphragm. Liver is an organ consisting of several lobes. It is reddish brown and is surrounded by a fibrous sheath.⁽²¹⁾ It is described as an accessory organ to digestion, but its functions are complex and affect many systems.⁽²²⁾ Liver is one of two principal accessory organs of the digestive system. Its metabolic capabilities are so crucial for maintaining several of the body's critical functions that a wide array of physiologic disturbances occur when there is damage to the liver.⁽²³⁾

1.1 Gross structure of human liver

Its anatomical position in the body is immediately under the diaphragm in the upper abdominal cavity at the right side. The liver lies on the right of the stomach and makes a kind of bed for the gallbladder. It has two major lobes consisting of right and left lobes which are divided by falciform ligament and left sagittal fissure.^(24, 25) Two major blood vessels, the hepatic artery and the portal vein, are the main blood supply of the liver. The hepatic artery usually comes off the celiac trunk. The portal vein brings venous blood from the spleen, pancreas, and small intestines, so that the liver can process the nutrients and byproducts of food digestion. The hepatic veins drain directly into the inferior vena cava.⁽²³⁾ The thoracic cage covers the vast majority of the right liver and most of the left side. The posterior surface straddles the inferior vena cava (IVC). A wedge of the liver extends to the left side of the abdomen. It is surrounded by a fibrous sheath name -Glisson's capsule. The liver is held in abdominal cavity by several ligaments. The round ligament is the remnant of the obliterated umbilical vein and enters the left liver hilum at the front edge of the falciform ligament. The falciform ligament separates the left lateral and left medial segments along the umbilical -fissure

and anchors the liver to the anterior abdominal wall. Deep in the plane between the caudate lobe and the left lateral segment is the fibrous ligamentum venosum (Arantius' ligament). It is the obliterated ductus venosus and covered by the plate of Arantius. The left and right triangular ligaments secure the two sides of the liver to the diaphragm. Extending from the triangular ligaments anteriorly on the liver are the coronary ligaments. The right coronary ligament also extends from the right undersurface of the liver to the peritoneum overlying the right kidney, thereby anchoring the liver to the right retroperitoneum. These ligaments (round, falciform, triangular, and coronary) can be divided into a bloodless plane to mobilize the liver to facilitate hepatic resection. Centrally and just to the left of the gall bladder fossa, the liver attaches via the hepatoduodenal and the gastrohepatic ligaments. The hepatoduodenal ligament is known as the porta hepatis and contains the common bile duct, the hepatic artery, and the portal vein.^(21, 26, 27)

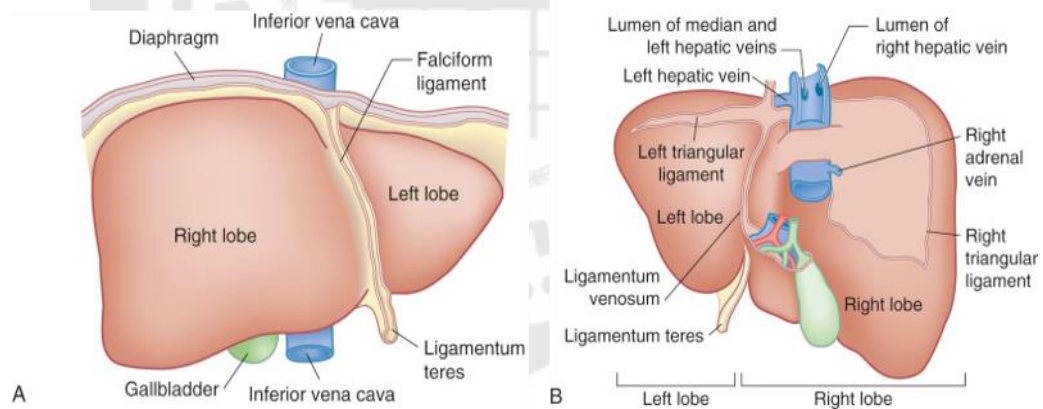


Figure 2 The human liver

The picture representing the anterior surface (A), the posterior and inferior surface (B) and ligamentous attachment of the liver.

Source: Blumgart L, Hann L. (2012). Surgical and Radiologic Anatomy of the Liver, Biliary Tract, and Pancreas: Blumgart's Surgery of the Liver, Biliary Tract, and Pancreas. p. 33-34.

1.2 Rat liver

The rat is the most used experimental animal model in various research because it is easy to handle and inexpensive. It is the most used animal model in many studies, for example, liver regeneration, liver immunology, liver fibrosis, liver cirrhosis, and liver cancer..⁽²⁸⁾

1.2.1 Liver anatomy

The liver of rats is multilobulated the same as in other mammals. The rat liver mass represents around 5% of the total body weight, whereas, in adult humans, it represents 2.5% approximately. Rat weighing between 250-300 grams has the liver mean weight of about 13.6 grams with 7.5 to 8.0 cm transverse liver diameter. It shows the superior-inferior diameter measured from 3.8 to 4.2 cm and has the anterior-posterior diameter ranged between 2.2 to 2.5 cm.^(28, 29)

1.2.2 Liver lobes

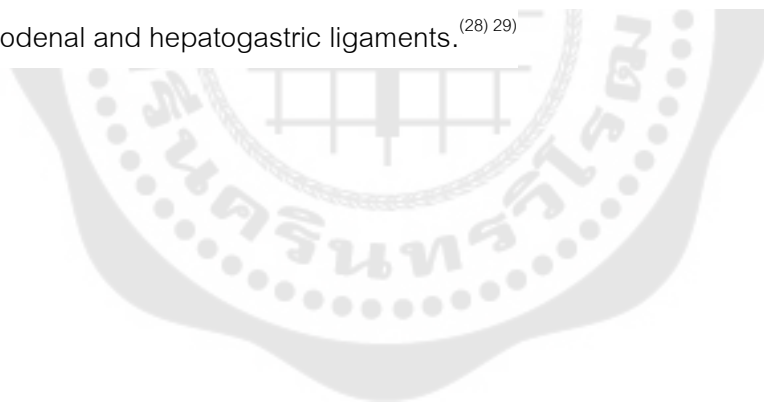
The liver lobes of the rat are named after the portal branches that its supply, same as the human liver. In mammals, the most constant anatomical reference is their portal system. Normally, it has four major lobes consisting of median lobe, left lobe, right lobe, and caudate lobe.

The median lobe (ML) is the largest lobe of the rat liver. It is about 38% of the liver weight, approximately. This lobe has a trapezoidal shape, and it is fixed in the diaphragm and abdominal wall by the falciform ligament and connected with the left lateral lobe (LLL). ML is divided by a vertical fissure (main fissure or umbilical fissure) into the right medial lobe (RML) and left medial lobe (LML). RML is 2/3 of the volume of the medial lobe, and LML is 1/3 of the medial lobe volume. The RML has both left and right hepatic vascular components.

The right lobe (RL) is positioned on the right of the vena cava and posteriorly in the right hypochondrium. The medial lobe almost entirely covers it. It contains about 22% of the liver weight. It is divided by a horizontal fissure into two pyramidal-shaped lobules: the superior (SRL, also called the right posterior lobe) and inferior (inferior right lobe, IRL, also called the right anterior lobe) lobules.

The left lateral lobe (LLL) is the lobe, which has a rhomboid shape and flattened without any fissures. LLL is located in the epigastric and left hypochondriac regions that over the stomach from the anterior aspect. The medial portion of LLL is covered by the left side of the medial lobe. The upper surface of LLL is slightly convex and is molded on the diaphragm.

The caudate lobe (CL) is located behind the LLL. It is on the left of the vena porta and inferior cava vein. CL comprises around 10% of the liver weight and is divided into two portions. About 2–3% of the liver mass is the paracaval portion (caudate process). It surrounds the inferior vena cava and bridges the CLs and the right lateral lobe, and the Spiegel lobe, which has an anterior (superior) and a posterior (inferior) portion in the form of discs. These are representing 4% of the liver mass each. The anterior part of the CL is situated anterior to the esophagus and stomach, and its pedicle lies superior. In contrast, the posterior is found behind these structures, and its pedicle lies inferior (figure 3). Both are covered by a skinny layer of peritoneum, the hepatoduodenal and hepatogastric ligaments.^{(28) (29)}



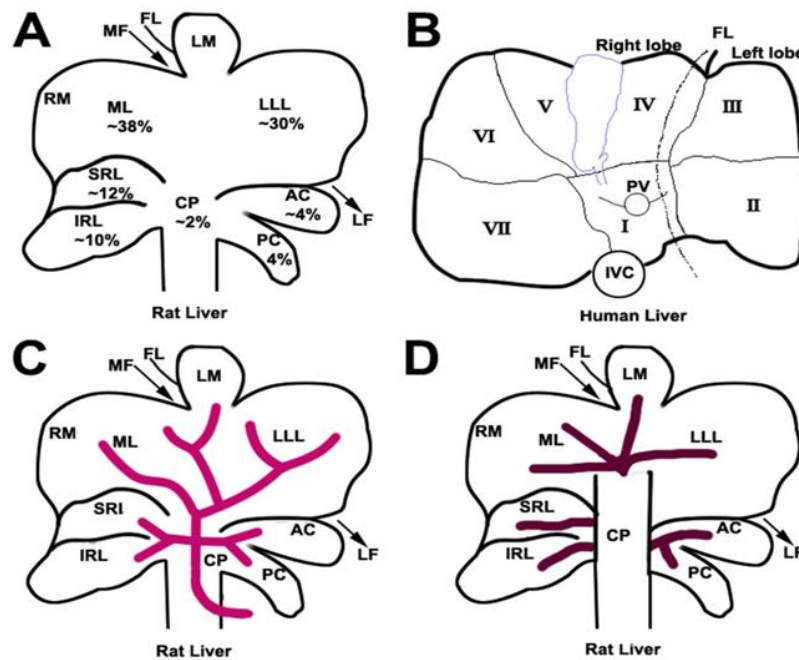


Figure 3 Anatomy of rat liver and human liver

(A) Visceral surface of the rat liver showing lobes and their mean relative weight. The caudate lobe (CL) is formed by the CP, AC and PC, the right liver lobe is formed by SRL and IRL and the medial lobe formed by SRL and IRL and the medial lobe formed by LML and RML. (B) Visceral surface of a human liver showing division into segments according to Couinaud's nomenclature. Most common anatomy of the portal vein (C) and hepatic veins (D) of the rat. In the rat, CL, LLL, LML, RML, (IRL+SRL) represent the human segments I and IX, segment II, segments III, IV, V and VIII; and segments VI and VII, respectively. In the rat, the left hemi-liver consists of the LLL, CL and LML while the right hemi-liver represents RL (SRL+IRL) and the RML. CP, caudate process; AC, anterior caudate lobe; PC, posterior caudate lobe; SRL, superior right lateral lobe; IRL, inferior right lateral lobe; ML, median lobe; RML, right portion of the medial lobe; LML, left portion of the medial lobe; LLL, left lateral lobe; MF, median fissure; LF, left fissure; RF, right fissure and FL, falciform ligament; PV, portal vein and IVC, inferior vena cava.

Source: Martins PNA, Neuhaus P. (2007) Surgical anatomy of the liver, hepatic vasculature and bile ducts in the rat. *Liver International*. p. 389.

1.3 Liver histology

1.3.1 Liver cell types

Liver cells can be classified into three groups: The first group is parenchymal cells include hepatocytes and bile duct epithelia. The second group is sinusoidal cells are composed of hepatic sinusoidal endothelial and Kupffer cells (hepatic macrophages), and the last group is perisinusoidal cells consist of hepatic stellate cells and pit cells.⁽³⁰⁾

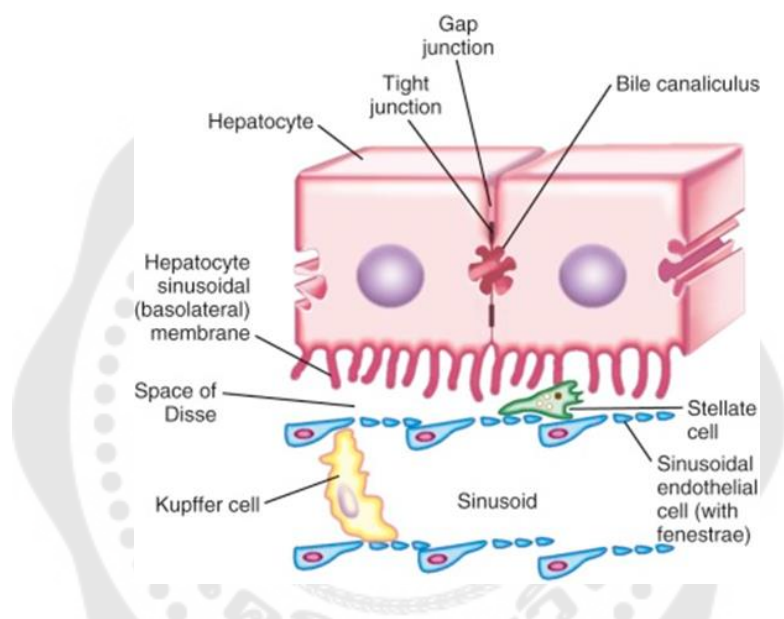


Figure 4 The spatial relationship among the different cell types of the liver

Sinusoidal plasma comes in direct contact with hepatocytes in the space of Disse. The endothelial cells are fenestrated and lack a basement membrane. Kupffer cells are located in the lumen of the sinusoid, where they are in direct contact with the sinusoidal endothelial cells and portal blood. Stellate cells are situated between the endothelial cells and hepatocytes, and come in direct contact with both cell types. The hepatocytes are joined with each other by tight junctions and the communicating gap junctions. The canalicular domain of the plasma membrane of two adjacent hepatocytes encloses the bile canaliculus.

Source: Roy-Chowdhury N, Roy-Chowdhury J. (2016) Liver Physiology and Energy Metabolism: Sleisenger and Fordtran's Gastrointestinal and Liver Disease. p. 1230.

1.3.1.1 Hepatocytes

Hepatocytes are the main cells in the liver. The hepatocyte is a polyhedral cell with a central spherical nucleus. Hepatocytes comprise 60% of the adult liver cell population, representing approximately 78% of the tissue volume. Hepatocytes are complex multifunctional cells. They perform the primary functions of the liver: uptake, storage, and release of nutrients; synthesis of glucose, fatty acids, lipids, and numerous plasma proteins, production and secretion of bile for digestion of dietary fats; and degradation and detoxification of toxins.^(27, 30) To carry out these functions, the plasma membrane of the hepatocyte is organized in a specific manner into three specific domains. The sinusoidal membrane is exposed to the space of Disse and has multiple microvilli that provide a surface specialized in the active transport of substances between the blood and hepatocytes. The lateral domain exists between neighboring hepatocytes and contains gap junctions that provide for intercellular communication. The canalicular membrane is a tube containing microvilli formed by two apposed hepatocytes. These bile canaliculi are sealed by zonula occludens (tight junctions), which prevent the escape of bile. The bile canaliculi form a ring around the hepatocyte that drains into small bile ducts known as canals of Hering, which empty into a bile duct at a portal triad. The canalicular membrane contains adenosine triphosphate (ATP)-dependent active transport systems that enable solutes to be secreted into the canalicular membrane against large concentration gradients.

Hepatocytes have only one or two nuclei. Each cell contains several types of organelle, as well as glycogen granules and lipid droplets. Organized into one- or two-cell-thick plates that are separated by sinusoids.⁽³¹⁾ The hepatocyte is one of the most diverse and metabolically active cells in the body, as reflected by its abundance of

organelles. There are 1000 mitochondria/hepatocyte, occupying approximately 20% of the cell volume. Mitochondria generate energy (ATP) through oxidative phosphorylation and provide the energy for the metabolic demands of the hepatocyte.

The hepatocyte mitochondria are also essential for fatty acid oxidation. An extensive system of interconnected membrane complexes made up of smooth and rough endoplasmic reticulum and the Golgi apparatus compose what is known as the hepatocyte microsomal fraction. These complexes have a diverse range of functions, including the following: synthesis of structural and secreted proteins; metabolism of lipids and glucose; production and metabolism of cholesterol; glycosylation of secretory proteins; bile formation and secretion; and drug metabolism. Finally, hepatocytes also contain lysosomes, which are intracellular single-membrane vesicles that contain a number of enzymes. These vesicles store and degrade exogenous and endogenous substances. Coordination of these numerous organelles in the hepatocyte allows these cells to accomplish a large variety of functions.⁽²⁷⁾

Blood flow into the liver sinusoids comes from terminal branches of both the hepatic portal vein and hepatic artery. The liver is therefore unusual in having both arterial and venous blood supplies, as well as separate venous drainage. With the exception of most lipids, absorbed food products pass directly from the gut to the liver via the hepatic portal vein. This brings blood that is rich in amino acids, simple sugars and other products of digestion but relatively poor in oxygen. The oxygen required to support liver metabolism is supplied via the hepatic artery. After passing through the sinusoids, venous drainage of blood from the liver occurs via the hepatic vein into the vena cava. The main blood vessels and ducts run through the liver within a branched collagenous framework termed the portal tracts. These tracts also contain the bile ducts that transport bile away from the liver to be secreted into the small bowel.⁽³²⁾

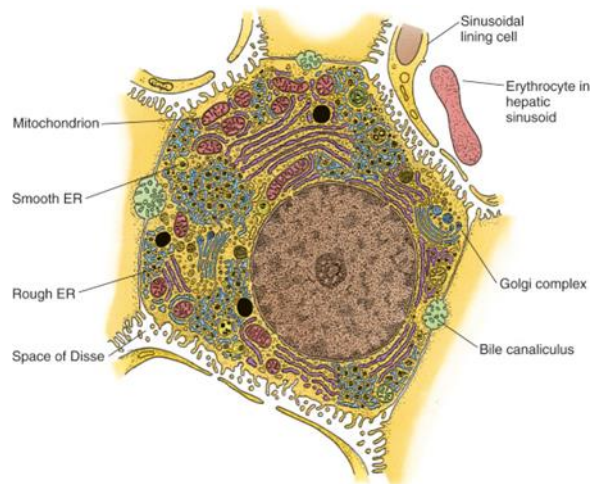


Figure 5 A hepatocyte

Its sinusoidal and lateral domains (ER, endoplasmic reticulum).

Source: Rogers AB, Dintzis RZ. (2012) Liver and Gallbladder: Comparative Anatomy and Histology. p. 195.

1.3.1.2 Kupffer cells

Kupffer cells (KC) are specialised macrophages, monocyte-derived members of the mononuclear phagocyte system.⁽³¹⁾ In KCs, the liver has the largest population of macrophages in the body. KCs are attached to the endothelial cells lining the sinusoids, so they can directly sample the slow-flowing blood for both gut-derived and systemic pathogens. KCs will either destroy pathogens or activate other immune cells to do so. They are also important in clearing activated platelets and leukocytes from the bloodstream, thus helping to limit coagulation and immune responses.⁽²²⁾ KCs are different from the endothelial cells when staining with standard H&E with phagocytosed colored particles (e.g., India ink) before fixation.⁽³¹⁾

1.3.1.3 Space of Disse

Space of Disse or the perisinusoidal space is located between hepatocytes and the endothelium of the hepatic sinusoids (figure 6). This structure contains microvilli of the hepatocytes, plasma, reticular fibers, and fat-storing cells (also called Ito cells or hepatic stellate cells). Blood plasma can enter this space through the openings between the endothelial cells, which are too small for blood cells to pass. Blood-borne substances thus directly contact the microvilli of hepatocytes. Hepatocytes absorb nutrients, oxygen, and toxins, and release endocrine secretions into the space of Disse. Its functions are the exchange of material between the bloodstream and hepatocytes, which do not directly contact the bloodstream. The cells that found in the space of Disse include the following;⁽³³⁾

a) Hepatic stellate cells (HSCs) (Ito cells, fat storing cells, lipocytes, pericytes) is the primary cell type in the liver and regulation for excess collagen synthesis during hepatic fibrosis.⁽³⁵⁾ HSCs store Vitamin A and manufacture and secrete several crucial hepatic growth factors and matrix components (collagens) and therefore play a role in liver regeneration and the development of liver fibrosis. Moreover, HSCs influence the growth and proliferation of hepatocytes and participate in the inflammatory reaction and the immune function of the liver.^(34, 35) In a healthy liver, stellate cells are largely inactive, contributing to immune surveillance and acting as the main reservoir of vitamin A in the body. If the liver is damaged, stellate cells are activated. They secrete collagen, to form a temporary scar at the site of injury, and signal molecules that stimulate hepatocytes in the area to divide and regenerate the damaged tissue. Repeated liver insults, such as in chronic liver disease, trigger ongoing stellate cell activation, which causes widespread formation of scar tissue known as Liver fibrosis. Fibrosis and ongoing stellate cell stimulation of hepatocyte proliferation are thought to trigger development of hepatocellular carcinoma (HCC). Activated stellate cells are also

contractile, constricting the sinusoids, which may contribute to the development of portal hypertension in liver failure.^(22, 31)

b) Pit cells, also known as large granular lymphocytes or natural killer cells, they are a primitive cellular immune host defense mechanism, active against viruses and tumor cells.

c) T and B lymphocytes.⁽³⁶⁾

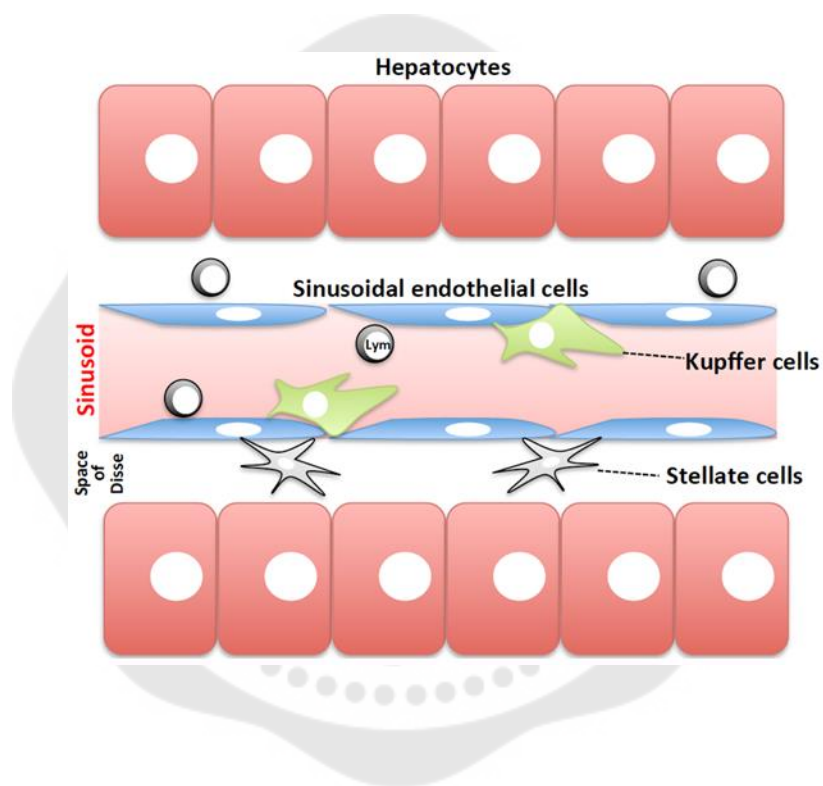


Figure 6 Schematic structure of the liver

Hepatic sinusoids are composed of sinusoidal endothelial and Kupffer cells. Blood circulates within the sinusoids in the liver. Hepatocytes, or liver parenchymal cells are localized to the space of Disse, distant from the sinusoid. Natural killer (NK) and invariant NK T (NKT) cells are abundant in the liver. Lym: lymphocytes, including NK cells, NKT cells, and other lymphocytes.⁽³⁷⁾

Source: Tsutsui H, Nishiguchi S. (2014) Importance of Kupffer cells in the development of acute liver injuries in mice: *Int J Mol Sci.* p. 7715.

1.3.2 Liver lobules

The relationship between hepatic structure and function is best demonstrated by three models of liver substructure: the classic lobule, the portal lobule, and the hepatic acinus.

1.3.2.1 Classic liver lobule

This model is based on the direction of blood flow. In sections, liver substructure exhibits a pattern of interlocking hexagons; each of these is a classic lobule. Human lobule boundaries are indistinct, but can be estimated by noting the portal triads at the lobule periphery, the central vein at its center, and the alternating hepatocyte plates and sinusoids between them.⁽³¹⁾ Each lobe of the liver has numerous lobules, which are in a hexagonal structure. The central vein occupies the center of each lobule, and the periphery of the lobule is called "portal triads." The portal triad is composed of the hepatic artery, portal vein. The portal triads appear at the vertices of the hexagonal lobule. The liver has both endocrine and exocrine functions.⁽³⁸⁾

Portal triad. One triad occupies a potential space (portal space) at each of the six corners of the lobule. Each triad contains three main elements surrounded by connective tissue: a portal venule (a branch of the portal vein; largest diameter), a hepatic arteriole (a branch of the hepatic artery; smaller diameter with a thick wall), and a bile ductule (tributary of a bile duct; small diameter with epithelial nuclei resembling a string of pearls). A lymphatic vessel also may be seen.

Central vein. A single vein marks the center of each lobule. It is easily distinguished from those in the portal triad by its lack of a connective tissue sheath.

Hepatocyte plates and hepatic sinusoids. Many such plates radiate from the central vein toward the lobule periphery (like the spokes of a wheel). The

plates are separated by hepatic sinusoids, which receive blood from the vessels in the triads, converging on the lobule center to empty directly into the central vein.⁽³¹⁾

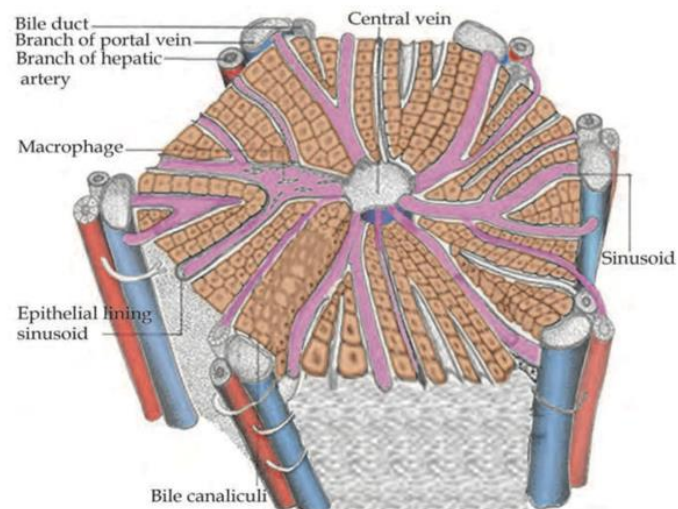


Figure 7 Histological structure of a liver lobule

Source: Tso P, McGill J. (2004) *The Physiology of the Liver: Medical Physiology* p. 519.

1.3.2.2 Portal lobule

This model is based mainly on the direction of bile flow, which is counter to that of blood. From this perspective, the liver parenchyma is divided into interlocking triangles, each with a portal triad at its center and a central vein at each of its three corners. Bile produced by the hepatocytes enters the membrane-bounded bile canaliculi between them and flows within the hepatocyte plates toward the bile duct in the portal triad. Liver lymph in the spaces of Disse flows in the same direction as bile, toward lymphatic vessels in the triad.

1.3.2.3 Hepatic acinus

This model is more abstract; it is based on changes in oxygen, nutrient, and toxin content as blood flowing through the sinusoids is acted on by

hepatocytes. Each diamond-shaped acinus contains two central veins and two portal triads that define its four corners. The diamond is divided into two triangles by a line connecting the portal triads. Along this line run terminal branches of the portal and hepatic vessels that deliver blood to the sinusoids. Each triangle is divisible into three zones, according to their distance from the terminal distributing vessels. Zone I, for example, is closer to these vessels, whereas zone III is closer to the central vein. Blood in zone I sinusoids has higher oxygen, nutrient, and toxin concentrations than in the other zones. As the blood flows toward the central vein, these substances are gradually removed by hepatocytes. Zone I hepatocytes thus have a higher metabolic rate and larger glycogen and lipid stores. They are also more susceptible to damage by blood-borne toxins, and their energy stores are the first to be depleted during fasting. This model helps explain regional histopathologic differences in patients with liver damage.⁽³¹⁾



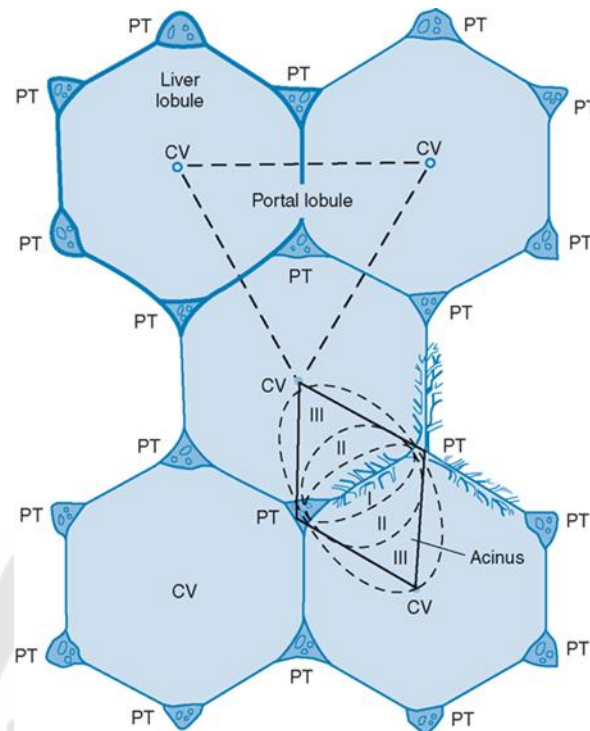


Figure 8 Schematic drawing of the territories of the classic liver lobules, hepatic acini, and portal lobules

The classic lobule has a central vein (CV) and is outlined by lines that connect the portal triads (PT; solid lines). The centers of the portal lobules lobules are located in the portal triads and are outlined by lines that connect the central veins (upper triangle). They constitute the portion of the liver from which bile flows toward a portal triad. The hepatic acinus is the region irrigated by one distributing vein (diamond-shaped figure). Zones of the hepatic acinus are indicated by roman numerals I, II, and III. (Revised, with permission, from Leeson TS, Leeson CR. *Histology*. 5th ed. Philadelphia, PA: WB Saunders; 1985.)

Source:<https://accessmedicine.mhmedical.com/content.aspx?bookid=563§ionid=42045311>

1.3.3. Biliary system

bile synthesis and secretion are the liver's main exocrine functions. Bile consists of bile acids, phospholipids, cholesterol, bilirubin, water, and electrolytes. This composition confers detergent properties that aid in digesting dietary fat. Approximately 90% of bile comes from recycled substances that are added to the intestinal contents in the duodenum and subsequently reabsorbed into the portal circulation by the epithelial lining of the distal part of the intestine. Hepatocytes merely reabsorb them from the sinusoids and transport them back to the bile canaliculi. Approximately 10% of bile is synthesized de novo in the hepatocyte's SER. a) Bile acids. Cholic acid is synthesized from cholesterol and conjugated with glycine or taurine to form glycocholic and taurocholic acid, respectively. b) Bilirubin is a water-insoluble by-product of the hemoglobin catabolism that accompanies the disposal of worn erythrocytes by cells of the mononuclear phagocyte system in the spleen, liver, and bone marrow. It is carried by the blood to the hepatocytes, which conjugate it with glucuronic acid to form bilirubin glucuronide. This now water-soluble substance is secreted, with other bile components, into the bile canaliculi.⁽³¹⁾ For the biliary tract, In the rat, it does not have a gallbladder. The extrahepatic biliary ducts are formed by first-order branches of each hepatic lobe and located superficially to the arterial and portal branches. Second-order branches exist for the superior and inferior CLs, right middle lobe, and caudate process. The rat biliary tract has several anatomical variations. Most generally, each lobe is drained by its bile ducts. The LLL is the most common (in 62.5% of cases) drained by two biliary branches. Branches drain the middle lobe from the right middle lobe (1–4 branches) and the LML. In around 60% of incidents, each CL has one branch that joins together to form a common branch before draining into the CBD. The superior part of the caudate process drains into branches of the right lateral lobe or the main biliary trunk. In contrast, the inferior part of it drains into the branches of the caudate process or to the branch of the right lateral lobe. The CBD is formed by the junction of the main hepatic ducts. The main hepatic ducts join together on the caudate process. In this series, the

CBD ranged from 12 to 16 mm in length and 0.6 to 1 mm in diameter, but it can be up to 45 mm long.

The CBD descends to the left of the hepatic artery and the portal vein on the surface of the caudate process and portal vein, and then along the right border of the lesser omentum, keeping some distance from them. A great extent of the CBD is completely imbedded in the pancreas, which has a diffuse and lobulated form. The CBD opens at the medial side of the descending portion of the duodenum, slightly below its middle and about 10–22 mm from the pylorus. The extrahepatic biliary system of the rat also has small intercommunicating branches.^(28, 39)

1.4 Liver function

In our body, the liver undertakes several vital functions. The major functions of the liver may be summarised as follows:

1. The uptake of nutrients delivered from the digestive tract via the portal vein.

2. The synthesis, storage, interconversion, and degradation of metabolites (metabolism). The liver involves in lipid synthesis, carbohydrate, fat, and hemoglobin metabolism. There are many chemicals, such as glycogens, vitamins, minerals, and several metabolites store in the liver.

- 2.1 Fat metabolism: Oxidising triglycerides to produce energy, synthesis of plasma lipoproteins and synthesis of cholesterol and phospholipid.

- 2.2 Carbohydrate metabolism: Converting carbohydrates and proteins into fatty acids and triglyceride and regulation of blood glucose concentration by glycogenesis, glycogenolysis and gluconeogenesis.

- 2.3 Protein metabolism: Synthesis of plasma proteins, including albumin and clotting factors, synthesis of non-essential amino acids, and Detoxification of metabolic waste products (e.g. deamination of amino acids and production of urea)

3. The regulated supply of energy-rich intermediates and building blocks for biosynthetic reactions.

4. The detoxification of harmful compounds by biotransformation: The liver also has a detoxification function. It can remove various toxic chemicals, including drugs, carcinogens, and several toxins through bile from the body.

5. The excretion of substances with the bile, as well as the synthesis and degradation of many blood plasma constituents.

6. Fighting infections (Kupffer cells-macrophages).⁽³⁸⁾

2. Hepatocellular carcinoma (HCC)

Hepatocellular carcinoma (HCC) is the most common type of primary liver cancer, followed by cholangiocarcinoma. HCC is the fifth most common cancer and the third most common cause of cancer-related death worldwide. The incidence rate is 2–3 times higher in developing countries than in developed countries. It usually occurs in older patients (> 60 years), but depends upon risk factors.^(1, 40)

2.1 Risk factors for development of HCC

Chronic hepatitis B and C virus (HBV and HCV) infection is the principal etiologic factor worldwide for HCC. Patients chronically seropositive for HBsAg constitute a high-risk group for development of hepatocellular carcinoma. Hepatitis B virus DNA has been detected integrated into the genome of host hepatocytes and hepatoma cells and has a direct oncogenic effect. Patients with chronic hepatitis B infection may therefore develop hepatocellular carcinoma in the absence of cirrhosis. By contrast, HCC arising in the setting of chronic hepatitis C infection is typically associated with cirrhotic change. Cirrhosis from almost any cause (eg, alcoholism, hemochromatosis, α_1 -antitrypsin deficiency, or primary biliary cirrhosis) is associated with an increased risk of hepatocellular carcinoma, and the great majority of these tumors arise in the setting of chronic underlying liver disease. With the increase in obesity in the United States, nonalcoholic fatty liver disease (NAFLD) has become the one of the most common causes of chronic liver disease; a subgroup of these patients with nonalcoholic steatohepatitis (NASH) are at high risk of cirrhosis and malignant transformation. Certain fungal metabolites called aflatoxins have been shown experimentally to be capable of producing liver tumors. These substances are present

in staple foods (eg, ground nuts and grain) in some parts of Africa where hepatocellular carcinoma has a high incidence.⁽⁴³⁾ In almost all cases (85–90%), HCC arises in the background of cirrhosis; therefore, HBV and HCV, Wilson disease, hemochromatosis, chronic alcoholism are risk factors, and *Aspergillus flavus* which produces aflatoxin.

2.2 Signs and symptoms

These signs and symptoms include abdominal pain, weight loss, weakness, abdominal fullness and swelling, jaundice, and nausea. Presenting signs and symptoms differ somewhat between high and low incidence areas. In high-risk areas, especially in South African blacks, the most common symptom is abdominal pain; by contrast, only 40–50% of Chinese and Japanese patients present with abdominal pain. Abdominal swelling may occur as a consequence of ascites due to the underlying chronic liver disease or may be due to a rapidly expanding tumor. Occasionally, central necrosis or acute hemorrhage into the peritoneal cavity leads to death. In countries with an active surveillance program, HCC tends to be identified at an earlier stage, when symptoms may be due only to the underlying disease. Jaundice is usually due to obstruction of the intrahepatic ducts from underlying liver disease. Hematemesis may occur due to esophageal varices from the underlying portal hypertension. Bone pain is seen in 3–12% of patients, but necropsies show pathologic bone metastases in 20% of patients. However, 25% of patients may be asymptomatic.⁽⁴¹⁾

The diagnosis at early and more treatable stages is often difficult, since symptoms are often absent. Screening and surveillance of high-risk patients (with cirrhosis, chronic hepatitis, etc) with ultrasonography of the liver has been recommended. Patients with more advanced tumors may have epigastric or right upper quadrant pain, which may be associated with referred pain in the right shoulder. Weight loss may be present. Jaundice is rare in patients with small tumors and good liver function; the presence of jaundice suggests either very advanced cancer or deteriorating liver function or both.

The patterns of presentation can thus be extremely variable and may include: (1) pain with or without hepatomegaly; (2) sudden deterioration of the condition

of a cirrhotic patient with the onset of hepatic failure, bleeding varices, or ascites; (3) sudden, massive intraperitoneal hemorrhage; (4) acute illness with fever and abdominal pain; (5) symptoms related to distant metastases; and (6) no clinical findings or symptoms.

2.3 Laboratory findings

Depending on the disease extent and underlying hepatic function, laboratory values may range from entirely normal to suggestive of impending liver failure.

2.3.1 Liver function test

Serum transaminase levels (AST and ALT) and alkaline phosphatase may be increased but are nonspecific and often seen in patients with chronic liver disease without hepatocellular carcinoma. The presence of a moderate to large liver tumor may bring about an increase in the serum alkaline phosphatase in the absence of underlying liver disease. An elevated serum bilirubin is a more ominous finding and reflects some degree of liver dysfunction, either from the underlying chronic liver disease or from a large volume of cancer within the liver. Tumor extension within the portal venous system is not uncommon, and involvement of the right and left portal trunks or the main portal vein may result in jaundice due to compromised portal venous inflow. Less often, jaundice is the result of tumor involvement of the biliary confluence by direct compression or by intrabiliary tumor extension. Other signs of compromised hepatic function include hypoalbuminemia, coagulopathy, and thrombocytopenia. A large number of patients may be positive for HBsAg or HCV antibody; the proportions of each vary somewhat by geography.⁽⁴²⁾

Abnormalities in laboratory tests are frequently the first or only sign of liver disease, and the pattern of abnormality is often suggestive of the underlying disease process. Gamma-glutamyltransferase (GGT) is particularly sensitive for liver disease. If the level of GGT is normal, there is only a 1–2% chance of liver disease. The levels of aspartate aminotransferase (AST) and alanine aminotransferase (ALT) are also very useful for the diagnosis of liver disease. An AST > 3000 U/L suggests a severe hypotensive episode causing centrilobular necrosis, a toxic injury such

as acetaminophen overdose, or acute viral hepatitis. On the other hand, chronic diseases of the liver such as alcoholic liver disease and chronic viral hepatitis are typically associated with smaller elevations of transaminases, in the 100–300 U/L range. Elevated ALT and AST with an AST/ALT ratio $> 2:1$ is classically associated with alcoholic hepatitis. Elevated alkaline phosphatase (ALP) can be seen in both liver and bone disease, whereas a concomitant elevation of ALP and GGT is consistent with cholestatic liver disease.

While the above enzymes (GGT, AST, ALT and ALP) indicate damage to the hepatocytes, serum albumin is more reflective of the functional status of the liver, since both albumin and clotting factors are produced by hepatocytes. Albumin is accurate at assessing a chronic change in liver function. Also, assessment of gamma globulins is useful for determining an acute versus chronic pathologic liver process. In acute processes, the gamma globulin level is normal, and in chronic processes, it is elevated (> 3 g/dL).

When assessing liver function tests, four general patterns are apparent: (1) acute hepatitis pattern, which has elevated transaminase levels and variable increases in other enzymes; (2) cirrhosis pattern, which has decreased albumin, elevated gamma globulins (with β - γ bridging on serum electrophoresis); (3) chronic hepatitis pattern, which has a combination of changes seen in acute hepatitis and cirrhosis patterns; and (4) obstructive liver disease pattern, also called cholestasis, which has an elevated ALP and bilirubin.⁽⁴³⁾

2.3.2 Tumor markers

Alpha fetoprotein (AFP), a glycoprotein normally present only in the fetal circulation, is present in high concentrations in the serum of many patients with hepatocellular carcinoma, testicular tumors, and hepatoblastomas. Increased levels are rarely seen as a product of other tumor types, such as the lung, stomach, pancreas, and biliary tree.

The upper limit of normal in the serum is 20 ng/mL; values above 200 ng/mL are suggestive of HCC, while levels above 400 ng/mL in a cirrhotic patients with a

hypervascular liver mass larger than 2 cm in diameter are diagnostic. Levels in the intermediate range are nonspecific and may occur with benign liver diseases, such as cirrhosis and chronic hepatitis, where they represent a manifestation of liver cell proliferation. As imaging methods have improved, the diagnosis of liver cancer is being made earlier, when AFP levels may be normal or only minimally elevated. Additionally, some patients may have normal AFP levels despite the presence of advanced disease. In general, AFP levels correlate with tumor size and vascular invasion, and a number of studies have shown a correlation between high AFP levels and recurrent cancer after resection.⁽⁴²⁾


AFP is the primary serum biomarker for HCC and is elevated in up to 40% of patients with early-stage HCC, with expression increasing in advanced disease. Although AFP is not specific for HCC and may be seen clinically in nonmalignant conditions such as chronic hepatitis, cirrhosis or fulminate hepatic failure, the elevation of AFP and confirming ultrasound findings clearly indicate malignant disease. AFP in preclinical studies is a reliable biomarker of the tumor take rate and growth. Serum AFP correlates well with the measurement of tumor size by caliper, weight of excised tumor tissue and ultrasound measurement of tumor volume.⁽⁴⁴⁾

2.4 HCC staging

Cancer staging is an important prognostic tool that provides a classification system to help guide patient management, provides a common language to compare results of various clinical trials, and is essential to the rational design of clinical trials. Based on common features shared by several staging systems, the key factors that have an impact on HCC prognosis and treatment option selection are solitary versus multifocal tumors, presence of macrovascular invasion, extrahepatic disease, high serum AFP levels, patient performance status, and degree of hepatic impairment. A number of staging systems for hepatocellular carcinoma are in current use when considering treatment options for patients with HCC: the Barcelona Clinic Liver Cancer (BCLC), Cancer of the Liver Italian Program (CLIP), Okuda, Chinese University Prognostic Index (CUPI), and Japan Integrated Staging (JIS); these classifications differ

on their assessment of tumor burden, related symptoms, and underlying liver dysfunction, and most cannot predict the survival in patients with advanced HCC.^(42, 45, 46)

The BCLC staging system (figure 9) has come to be widely accepted in clinical practice and is also being used for many clinical trials of new drugs to treat HCC. Therefore, it has become the de facto staging system that is used. The recommendations for liver transplantation have not changed. No new data have emerged that can be used to define a new limit for expanding the patient selection criteria. The usefulness of portal pressure measurement to predict the outcome of patients and define optimal candidates for resection has been validated in Japan. Thus, resection should remain the first option for patients who have the optimal profile, as defined by the BCLC staging system. Although resection can be performed in some of these patients with advanced liver disease, the mortality is higher and they might be better served by liver transplantation or ablation. A cohort study of radiofrequency ablation demonstrated that complete ablation of lesions smaller than 2 cm is possible in more than 90% of cases, with a local recurrence rate of less than 1%.¹³ These data should be confirmed by other groups before positioning ablation as the first-line approach for very early HCC.⁽⁴⁶⁾



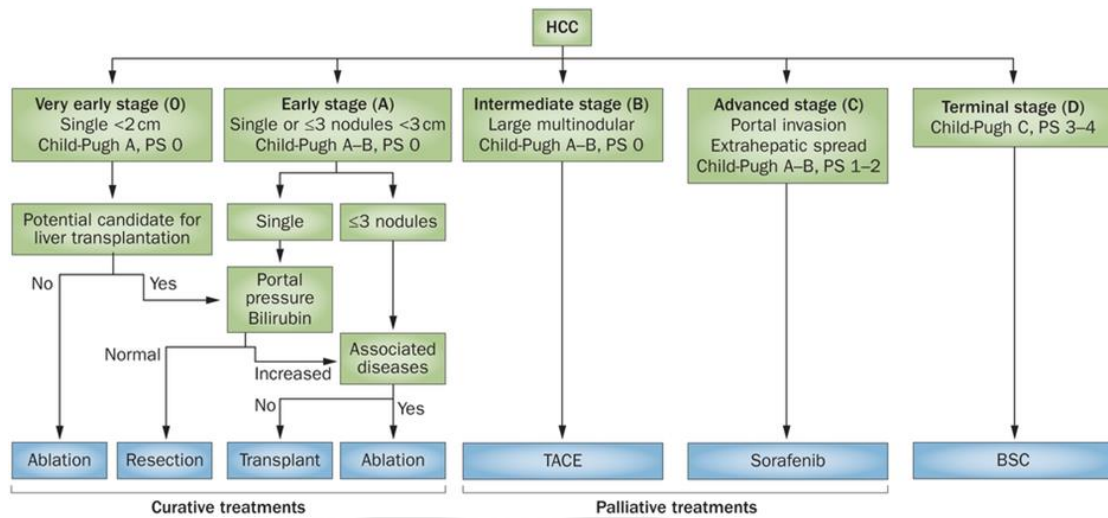


Figure 9 The BCLC staging system

The BCLC algorithm classifies HCC into five stages—based on the extent of disease, Child-Pugh score, and ECOG performance status—that enables prognostication and informs allocation of first-line treatment. If the proposed first-line treatment is contraindicated owing to a patient's clinical status, the treatment approach recommended for the subsequent disease stage should be considered. For example, a patient with early stage HCC (BCLC stage A) might benefit from TACE. Abbreviations: BCLC, Barcelona Clinic Liver Cancer (group); BSC, best supportive care; ECOG, Eastern Cooperative Oncology Group; HCC, hepatocellular carcinoma; PS, performance status; TACE, transarterial chemoembolization. Reprinted from The Lancet, 379, Forner, A., Llovet, J. M. & Bruix, J. Hepatocellular carcinoma, 1245–1255 © 2012, with permission from Elsevier.⁽⁴⁷⁾

Source: Forner A, Gilabert M, Bruix J, Raoul JL. (2014) Treatment of intermediate-stage hepatocellular carcinoma: Nat Rev Clin Oncol. p. 528.

2.5 Pathological analysis of HCC

Pathological analysis of HCC is an overall procedure able to provide its accurate diagnosis and prognosis by evaluating both tumor macroscopic (including tumor size, growth pattern of development) and microscopic features including grade of differentiation, vascular invasion, and aspect of non-tumoral liver, especially the identification of preneoplastic changes. At last, pathogenesis of HCC is complex, involving different molecular pathways that may reflect both underlying etiologies and biological tumor behavior.⁽⁴²⁾

Pathological analysis of HCC is based on macroscopic and microscopic features that are highly diversified and correlated with prognosis for some of them.⁽⁴⁰⁾ HCC typically form soft masses with a heterogeneous macroscopic feature, polychrome with foci of hemorrhage or necrosis. They could be single or multiple with a size ranging from less than 1 cm to over 30 cm. Usually, on cirrhosis, size of HCC is smaller compared to those developed in the non-fibrotic liver.^(40, 48) The hepatocellular carcinoma progression can be macroscopically classified into nodular, massive, and diffuse. First, the nodular type, it can either consist of a single or multiple nodules. Single nodules are usually encapsulated and may show extracapsular growth in the region of the primary nodule. The multinodular type is an aggregation of a diverse amount of small nodules. The second type is the massive type. This type is defined as a large tumor with irregular demarcation. These morphologic features can also be seen in advanced HCC. The last type is the diffuse type; it has several small nodules in a hepatic lobe or the entire organ.^(42, 49)

A large proportion of patients have intrahepatic or extrahepatic metastases at presentation. Multiple intrahepatic tumors can arise as a result of infiltration of the portal venous system with subsequent dissemination of tumor cells. Vascular invasion is more common with larger tumors (> 5 cm). The extrahepatic sites most commonly involved with metastatic disease include the hilar and celiac lymph nodes and the lungs; metastases to bone and brain are less common, and peritoneal disease (ie,

carcinomatosis) is distinctly unusual. Major portal or hepatic veins are often invaded by tumor, and venous occlusion may occur as a result.⁽⁴²⁾

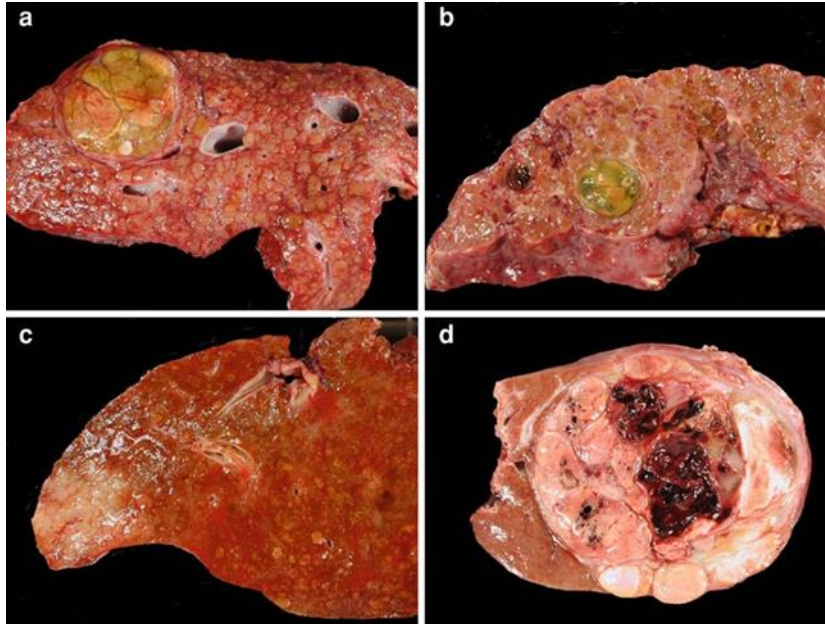


Figure 10 Macroscopic aspects of Hepatocellular carcinoma

a) Nodular pattern of HCC developed in a cirrhotic liver. b) Infiltrative pattern of HCC developed in a cirrhotic liver. c) Early HCC (progressed type) on a cirrhotic tissue. d) Nodular HCC developed in a normal liver in the context of metabolic syndrome.⁽⁴⁰⁾

Source: Paradis V. (2013) Histopathology of Hepatocellular Carcinoma: Multidisciplinary Treatment of Hepatocellular Carcinoma. Berlin, Heidelberg: Springer; 2013. p. 25.

The classical histomorphological appearances of HCC are well-vascularized tumors with wide trabeculae (more than 3 cells) or thick hepatic cell cord, prominent acinar pattern, small cell changes, cytologic atypia, mitotic activity, vascular invasion, loss of Kupffer cells and the lack of the reticulin network.⁽⁵⁰⁾ The most typical histologic growth patterns are trabecular-resembling normal liver tissue, pseudoglandular or acinar with possible bile or fibrin content, and the solid pattern. Bile production can often be observed. Mallory-bodies and pale bodies can present within the tumor cells. Histomorphological features of HCC are varies greatly from patient to

patient, and even in a single patient, different stages of intratumoral differentiation and growths patterns can be observed. There are some authors assume a step-wise dedifferentiation of an initially well differentiated small lesion into a larger, less differentiated tumor which leads to intratumoral heterogeneity. The well-differentiated lesion is usually replaced by tissue of the dedifferentiated component in advanced disease and therefore leads to a nodule in nodule present. In contrast, HCC progression shows an expansive and infiltrative histological growth pattern with a completely new blood vessel forming with unpaired arteries and possible vascular infiltration. There are no portal tracts appear within the tumor, and all the classical histological patterns such as trabecular/sinusoidal, pseudoglandular, solid, and undifferentiated, that are often seen. The tumors are mostly encapsulated, and septae are detected. Encapsulation is found to be more common in tumor arising in a cirrhotic liver than in non-cirrhotic livers.⁽⁴⁹⁾ Most tumors show satellite nodules within 2 cm of the primary tumor nodule as well as metastasis in the liver. In HCC, the structure of the blood vessel plays a critical role during tumor growth and is also a vital part of modern imaging modalities. The progressed HCC has classical unpaired arteries positive for SMA and CD34. These arteries are not associated with a portal tract and hence have no association with bile ducts. They also show less elastic fibers compared to normal intrahepatic arteries. Early HCC of the vaguely nodular type has a reduced density of unpaired arteries compared to progressed HCC and therefore appears hypovascular in imaging. Due to the appearance of portal tracts within the tumor, although less in number than in normal liver tissue, these lesions also obtain blood from the portal vein.^(51, 52) The distinctly nodular type in early HCC, as well as progressed-HCC, produce and develop hypervascular because of earlier blood vessel formation with unpaired arteries.⁽⁴⁹⁾

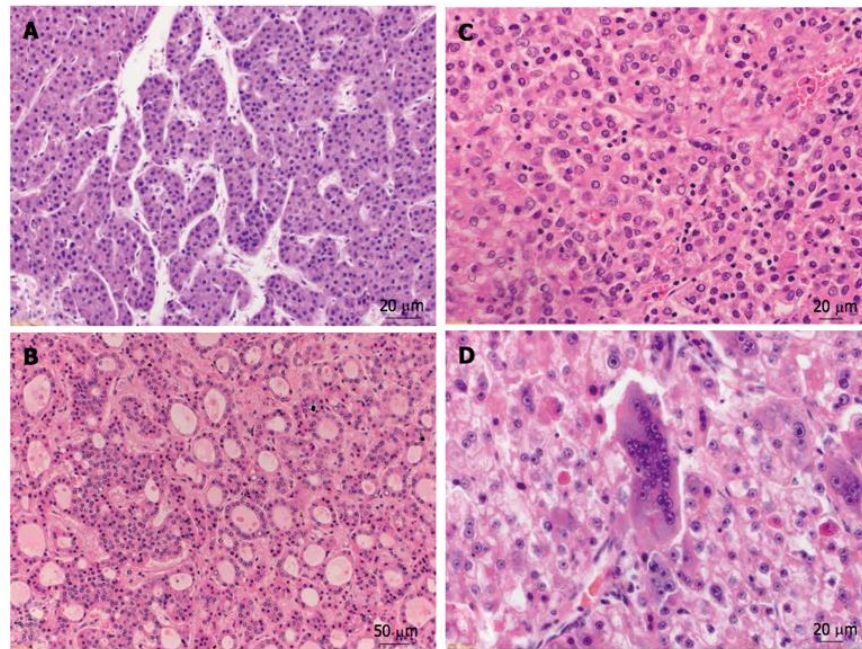


Figure 11 Growth patterns of progressed hepatocellular carcinoma

A: Hepatocellular carcinoma (HCC) with trabecular growth pattern stained with hematoxylin and eosin (HE), $\times 300$; B: HCC with pseudoglandular growth pattern (HE, $\times 100$); C: HCC with solid growth pattern (HE, $\times 200$); D: HCC with giant cell formation (HE, $\times 200$).⁽⁴⁹⁾

Source: Schlageter M, Terracciano LM, D'Angelo S, Sorrentino P. (2014) Histopathology of hepatocellular carcinoma: World J Gastroenterol. p.15958.

2.6 Treatment of HCC

Long-term survival is associated with resection or ablation or transplantation, all of which can yield $>70\%$ 5-year survival. Liver transplant is the only therapy that can treat the tumor and the underlying liver disease simultaneously and may be the most important advance in HCC therapy in 50 years. Unfortunately, it benefits only patients with limited size tumors without macrovascular portal vein invasion. Untreated patients with multinodular asymptomatic tumors without vascular invasion or extrahepatic spread have a median survival of approximately 16 months. Chemoembolization (TACE) improves their median survival to 19–20 months and is

considered standard therapy for these patients, who represent the majority of HCC patients, although ⁹⁰Yttrium therapy may provide similar results with less toxicity. Patients with advanced-stage disease, vascular invasion, or metastases have a median survival of around 6 months. Among this group, outcomes may vary according to their underlying liver disease. It is this group at which kinase inhibitors are directed. A number of new kinase inhibitors are being evaluated for HCC. These include the biologicals, such as Raf kinase and vascular endothelial growth factor (VEGF) inhibitors, and agents that target various steps of the cell growth pathway.⁽⁴¹⁾

2.6.1 Sorafenib

Sorafenib (Nexavar, BAY 43-9006) was approved for HCC in 2007 and it is the standard of care for patients with advanced-stage HCC (BCLC-C).⁽⁵³⁾ Sorafenib is the current standard of care for patients with advanced HCC who have preserved liver function. It is an oral multikinase inhibitor approved by the U.S. Food and Drug Administration for the treatment of patients with advanced renal cell carcinoma (RCC). Clinical trials have demonstrated the effectiveness and relative safety of sorafenib, and thus the drug is used in unresectable HCC.^(54, 55) In two randomized controlled phase III trials, sorafenib significantly extended survival compared with placebo.⁽¹¹⁾ Recommended daily dosing is 400 mg p.o. bid. Sorafenib is undergoing phase II/III clinical evaluation in a wide variety of other solid tumors, including melanoma and non-small cell lung cancer.

Sorafenib is an oral multikinase inhibitor with antiproliferative and antiangiogenic effects.⁽⁵⁵⁾ It has been shown to inhibit the activity of the serine/threonine kinases. Sorafenib inhibits Raf kinases, including Raf-1 and B-Raf, which are members of the Raf/ MEK/ERK signaling pathway.⁽⁵⁸⁾ It has been shown to block tumor cell proliferation and angiogenesis by inhibiting serine/threonine kinases (c-RAF, and mutant and wild-type BRAF) as well as the receptor tyrosine kinases vascular endothelial growth factor receptor 2 (VEGFR2), VEGFR3, platelet-derived growth factor receptor (PDGFR). However, sorafenib is a potent inhibitor of VEGFR and PDGFR, and these receptor tyrosine kinases are likely to be among its clinical targets.^(2, 56) Moreover, it

inhibits proliferation and induces apoptosis in various tumor cell lines. Cyclins and Cyclin-dependent kinases (Cdks), are associated with cellular proliferation and clinical outcome by sorafenib.⁽⁵⁷⁾ The intracellular signalling pathway Raf/MEK/ERK and the extracellular receptors VEGFR and PDGFR have been implicated in the pathogenesis of hepatocellular carcinoma.⁽⁵⁴⁾

However, many patients may develop acquired resistance to sorafenib, so their response to sorafenib is eventually lost. Sorafenib may induce autophagy, which leads to apoptosis.⁽¹⁰⁾ Patients treated with sorafenib should be monitored every 4–6 weeks for toxicities; patients should be educated about possible side effects before they start therapy. Skin reactions are among the most frequent, occurring in 20%–40% of patients, and including hand and foot reactions, dry skin, pruritus, rash or desquamation, alopecia, and psoriasiform eruptions (these are rarely severe enough to require dose reduction or temporary treatment withdrawal). Gastrointestinal toxicities occur among 20%–30% of patients with HCC who receive sorafenib, including severe diarrhea in 10% of patients. Other potential side effects include anorexia, stomatitis, nausea or vomiting, voice changes, fatigue, weight loss, and hypertension.⁽⁵³⁾ The most common toxicities include fatigue, hypertension, diarrhea, mucositis, and skin changes, such as the painful hand-foot syndrome, hair loss, and itching, each in 20–40% of patients. Several “look-alike” new agents that also target angiogenesis have either proved to be inferior or more toxic. These include sunitinib, brivanib, linifanib, everolimus, and bevacizumab.⁽⁴¹⁾

2.7 Induction of HCC

2.7.1 Carcinogenesis

The process of carcinogenesis may be divided into at least three stages: initiation, promotion, and progression. The first stage of carcinogenesis, initiation, results from an irreversible genetic alteration, most likely one or more simple mutations, transversions, transitions, and/or small deletions in DNA.⁽⁵⁸⁾ Carcinogenesis proceeds in three steps: initiation, promotion, and progression. Many efforts have been made to elucidate the factors related to each step and their effects on cells and tissues to enable the creation of a model system for use in the evaluation of carcinogens. An animal

model has been developed for this purpose because studies in human patients are very limited.

Nowadays many animal models have enabled study of the mechanism of cancer and the development of possible strategies for treatment including HCC treatment. Carcinogenesis is one of the mechanisms to elucidate the progression of cancer on animal models. Normally, carcinogenesis proceeds in three steps: initiation, promotion, and progression.⁽¹⁾ First, the stage of initiation, It has been studied in detail in few systems because of the inability to identify, isolate, and specifically characterize initiated cells.⁽⁵⁸⁾

Many chemical and physical carcinogens can induce one or more of a variety of mutations in cells when given chronically, such as occurs in many current carcinogenesis protocols.⁽⁵⁹⁾

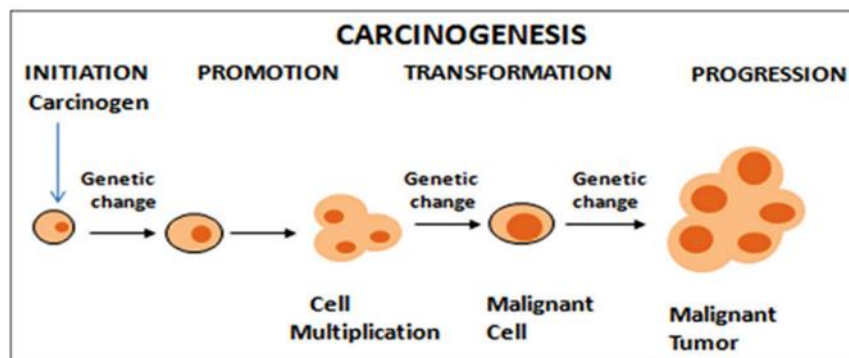


Figure 12 Different stages of carcinogenesis

Source: Kaur S, Singh G, Kaur K. (2014) Cancer stem cells: an insight and future perspective: J Cancer Res Ther. p. 849.

Liver carcinogenesis is a multistep process: the presence of specific risk factors promotes gene damage, which leads to a cascade of molecular and cellular deregulations that ultimately result in transformation of hepatocytes. Carcinogenesis may arise as a result of chemical or biological damage to normal cells in a multistep process that involves changes at the initiation level followed by promotion and

progression which lead to malignancy. The promotional stage of cancer is reversible stage and appears to be most appropriate target stage for chemopreventive intervention. Chemoprevention is one of the strategies by which we can revert or delay the response of carcinogen. Cancer chemopreventive agents are able to reduce the incidence of tumorigenesis by intervening in one or more stages of carcinogenesis initiation, promotion or prolongation.⁽⁶⁰⁾

Hepatocarcinogenesis (liver carcinogenesis) is the development of liver cancer due to the exposure of carcinogens, a chemical that produces cancer. Various hepatocarcinogens, including aflatoxins, acetylaminofluorene, diethylnitrosamine, have been used to develop hepatocarcinogenesis in animals successfully. From many experiments, either different carcinogens and animal species could develop hepatocarcinogenesis. Many genetic and epigenetic alter chromosomal deletions, rearrangements, aneuploidy, gene amplification, genetic mutations, DNA adducts formation, DNA strand-break, DNA methylation modulation, and modulate cell signaling pathways. Carcinogen exposure causes a direct or indirect effect, which leads to the tumor transformation of liver cells in experimental animals. The hepatocarcinogenesis is a multistage process, initiated by an early feature of morphologically and genetically changed hepatic focal lesions, also called preneoplastic lesions. Originally monoclonal groups of liver cells develop primarily due to carcinogenic insult. These aberrant monoclonal groups of regenerative liver cells (focal lesions) develop hyperplastic nodules to dysplastic nodules, leading to HCC.⁽⁶¹⁾

The first step of hepatocarcinogenesis is initiation. Initiation step initially from the liver cells is exposed carcinogens or genotoxic agents such as aflatoxins, 2-acetylaminofluorene, diethylnitrosamine, ionizing radiation, which alters DNA sequence and DNA mutations in the liver cells then develop and transform normal cells into cancer cells. The mutations frequently activate proto-oncogenes and/or inactivate tumor suppressor genes to develop HCC in the carcinogenic mechanism. The chemicals or carcinogens that cause the initiation process are called "initiators." This process is an irreversible process for a small population of cells. Generally, Genotoxic agents

produce the electrophilic moieties that bind with DNA to form DNA adduct, hamper cellular DNA repair mechanism, and develop permanent DNA lesions. Hence, the normal cell becomes an initiated cell. The initiated cells can develop focal lesions, which can act as an origin site for the subsequent development of malignant neoplasia.

After the initiation step is promotion, in this step, the initiated cells are incapable of growing autonomously. However, they get the potential to promote proliferation by maintaining alterations in gene and protein expressions. Upon exposure to an environment where initiated cells are at higher risk, further genetic alterations begin, making some reversible changes in the initiated cell populations. If promoting agents such as phenobarbital, dietary fat, ethanol, estrogens, even some partial hepatectomy or diseased liver (from virus infection or cirrhosis) are repeated or long term exposure to the cell, the initiated cells will induce the focal proliferations.

Progression is the last step of hepatocarcinogenesis. The focal lesions from the promotion process further promotion for more genetic and enzymatic changes in the constituted liver cells, forming enzyme-altered foci. A lesion may form from a single or by merging numerous lesions and maybe big enough to create a macroscopic structure (hepatic or liver nodule) in the liver. They sometimes look grey or whitish gray or greenish (because of the presence of bile in them). Finally, by a gradual process through many biochemical and genetic alterations, those altered hepatic foci or hepatic nodules progress more malignant cellular characteristics. They are transformed into neoplasia without any additional external stimulus or intervention..^(61, 62)

Oxidative stress is associated with damage to a wide range of macromolecular species including lipids, proteins, and nucleic acids thereby producing major interrelated derangements of cellular metabolism including peroxidation of lipids. Free radicals and nonradicals oxidizing species were produced in animals treated with carcinogens, and also in human tissues. Reactive oxygen species (ROS) is formed from endogenous or exogenous sources are highly reactive, toxic, and mutagenic. Lipid peroxidation plays an important role in carcinogenesis is the most studied biologically relevant free radical chain reaction and measured as malonaldehyde (MDA).⁽⁶⁰⁾

Antioxidants possess a variety of biological activities, including the induction of drug-metabolizing enzymes, inhibition of prostaglandin synthesis, inhibition of carcinogen-induced mutagenesis, and scavenging of free radicals. Antioxidants may protect membrane from ROS toxicity by prevention of ROS formation by the interruption of ROS attack, by facilitating the repair caused by ROS and by providing cofactors for the effective functioning of other antioxidants. Development of life threatening diseases like cancer is linked to the availability of these antioxidants.⁽⁶³⁾ Oxidative stress is important in the development and progression of liver disease and the use of antioxidants is an established treatment modality in this condition. Oxidative stress has been implicated in the pathogenesis of hepatic encephalopathy.⁽⁶³⁾

2.7.2 Chemically induced models

Causative agents for HCC have been studied along two general lines. First are agents identified as carcinogenic in experimental animals (particularly rodents) that are thought to be present in the human environment. Second is the association of HCC with various other clinical conditions. Probably the best-studied and most potent ubiquitous natural chemical carcinogen is a product of the *Aspergillus* fungus, called aflatoxin B₁. This mold and aflatoxin product can be found in a variety of stored grains in hot, humid places, where peanuts and rice are stored in unrefrigerated conditions. Aflatoxin contamination of foodstuffs correlates well with incidence rates in Africa and to some extent in China. In endemic areas of China, even farm animals such as ducks have HCC. The most potent carcinogens appear to be natural products of plants, fungi, and bacteria, such as bush trees containing pyrrolizidine alkaloids as well as tannic acid and safrole. Pollutants such as pesticides and insecticides are known rodent carcinogens.⁽⁴¹⁾

Several chemical reagents induce tumor formation when administered in sufficient high doses and time span. There are two types of carcinogenic compounds: (i) genotoxic compounds which are characterized by their capacity to induce structural DNA changes and (ii) promoting compounds which lack direct genotoxic capability, but enhance tumour formation after initiation by a hepatotoxic compound.⁽⁶⁴⁾ Treatment with

a tumor-promoting agent facilitates the clonal expansion of the preneoplastic cells. Toxic industrial chemicals, air and water pollutants, food additives and fungal toxins are major sources of hepatocarcinogenesis. Although these agents have been suspected, the molecular pathogenesis of HCC remains unclear.

2.7.2.1 Dinitrosodiethylamine (DEN)

Diethylnitrosamine (DEN) is a representative chemical carcinogen with the potential to cause tumors. Specifically in HCC, DEN is a complete carcinogen. At subcarcinogenic doses it induces only the initiation of carcinogenesis, and hepatic fibrosis is induced at 10mg/kg of body weight ; however, at doses above 25–30mg/kg of body weight, DEN leads to the next steps in carcinogenesis, promotion and progression.⁽¹⁾ As an established environmental hepatocarcinogen, diethylnitrosamine (N-nitrosodiethylamine; DEN), which produces primary metabolic activation resulting in initiation of liver carcinogenesis and formation of liver tumors after repeated administration, is normally used to induce liver cancer in several animal models. DEN-induced hepatocarcinoma in animals serves as a standard model to study the beneficial effects of many drugs and treatments on HCC. Prior studies have shown the histopathological similarities of human HCC and chemical-induced experimental liver tumors in Wistar rats and Syrian golden hamsters^(68,69) DEN is a hepatocarcinogen known to cause DNA ethylation and mutagenesis. It is commonly used to induce liver cancer in animal models, and in rodents, it induces tumors that closely mimic a subclass of human hepatocellular carcinoma (HCC).^(65, 66)

DEN is found in a wide variety of foods such as cheese, soybeans, smoked, salted and dried fish, cured meat, alcoholic beverages as well as in ground water having a high level of nitrates. In rats, DEN is a potent hepatocarcinogen influencing the initiation stage of carcinogenesis during a period of enhanced cell proliferation accompanied by hepatocellular necrosis and induces DNA carcinogen adducts, DNA-strand breaks and in turn hepatocellular carcinomas without cirrhosis

through the development of putative pre-neoplastic focal lesions.⁽⁶⁷⁾ DEN has been shown to generate free radicals, an uncompromising free radical generation in the liver overwhelms the antioxidant status and ultimately proceeds to oxidative stress paving way to carcinogenesis.⁽⁶⁰⁾ It is a widely occurring nitrosamine that is one of the most important environmental carcinogens and hepatotoxin. These compounds are considered to be effective health hazards to human beings because N-nitrosamines have widespread industrial uses and readily form DNA adducts. DEN is normally used as a carcinogen to induce liver cancer in animal models, especially in rats.⁽⁶⁸⁾ DEN is carcinogenic in at least 17 species. While the exact mechanisms of action of chemical carcinogens remain to be elucidated, investigations have implicated as a possible precursor to cancer induction the metabolic conversion of these compounds to electrophiles which covalently bind to cellular macromolecules, including DNA.^(65, 69) Moreover, oxidative stress caused by DEN can contribute to hepatocarcinogenesis.⁽⁷⁰⁾ Reactive oxygen species (ROS) generated by the P450-dependent enzymatic system might induce oxidative stress by the formation of hydrogen peroxide and superoxide anions. Production of ROS is known to cause DNA, protein and lipid damage; therefore, oxidative stress can play an important role in carcinogenesis.⁽⁷¹⁾

Furthermore, it was found that the chemical carcinogen diethylnitrosamine (DEN) leads to the initiation of hepatocytes or to the death of hepatocytes through both necrosis and apoptosis. In the case of a deficiency in IKK- β (inhibitor-of-nuclear-factor- κ B (NF- κ B) kinase- β), necrotic cell death of DEN-exposed hepatocytes is augmented by increased accumulation of reactive oxygen species and sustained activation of JUN amino-terminal kinase (JNK). This leads to the release of as-yet-unknown cellular constituents — possibly HMGB1 (high-mobility group box 1 protein), S100 calcium-binding proteins, heat-shock proteins or purine metabolites — that activate IKK- β and NF- κ B in adjacent Kupffer cells. Activated Kupffer cells then release pro-inflammatory cytokines, such as tumour-necrosis factor (TNF) and

interleukin-6 (IL-6), and stimulate the production of hepatocyte growth factor by stellate cells, which together stimulate the proliferation of surviving, mutated hepatocytes.⁽⁶⁹⁾

2.7.2.2 Thioacetamide (TAA)

The acute liver injury induced by a necrogenic dose of thioacetamide (TAA), a potent hepatotoxic agent, is characterized by a severe perivenous necrosis. Numerous investigators use TAA to study mechanisms of hepatic necrosis because of its relatively short half-life, well known ability to cause acute toxicity, and a large window of time between its necrogenic effects and liver failure.⁽⁷²⁾ The reactive metabolites responsible for TAA hepatotoxicity are the radicals derived from thioacetamide-S-oxide and the reactive oxygen species derived as subproducts in the process of microsomal TAA oxidation which can deplete reduced glutathione leading to oxidative stress.⁽⁴⁸⁾

Thioacetamide has been used in many studies to explore different aspects of liver cirrhosis and its possible reversibility. Interest of thioacetamide was first shown in 1943 when this substance, used on oranges as an antifungicide, was found to be a contaminant in orange juice and thus a danger to public health.⁽⁷³⁾ The hepatotoxicity of TAA has been known since 1948. In rats, single doses cause centrilobular necrosis accompanied by increases in plasma transaminases and bilirubin. To elicit these effects, TA requires oxidative bioactivation, to elicit its toxicity leading first to its S-oxide (TASO) and then to its chemically reactive S,S-dioxide (TASO₂), which ultimately modifies amine-lipids and proteins.⁽⁷⁴⁾ TAA, a model hepatotoxicant, has been shown to require metabolic activation to initiate hepatocellular necrosis. It is S-oxidized to thioacetamide sulfoxide (TASO) and further to thioacetamide-S,S-dioxide (TASO₂) via hepatic CYP2E1. The obligate reactive metabolite of TAA, presumably TASO₂, covalently binds to proteins with the formation of acetylimidolysine derivatives that are responsible for TAA-induced hepatotoxic effects.⁽⁷⁵⁾ Biotransformation of chemical toxicants and carcinogens is mediated by cellular enzymes including the cytochromes P450 (CYP) system. CYP is a heme

containing enzyme that catalyzes the oxidation of a wide variety of endogenous and exogenous compounds including drugs, carcinogens and other xenobiotic chemicals. Earlier experiments revealed that treatment of mice and rats with thioacetamide (TAA) induced liver cell damage, fibrosis and/ or cirrhosis, associated with increase of oxidative stress and activation of hepatic stellate cells. TAA is generally thought to be bioactivated by CYP and/or flavin-containing monooxygenase (FMO) systems to sulfine (sulfoxide) and sulfene (sulfone) metabolites. Phenobarbital pretreatment potentiated TAA toxicity, parallel to the induction of CYP and FMO. These results suggested that induction of CYP and/or FMO may be a primary mechanism of increased bioactivation-based liver injury of TAA.⁽⁷⁶⁾

Liver injury begins with bioactivation of TAA to thioacetamide sulfoxide (TASO) (step I) and further to thioacetamide-S,S-dioxide. These (TASO₂) (step II) (figure 13). Thioacetamide-S,S-dioxide, an unstable, reactive metabolite, is thought to initiate necrosis by covalently binding to liver macromolecules. The advantages of using TAA as a model hepatotoxicant include high specificity for liver as a target organ. When a lethal dose is administered to rats, death occurs 3.5 to 7 days after administration due to fulminant hepatic failure. This allows the luxury of a long window of time for studying the incline and decline slopes of injury and recovery by conducting time course studies after administration of low to moderate doses. CYP2E1 metabolizes a large number of low-molecular-weight compounds, many of which are industrial solvents, chemical additives, halogenated anesthetics, and drugs. Most importantly, CYP2E1 activates many xenobiotics to hepatotoxic or carcinogenic products. Also, a wide variety of CYP2E1 substrates are known to exhibit saturation kinetics.⁽⁷²⁾ TAA and its initial metabolite elicit a variety of hepatotoxic responses in rats depending on the dose and duration of administration.^(73, 77) Accordingly, it has been reported that the hepatotoxic effects of thioacetamide are only expressed after metabolic conversion to thioacetamide

S-oxide that undergoes further metabolic conversion to an as yet unidentified metabolite, probably the reactive unstable thioacetamide sulfone.⁽⁷⁸⁾

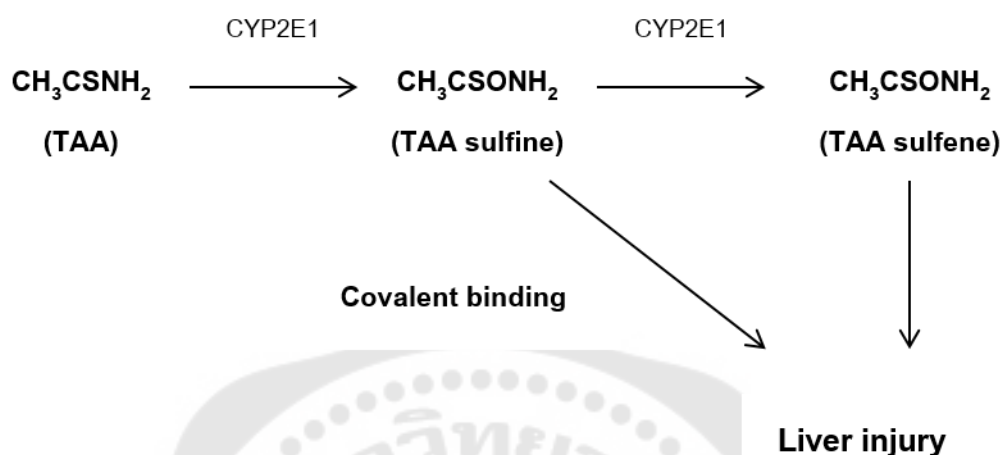


Figure 13 Mechanism-based liver injury of thioacetamide

Source: Ramaiah SK, Apte U, Mehendale HM. (2001) Cytochrome P4502E1 induction increases thioacetamide liver injury in diet-restricted rats: Drug Metab Dispos. p. 1089.

2.8. Molecular pathogenesis of HCC

Pathological analysis of HCC is based on macroscopic and microscopic aspects that are highly diversified and associated with prognosis for some of them. At last, pathogenesis of HCC is very complex, involving different molecular pathways that may reflect both underlying etiologies and biological tumor behavior.⁽⁵³⁾

2.8.1 PI3K/AKT/MTOR pathway

The phosphatidylinositol-3 kinase (PI3K) pathway plays an important role in the proliferation and survival of cancer cells in various solid tumors, including HCC.⁽³⁾ Constitutive activation of the PI3K/AKT/mTOR signaling pathway has been firmly established as a major determinant of tumor cell growth and survival in a multitude of solid tumors.⁽⁵⁵⁾ The PI3K/AKT/mTOR signaling pathway can be overactivated by enhanced stimulation of receptor tyrosine kinases, particularly the IGF receptor and EGFR. It was found that HCC and human cirrhotic liver were upregulated both of IGF

and IGF receptor expression⁽⁷⁹⁾, resulting in stimulation of the PI3K/AKT/ mTOR signaling pathway. Similarly, EGF and related growth factors are commonly overexpressed in HCC.⁽²⁾

In the PI3K/AKT/mTOR signaling pathway, binding of growth factors (most notably IGF and EGF) to their receptors activates PI3K. PI3K subsequently produces the lipid second messenger PIP3b (phosphoinositoltriphosphate), which in turn activates the serine/threonine kinase AKT. PI3K activates AKT, which is a lipid second messenger. Since Akt is involved in a number of biological processes, such as cell survival, cell growth, apoptosis and differentiation, its deregulation has been implicated in many human cancers. Subsequently, AKT phosphorylates various intracellular proteins, including mTOR⁽²⁾, activated AKT also phosphorylates several cytoplasmic proteins, most notably mTOR and BCL-2-associated death promoter. The mTOR activation increases proliferation of cell, and BAD inactivation decreases apoptosis and increases survival of cell.⁽⁸⁰⁾ Therefore, the activation of mTOR and BAD inactivation are important for cancer cells to survive by regulating apoptosis.

The PI3K pathway is regulated by phosphatase and tensin homolog deleted on chromosome 10 (PTEN) negatively and the expression of PTEN is suppressed in half of HCC cells clinically.⁽³⁾ In normal tissue, this pathway is negatively regulated by the phosphatase and tumor suppressor phosphatase on chromosome 10 (phosphatase and tensin homolog (PTEN)), which targets the lipid products of PI3K for dephosphorylation. AKT phosphorylation has been implicated in early HCC recurrence and poor prognosis, and a recent microarray study found that 23% of HCC patients had elevated levels of AKT phosphorylation on Ser473. Aberrant mTOR signaling was observed with activation of either the IGF and/or EGF cascade. mTOR blockade with everolimus slowed tumor growth and increased survival in the HCC xenograft model, an effect that was enhanced in vivo with EGFR/VEGFR blockade. These results add considerably to the body of research suggesting that mTOR pathway activation has a crucial role in the pathogenesis of HCC.

Taken together, these data suggest that the PI3K/AKT/mTOR pathway has a critical role in the pathogenesis of HCC. Indeed, levels of the phosphorylated form of mTOR have been shown to be elevated in 15% of cases of HCC, and levels of total p70 S6 kinase (the immediate substrate for phosphorylated mTOR) have been shown to be increased in 45% of cases.⁽²⁾

2.8.2 RAS/RAF/MEK/ERK pathway

Preclinical studies demonstrated that Raf/ MAPK-ERK kinase (MEK)/extracellular signal regulated kinase (ERK) pathway has a role in HCC.⁽⁸¹⁾ Tyrosine kinase type receptors, such as VEGFR, PDGFR, EGFR, FGFR, and IGFR, activate intracellular RAS in the RAF/MEK/ERK pathway. Subsequently, AP-1 family members such as c-JUN and c-FOS activate expression of various genes that induce cell proliferation and vasculogenesis. The activation of the RAF/MEK/ERK pathway is related to the disease progression of HCC and HBV-related HCC development. Furthermore, HCV core protein activates RAF and is considered to play a role in the development of HCC. RAS and RAF play important roles in which intracellular signals activate expression of various genes. RAS activates RAF, which induces activation of MEK. MEK activates ERK and its phosphorylation. ERK regulates more than one hundred intracellular substrates directly and gene expression indirectly as cell kinase to activate transcription factors and cell cycle regulators. Activation of ERK is closely related to cancer cell proliferation and, thus, inhibition of ERK could have an anticancer effect.⁽³⁾

The MAP kinase pathway has been known the most extensive characterization in the process of HCC development. The growth factor that binds to tyrosine kinase receptor resulting in receptor phosphorylation, leading to a molecular complex formation with an adaptor protein growth factor receptor bound-2 (Grb2), Grb-2 associated binder 1 and signal relay protein SH-2 domain-containing tyrosine phosphatase- 2 which localized in the plasma membrane. An exchange factor, Son-of-sevenless (SOS), is also joining the complex. The complex then activates Ras while

exchange GDP to GTP in the ras/raf/MEK/ERK/MAP kinase pathway. Ras/Raf/MEK/ERK/MAP kinase pathway is identified to involve in cell proliferation, differentiation, angiogenesis, and cell survival. The components of this pathway activation have been reported to contribute to tumorigenesis, including HCC. The GTPase (Guanine nucleotides triphosphate)-Ras and the serine/threonine kinase Raf (signaling regulators) control the signaling process immediately by activating Raf. Thus, Raf phosphorylates the mitogen/extracellular protein kinase kinases, MEK-1, and MEK-2. After that, MEK proteins then phosphorylate the downstream extracellular signal-regulated kinase (ERK) signaling molecules, ERK-1 and ERK-2. GTPase-Ras is a switch protein that alternates between an active on a state with a bound GTP and an inactive off state with a bound GDP. ERK-1 and ERK-2 activation regulate several target proteins and gene regulatory proteins in the cytoplasm and nucleus. It was found that Ras protein is involved in other signaling pathways such as phosphoinositol-3-kinase/Akt pathway, Phospholipase C/protein kinase C pathway..

In HCC, the RAF/MEK/ERK pathway is constitutively activated, suggesting a possible role for this pathway in tumorigenesis. Hwang et al. (2004) reported overexpression of CRAF in 100% of 30 HCC tissue specimens tested, and concluded that CRAF activation may have an important role in HCC. Furthermore, after immunohistochemical evaluation of tissue samples, there was an approximately sevenfold increase in MEK1/2 phosphorylation in HCC tissues, compared with that in adjacent benign liver tissues.⁽²⁾

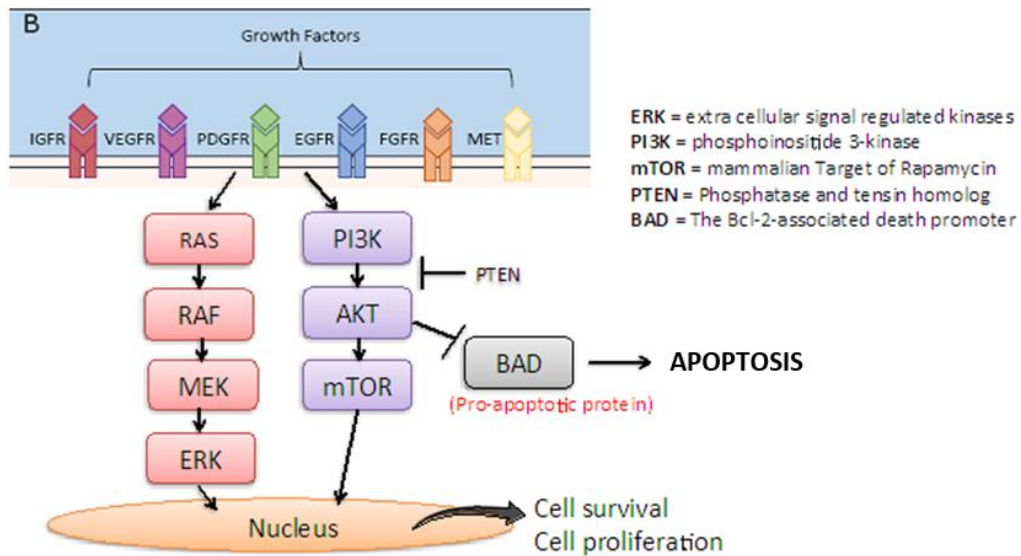


Figure 14 The RAF/MEK/ERK and the PI3K/AKT/mTOR signaling pathways

Proangiogenic and proliferative growth factors activate the RAF/MEK/ERK pathway. The small GTPase RAS and the serine/threonine kinase RAF are the key molecular signal regulators. Intermediate signaling is regulated by MEK, which is responsible for phosphorylating and activating the final downstream signaling ERK molecules. ERK regulates cellular activity, indirect inducers of gene expression, and transcription factors in the AP-1 family such as c-JUN and c-FOS and cell cycle-related kinases. Binding of these growth factors to their receptors also activates PI3K, which subsequently produces the lipid second messenger, and in turn activates serine/threonine kinase AKT. Activated AKT also phosphorylates several cytoplasmic proteins, most notably mTOR. The activation of mTOR increases cellular proliferation, and inactivation of BAD decreases apoptosis and increases cell survival. This pathway is negatively regulated by the phosphatase and tensin homolog deleted on chromosome 10 (PTEN), which targets the lipid products of PI3K for dephosphorylation. (Adapted from Meguro M. et al., 2011)⁽³⁾

Source: Meguro M, Mizuguchi T, Kawamoto M, Hirata K. (2011) The molecular pathogenesis and clinical implications of hepatocellular carcinoma: *Int J Hepatol.* p. 3

2.8.3 Wnt/Beta-catenin pathway

This developmental pathway is commonly known for its fundamental role in embryogenesis, which aids the cell in differentiation, proliferation and apoptosis. In the absence of Wnt signaling, cytoplasmic b-catenin complexes with the tumor suppressors: adenomatous polyposis coli (APC) and Axin1, as well as the glycogen synthase kinase-3b (GSK-3b). In this complex, GSK-3b phosphorylates b-catenin, targeting it for ubiquitination and subsequent degradation. In the event that Wnt signaling receptors are engaged, conformational changes in the Axin complex cause the release of beta-catenin, which then localizes to the nucleus and activates the transcription of Myc, cyclin D1 and COX2 amongst others. In HCC, a number of other transcriptomic and proteomic studies have indicated an increase in Wnt signaling, possibly as a result of an accumulation of Axin1 mutations at sites that bind b-catenin and/or CTNNB1 mutations along sites marked for phosphorylation by GSK-3b. It is hypothesized that an increase in signaling from the Wnt pathway is necessary to maintain “stemness” in HCC, characterized by cell proliferation and immortality.⁽⁸²⁾

A major and early carcinogenic event in the development of HCC seems to be the abnormal regulation of the transcription factor beta-catenin, a key component of the WNT signaling pathway. In the absence of WNT stimulation, a destruction complex containing the proteins adenomatous polyposis coli (APC), glycogen synthase kinase 3 β (GSK3 β) and AXIN phosphorylates and targets CTNNB1 for ubiquitylation (Ub) and proteasomal degradation. In the normal state, the binding of members of a family of soluble cysteine-rich glycoprotein ligands, the WNTs, to members of the Frizzled family of cell-surface receptors results in the activation of the WNT signaling pathway. Receptor binding activates DSH (downstream effector Dishevelled), which consequently prevents phosphorylation of beta-catenin by GSK3 β and its subsequent ubiquitination and proteasomal degradation. Activated DVL inhibits the destruction complex, resulting in the accumulation of CTNNB1, which then enters the nucleus where it can act as a co-activator for TCF/LEF-mediated transcription. An ensuing increase in the cytoplasmic concentrations of beta-catenin results in its translocation from the

cytoplasm to the nucleus. Once in the nucleus, b-catenin acts as a co-activator to stimulate the transcription of genes and expression of gene products involved in cell proliferation (for example, MYC, MYB, CJUN and CYCD1), angiogenesis, anti-apoptosis and the formation of extracellular matrix. This accumulation of beta-catenin provides a growth advantage to tumor cells by promoting proliferation and suppressing differentiation. Studies with b-catenin transgenic mouse models indicate that abnormal WNT signaling can cause severe hepatomegaly, but is not sufficient for carcinogenic transformation.^(2, 4, 83)

2.8.4 Angiogenesis

A specific pathological feature of HCC is high vascularity of the tumor. It is necessary to increase vascularity for cancer cell proliferation. VEGF, PDGF, EGF, FGF, and IGF, growth factors that facilitate high vascularity and cancer cell proliferation, are expressed not only in cancer cells but also in other surrounding cells. The high expression of the growth factors is also associated with tumor invasion and portal thrombosis.⁽³⁾

The liver is a highly vascular organ that depends on effective angiogenesis for cellular regeneration. Similarly, tumor growth, vascular invasion (the hallmark of invasive disease) and metastasis are also critically dependent on efficient angiogenesis. In HCC, angiogenesis relies on autocrine and paracrine interactions between tumor cells, vascular endothelial cells and pericytes. During the angiogenic process, the existing microvasculature is destabilized, leading to vascular hyperpermeability, remodeling of the cellular matrix and activation of endothelial cells. Once activated, endothelial cells proliferate, migrate and undergo cord formation to form new microvessels. Finally, pericytes are activated and recruited to stabilize the new blood vessels.

Normal angiogenesis is maintained by the balance between proangiogenic and antiangiogenic factors. The angiogenic balance is disturbed in HCC as tumor cells, endothelial cells and pericytes secrete a net excess of angiogenic factors, which support the recruitment and activation of endothelial cells and pericytes.

A number of angiogenic growth factors, including VEGF-A, angiopoietin-2 and PDGF, have been shown to be upregulated in HCC tumors at the level of gene expression and at the plasma protein level in patients with HCC compared with cirrhotic patients. The principal angiogenic factors involved are VEGFs, PDGFs, placental growth factors, transforming growth factor (TGF)- α and - β , basic fibroblast growth factor, EGF, HGF, angiopoietins and interleukin-4 and -8. These growth factors and cytokines induce angiogenic signaling through a variety of mechanisms, including activation of the RAF/MEK/ERK, PI3K/AKT/mTOR and Janus kinase (JAK)/signal transducer and activator of transcription pathways.⁽²⁾ Tumor angiogenesis performs a critical role in tumor progression through which the tumor establishes an independent blood supply, consequently facilitating tumor growth and favoring the transition from hyperplasia to neoplasia. Researchers have found out that VEGF seems to be the most potent and predominant angiogenic cellular factor sustaining tumor growth.^(2, 82)

2.8.5 Apoptotic pathway

Apoptosis is one of the mechanisms leading to cell death when cells have sustained damage to their DNA or cytoskeleton. Evasion of this mechanism is one of the hallmarks of cancer.⁽¹²⁾ Several of the genetic alterations observed in HCC lead to an imbalance in the pro- and anti-apoptotic members of the Bcl-2 family is mentioned. The overexpression of Bcl-XL is in a high percentage of HCC. In contradiction, the downregulation of pro-apoptotic members of the family, for example, Bax or Bcl-XS in HCC was found with dysfunction in the p53 pathway. Moreover, the report indicated that some pro-apoptotic members of the BH-3-only family, for example, Bid, is down expression in HCC related to hepatitis B or C virus infection. A recent report has exhibited that X-linked inhibitor-of-apoptosis protein (XIAP), a well-known inhibitor of caspases were high express in approximately 90% of clinical tumors from advanced HCC patients. In vitro studies, in HCC cell lines with different metastatic capabilities, showed a correlation of metastasis with resistance to apoptosis and up-regulation of XIAP. It also had been proposed that XIAP might function as a cofactor in TGF- β signaling. Therefore, XIAP overexpression might present resistance to the apoptotic

effects of TGF- β , providing HCC cells to respond to this cytokine in terms of migration and invasion.^(84, 85)

The mechanisms of apoptosis are highly complex. To date, research indicates that there are two main apoptotic pathways: the extrinsic or death receptor pathway and the intrinsic or mitochondrial pathway. However, there is now evidence that the two pathways are linked and that molecules in one pathway can influence the other.⁽⁸⁶⁾ Both of these pathways lead to caspase activation and cleavage of specific cellular substrates. The receptor-triggered-apoptosis pathway includes ligands and their receptors such as FAS, TNF, TRAIL, and downstream molecules, such as caspases and BCL2 family members. The mitochondria-apoptosome-mediated pathway includes apoptotic stimuli induced by radiation therapy and chemotherapy, mitochondria, apoptosome, and key effector caspases. Caspases are activated in a cascade-like fashion. Initiator or upstream caspases (caspases 8, 9, and 10) can activate effectors or downstream caspases, including caspases 3, 6, and 7, which leads to induction of apoptosis. Crosstalk also exists between the two apoptotic pathways. For example, FAS is linked to the mitochondria-apoptosome-mediated pathway that is mediated through the activation of caspase 8 to cleave the BID protein resulting in the release of cytochrome c from mitochondria. The inhibitors of apoptosis proteins, including XIAP, cIAPs, the PI3K/AKT/NF- κ B pathway, and heat shock proteins (HSPs), can interact with the caspases and cause inhibition of apoptosis.⁽⁸⁷⁾

Apoptosis is characterized by a series of typical morphological features, such as shrinkage of the cell, fragmentation into membrane-bound apoptotic bodies and rapid phagocytosis by neighbouring cells. This paper reviews the current knowledge on the molecular mechanisms of apoptosis as they relate to the morphologic hallmarks and their implications for the detection of apoptosis in cardiac tissue. Activation of cysteine proteases called caspases plays a major role in the execution of apoptosis. These proteases selectively cleave vital cellular substrates, which results in apoptotic morphology and internucleosomal fragmentation of DNA by selectively activated Dnases. In response to several pro-apoptotic signals, mitochondria release

caspase activating factors, that initiate an escalating caspase cascade and commit the cell to die.⁽⁸⁸⁾ An imbalance of pro-apoptotic and anti-apoptotic proteins expression was showed in HCC cells, which favors cell survival.⁽⁸⁵⁾

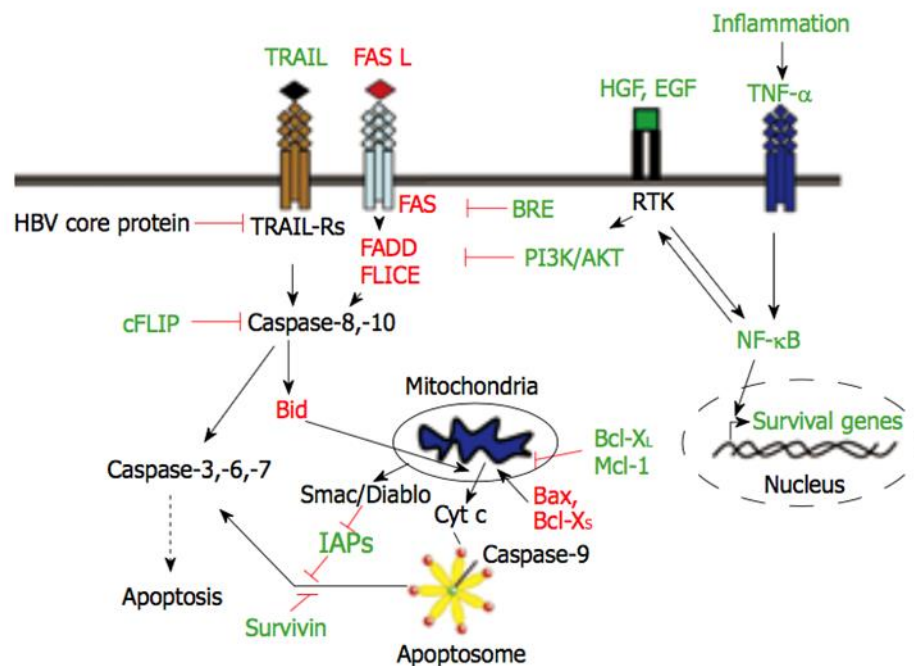


Figure 15 The Alterations in the expression or functions of death receptor pathways and apoptosis regulatory proteins in HCC cells

In red, proteins either down-regulated or inactivated; in green, proteins either up-regulated or overactivated.

Source: Fabregat I. (2009) Dysregulation of apoptosis in hepatocellular carcinoma cells. *World J Gastroenterol.* p. 516.

2.9. Proteomics study in HCC

In spite of the relatively well-established etiological study in HCC risks, the molecular mechanisms underlying the hepatocarcinogenesis remain to be unequivocally defined. As such, identification of tumor-associated biomarkers will provide new insight

into the mechanism of tumor progression as well as molecular targets for early intervention in human liver cancer. To this end, several groups have recently employed the proteomic profiling approaches with attempts to unveil the differential expression patterns between HCC and adjacent non-tumor liver tissues.⁽⁹⁾

There has been ongoing development in treatment for HCC, an effective marker for diagnose or treatment for HCC is yet to be found. Presently, factors such as transforming growth factor, and p53 are known to have important roles in hepatocarcinogenesis. However, these genetic changes do not precisely reflect the biological nature of cancer cells or the clinical characteristics of individual HCC patients. Hence, expression profile analysis of a large number of genes in clinical HCC tissue samples is an essential step in understanding the mechanisms of hepatocarcinogenesis and in discovering diagnostic markers and therapeutic targets for HCC.⁽²⁰⁾ Although many tumor markers have been discovered and investigated experimentally, there is little consensus on their clinical use. Better methods for discovering sensitive and specific markers are needed.⁽⁸⁹⁾

Over the past few years, the concept of the 'Proteome' has been formulated. The term 'proteome' was designated to describe an organism's entire protein complement based on the idea of screening and determining all the proteins produced by the DNA of an organism rather than sequencing its genes. It was later defined as the entire protein complement expressed by a genome or by a cell or tissue type.⁽⁸⁹⁾ Proteomics combines high-resolution separation techniques applied to complex protein mixtures with identification methods such as mass spectrometry (MS).⁽⁹⁰⁾ Proteomics refers to the study of the proteome, which is the total protein complement of a genome. It is presently considered to be the key technology in the global analysis of protein expression and in the understanding of gene function. The application of proteomics has been the most established in the clinical and biomedical fields. For example, in the study of human diseases, disease specific/associated proteins can be identified by comparing the protein profiles of normal versus diseased tissues or biological fluids. Since these proteins are potential diagnostic tools or leads for the development of

drugs, proteomics has great potential in the drug discovery process.⁽⁹¹⁾ Besides studying the proteins involved in carcinogenesis, it is also applicable to the discovery of serological tumor markers for clinical uses, such as for hepatocellular carcinoma.⁽⁸⁹⁾

Expression of genes and proteins are not always uniform. Moreover, recent studies have demonstrated that mRNA and protein expression do not always correlate.⁽⁷⁾ Therefore, recently many studies of proteome were reported for understanding of mechanism of diseases by proteomics technique. For example, the study showed that insulin growth factor II, a disintegrin and metalloproteases, signal transducers and activators of transcription 3, suppressors of cytokine signaling 3, and cyclin D1 were significantly upregulated and collagen 1, SMAD 4, fragile histidine triad, and suppressors of cytokine signaling 1 were downregulated in HCC by protein microarrays. Moreover, proteomic analysis has been applied to human HCC cell lines and HCC tissues. Those studies were performed with 2-DE and MALDI-MS analysis. One of the limitation of the studies was the inclusion of patients with various causes of liver disease (hepatitis C or B, alcohol consumption), who also presented different degrees of severity of the underlying liver disease, leading to the study of a heterogeneous population.⁽⁷⁾

Tools such as 2-dimensional polyacrylamide gel electrophoresis (2-DE) and matrix associated laser desorption/ionization time-of-flight (MALDI-TOF) mass spectrometry (MS), enable the study of cancer proteomics. The value of this technique for detecting novel cancer-related proteins and for classifying human cancer (e.g., breast cancer, colon cancer, lung cancer, etc.) has been exhibited by several studies. Using this technology, the change in protein expression levels in tissue samples from HCC patients can also be demonstrated.⁽²⁰⁾ MALDI-TOF mass spectrometry (MALDI-TOF MS) is renowned for its easy operation and requirement of inexpensive matrixes for preparation of a sample. However, the instrumentation is more important which is fully automated and thus it can provide the screening of a large set of samples in a short period of time of analysis due to advanced laser technology and hardware.⁽⁹²⁾

3. *Dioscorea membranacea* (DM)

Selective interviews of traditional doctors of Southern Thailand found that they used Hua-Khao-Yen as one of the ingredients in 18 out of 30 formulae of drugs for cancer listed. They further found that Thai traditional doctors used five species of Hua-Khao-Yen, including *Dioscorea birmanica*, *Smilax corbularia*, *Smilax glabra*, *Pygmaepremna herbacea* and *Dioscorea membranacea*, to treat cancers, AIDS, septicemia and lymphatic diseases.⁽⁹³⁾ Among the five species, *Dioscorea membranacea* Pierre, called Hua-Khao-Yen-Tai, showed the highest cytotoxic activity against a human breast cancer cell line, but was less active for normal cells.⁽⁹⁴⁾ These preparations have been used to treat dermatopathy, lymphopathy, leprosy, venereal diseases, inflammations, bacterial infections as well as inflammatory conditions associated with diseases such as rheumatism, infectious diseases and other pain-causing condition in Thai traditional medicine. In the current study the liver cancer cell line HepG2 showed cytotoxicity to compounds isolated from *D. membranacea* extract with an $IC_{50} = 18.5 \pm 2.0 \mu\text{g/ml}$.⁽¹⁴⁾ Besides the extract also showed less toxicity to normal cells.⁽¹⁷⁾ The extracts are usually prepared with boiling water or soaking with ethanol.^(95, 96) Plant materials were dried at 50 °C, powdered and extracted by methods corresponding to those practiced by Thai traditional doctors. For the ethanolic extracts, dried ground plant material (100 g) was percolated with 95% ethanol, then concentrated to dryness under reduced pressure.⁽¹⁵⁾

3.1 General description of *Dioscorea membranacea*

Dioscorea membranacea Pierre (Dioscoreaceae), its Thai vernacular names are Phak Lum Phua, Phak Khanong Ma, Khao-Yen-Tai and Khrua That. It is distributed from Thai westwards to north Myanmar and eastwards into Cambodia; southwards passing beyond the Isthmus of Kra into Malaysia, it grows on limestone at its southern limit. Its rhizome is edible and medicinally used for long time by local people to treat cancer.

Descriptive of *Dioscorea membranacea* Pierre (figure 16): rhizome wide-running, perhaps even to 2 m, dark brown, with white flesh. Stem slightly ridged, unarmed. Leaves deeply trifid above a cordate base, shortly acuminate, 9 nerved, two primary

nerves reaching the forerunner tip along with the midrib and the second pair reaching the tips of the lateral lobes; petiole 1/2-2/3 the length of the blade. Male flowers in small subsessile cymes with up to 4 flowers, tepals 1 mm long, long-ovate. Stamens all alike, the filaments inserted just below the tepals, 0.3 mm long; anther introse, small. Female flowers on down-wardly directed spike-like racemes. Tube of flower absent. Outer tepals obovate, inner ones lanceolate, a little shorter than the outer. Style short. Capsules 1-2 cm apart.^(95, 96)



Figure 16 Plants called Hua-Khao-Yen; *Dioscorea membranacea* Source: Maneenoon K. (2013) Medicinal plants of the genus *Dioscorea* L. used in traditional Thai medicine prescriptions: KKU Science Journal. p. 801.

3.2 Chemical compounds

Many studies examined the effect of extracts of the rhizomes of *D. membranacea* for treatment *in vitro*. The result showed that this extract has many properties including anti-cancer, anti-inflammation, antioxidant, anti-allergy, and anti-HIV. Moreover, investigators isolated many compounds from such extracts to identify the active compounds. Eight compounds were isolated from crude ethanolic extracts, [two naphthofuranoxepins (1,2), one phenanthraquinone (3), three steroids (4-6), and two steroidal saponins (7,8)](Figure 17).⁽¹⁸⁾

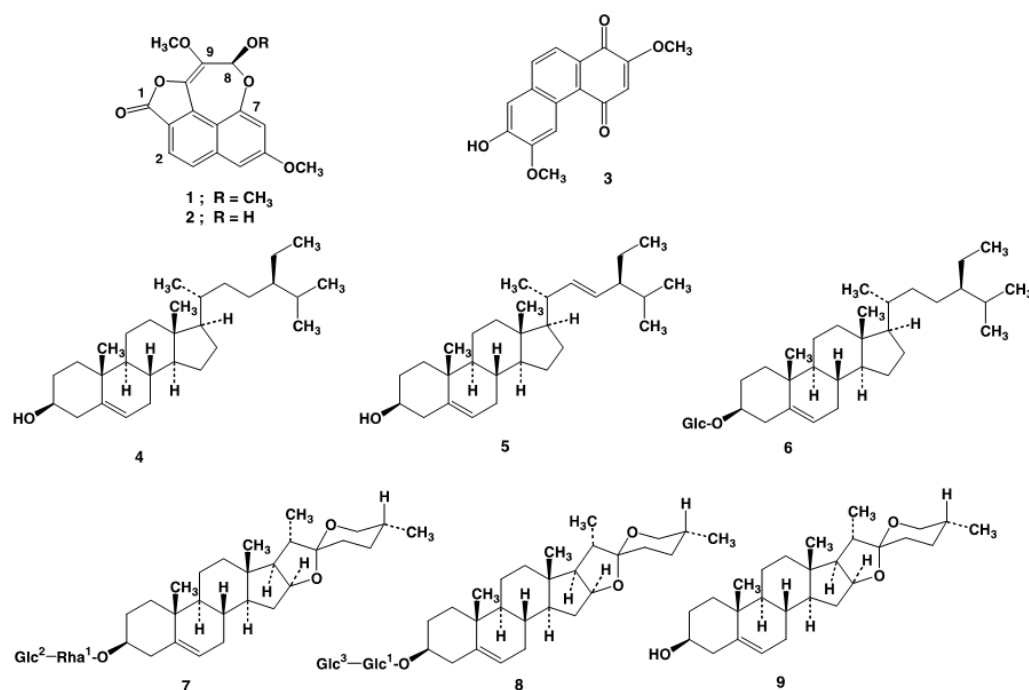


Figure 17 Chemical structures of compounds 1–9 isolated from *Dioscorea membranacea*

Dioscorealide A (1), dioscorealide B (2), and dioscoreanone (3), β -sitosterol (4), stigmasterol (5), diosgenin 3-O- β -D-glucopyranosyl (1 \rightarrow 3)- β -D glucopyranoside (6), diosgenin 3-O- α -L-rhamnopyranosyl(1 \rightarrow 2)- β -D glucopyranoside (7), β -D-sitosterol glucoside (8) and diosgenin (9)⁽¹⁸⁾

Source: Tewtrakul S, Itharat A. (2006) Anti-allergic substances from the rhizomes of *Dioscorea membranacea*: Bioorg Med Chem. p. 8708.

3.3 The extract properties

3.3.1 Anti-cancer property

By following the cancer treatments program of Thai traditional doctors in Songkhla province, it was found that the formula with *D. membranacea* could extend lifespan by 2-3 years for elderly patients and more than ten years for the young patients.

In 2011, the effects of crude ethanolic extract from the rhizome of this plant on cell growth and division, cell cycle distribution, and apoptotic induction in

human lung cancer cell lines were analyzed. The results showed that the crude extract selectively inhibited cell growth on all types of cell lines through the induction of G1 cell cycle arrest, cell division inhibition, and apoptosis.⁽⁹⁷⁾ It was further found that the cytotoxic activity of dioscorealide B against human breast cancer cells (MCF-7) had an $IC_{50} = 0.94 \mu\text{g/ml}$. To determine whether this active compound induced apoptosis in MCF-7 cells, an Annexin-V assay showed that the number of apoptotic cells increased to 7-12 folds after treatment with 1-4 $\mu\text{g/ml}$ dioscorealide B for 24 hours. In addition, the data revealed that dioscorealide B induced the activation of caspase-7, -8, and -9. These data suggested that this compound activated both the intrinsic and extrinsic apoptotic pathway. Moreover, an increase in the pro-apoptotic protein (Bax) expression was observed at 6 hours and a decrease in the anti-apoptotic protein (Bcl-2) expression was observed at 3 hours after the treatment with 1 $\mu\text{g/ml}$ dioscorealide B. Together, the results indicated that dioscorealide B possessed cytostatic effect against human breast cancer cells that was mediated via the apoptotic pathway.^(95, 97)

3.3.2 Anti-oxidant and anti-inflammatory properties

Thai medicinal plants locally known as Hua-Khao-Yen were examined for their inhibitory activities against lipopolysaccharide (LPS) induced nitric oxide (NO) production in RAW264.7 cell lines. Among the plant species studied, an ethanolic extract of *Dioscorea membranacea* exhibited the most potent inhibitory activity, with an IC_{50} value of 23.6 $\mu\text{g/ml}$.⁽¹⁹⁾

From this extract, eight compounds were isolated and further investigated for their inhibitory properties of NO production. It was found that diosgenin 3-O- α -L-rhamnopyranosyl(1 \rightarrow 2)- β -D glucopyranoside (7) possessed the highest activity, followed by dioscoreanone (3), and dioscorealide B (2). Regarding structural requirements of diosgenin derivatives for their inhibitory activity on NO production, compound (7) which has a rhamnoglucosyl moiety at C-3 exhibited much higher activity than compounds that have either a diglucosyl substitution (8) or its aglycone (9). Furthermore, hydroxyl substitution at position 8 of naphthofuranoxepin derivatives conferred a higher activity than the methoxyl group. It was concluded that diosgenin 3-

O- α -L-rhamnopyranosyl(1 \rightarrow 2)- β -D glucopyranoside (7), dioscoreanone (3) and dioscorealide B (2) were the active principles for NO inhibitory activity of *D. membranacea*. Compounds 1–3 were also tested for their inhibitory effect on LPS-induced TNF- α release in RAW264.7 cells. The result revealed that dioscoreanone (3) possessed potent activity against TNF- α release with an IC₅₀ value of 17.6 μ M, whereas compound (1) and (2) exhibited mild activity. The result revealed that dioscoreanone possessed potent activity against TNF- α release and strong inhibition of nitric oxide (NO) production.⁽¹⁹⁾ Moreover, in 2007, the research has established that dioscoreanone in *D. membranacea* extract have the highest antioxidant activity in DPPH test.⁽⁹⁸⁾

In conclusion, diosgenin 3-O- α -L-rhamnopyranosyl(1 \rightarrow 2)- β -D glucopyranoside (7), dioscoreanone (3) and dioscorealide B (2) are active principles for NO inhibitory activity of *D. membranacea*, and dioscoreanone also exhibited potent inhibitory effect on TNF- α release.^(99, 100)

3.3.3 Anti-allergic property

Extracts of five species of Thai medicinal plants, locally known as Hua-Khao-Yen, were screened for anti-allergic activities using RBL-2H3 cells. Among the five species of Hua-Khao-Yen, the ethanol extract of *D. membranacea* exhibited the potent inhibitory activity against β -hexosaminidase release as a marker of degranulation in RBL-2H3 cells, with an IC₅₀ value of 37.5 μ g/ml. Eight compounds were isolated from this crude ethanolic extract, and tested for their anti-allergic activities. The results showed that dioscorealide B (2) possessed the highest activity.⁽⁹⁸⁾

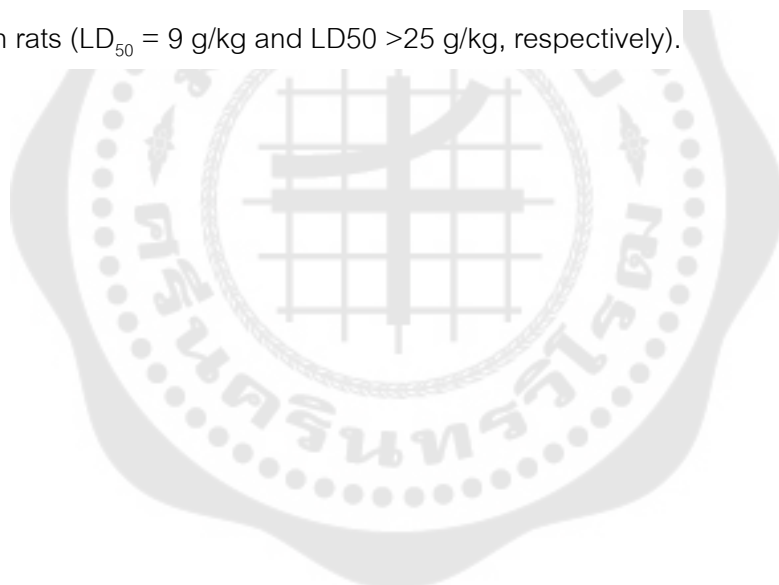
In addition, the ethanol and aqueous extract of *D. membranacea* rhizome suppressed the paw edema induced by carrageenin in rats. Oral administration of the ethanol *D. membranacea* extract at the dose of 1600 mg/kg significantly decreased the paw edema induced by carrageenin in rats and the aqueous extract (1600 mg/kg) also significantly suppressed the carrageenin-induced paw edema in rats, but the ethanol extract had no significant effects on antinociceptive response in writhing, formalin and hot plate tests and antipyretic.⁽¹⁵⁾

3.3.4 Anti-HIV property

The extracts of five species of Hua-Khao-Yen were determined to test on anti-HIV effects. Interestingly, only the ethanol extract of *Dioscorea membranacea* showed appreciable activity ($IC_{50} = 48 \mu\text{g/ml}$) against HIV-1 protease, while the other extracts possessed mild activity and exhibited anti-HIV-1 integrase instead. This result strongly supported the basis for the use of two species of Hua-Khao-Yen, *Smilax corbularia* and *D. membranacea* for AIDS treatment by Thai traditional doctors.⁽¹⁰¹⁾

3.3.5 Toxicity

Itharat and Ooraikul (2007) tested for acute toxicity of ethanolic and water extracts of *D. membranacea* at Department of Medical Sciences, Ministry of Public Health. The result showed that both ethanolic and water extracts had no acute toxicity in rats ($LD_{50} = 9 \text{ g/kg}$ and $LD_{50} > 25 \text{ g/kg}$, respectively).



CHAPTER 3

MATERIALS AND METHODS

1. Chemicals and reagents

Diethylnitrosamine (DEN), thioacetamide (TAA), hematoxylin-eosin stain, and lipid peroxidation (MDA) assay kit were purchased from Sigma-Aldrich (St. Louis, MO). Paraformaldehyde and paraffin were purchased from Electron Microscopy Science (Hatfield, PA, USA). High-Capacity cDNA reverse transcription kit, and TRIzol reagent were purchased from Invitrogen (Carlsbad, CA, USA). SsoAdvanced SYBR® Green Supermix, and PrimePCR SYBR® Green gene assay were purchased from Bio-Rad (Hercules, CA, USA). Diethylpyrocarbonate (DEPC)-treated water was purchased from Applied Biosystems (Foster City, CA, USA). Copper (II) sulphate, dimethyl sulfoxide, and Permout® were purchased from Fisher Scientific (Loughborough, UK). All other chemicals used in this study were of analytical grade and obtained from Sigma-Aldrich (St. Louis, MO, USA) or Bio-Rad (Hercules, CA, USA).

2. Plant extract

Dioscorea membranacea (DM) extract was obtained from Assoc.Prof.Arunporn Itharat, Center of Excellence of Applied Thai Traditional Medicine, Thammasat University, Thailand. Briefly the extraction process of the DM was documented.⁽¹⁵⁾ Dried ground DM plant material (100 g) was percolated with 95% ethanol, then was dried under reduced pressure to prepare the concentrated plant extract stock.

3. Experimental animals

Thirty six male Wistar rats (*Rattus norvegicus*) with 6-7 weeks old weighing between 200-250 g were obtained from the National Laboratory Animal Center, Mahidol University, Thailand. The animals were allowed free access to food and water in a temperature- and humidity-controlled environment and maintained on a 12 h light/dark cycle. All procedures involving animals were followed and approved by the Animal Ethics Committee of the Faculty of Medicine, Srinakharinwirot University (license No. 2/2559).

4. Experimental designs

After acclimatization, the rats were weighed and randomly divided into six groups of six rats each. Group 1 was the standard control group and group 2 the control group treated with DM extract at 40 mg/kg. Groups 3-6 were subjected to HCC induction by initially injection intraperitoneally with a single dose of 200 mg/kg diethylnitrosamine (DEN; Sigma-Aldrich, St. Louis, MO, USA). Subsequent 2 weeks, the rats were intraperitoneally administered with 300 mg/kg of thioacetamide (TAA; Sigma-Aldrich, St. Louis, MO, USA) three times weekly for consecutive 4 weeks. The rats were then left for a further 2 weeks without any treatment for allowing the cancer to develop (adapted protocol from Nahla E. El-Ashrawy et al., (2014)⁽¹¹¹⁾(Figure 18). At week 8, all animal groups were subjected to daily oral administration of different compounds for another period of 8 weeks. Groups 1 and 3 were administered with the vehicle (propylene glycol:tween80:water (4:1:4 v/v), group 4 with 4 mg/kg of DM extract, groups 2 and 5 with 40 mg/kg of DM extract and group 6 with 30 mg/kg sorafenib.⁽¹⁰²⁾

Doses of DM extract used in the present study were based on those used *in vitro*⁽¹⁴⁾ and were demonstrated to be safe in a toxicity test in rats (Itharat, preliminary study report). During the time course of the experimental tumor study (16 weeks), a set of criteria was developed to follow the rats' condition. These included their external physical appearance, appearance of any visible lesions, changes in body weight and behavioral responses to external stimuli (including light or noise, etc.), which reflect pain and distress in the animals. The humane endpoint in the present study was based on a weight loss exceeding 20% of the body weight of the rats in the control group. At the end of the experiment at week 16, experimental rats (n=6 per group) were anesthetized with an intraperitoneal injection of 45 mg/kg Nembutal. Liver tissues and blood samples were collected and processed for histological and immunohistochemical analyses, liver function tests, lipid peroxidation, reverse transcription-quantitative PCR (RT-qPCR) and proteomic analyses.

Table 1 Experimental animal groups.

Group	Treatment
1	Normal control
2	Control + DM 40 mg/kg
3	HCC control
4	HCC + DM 4 mg/kg
5	HCC + DM 40 mg/kg
6	HCC + Sorafenib 30 mg/kg

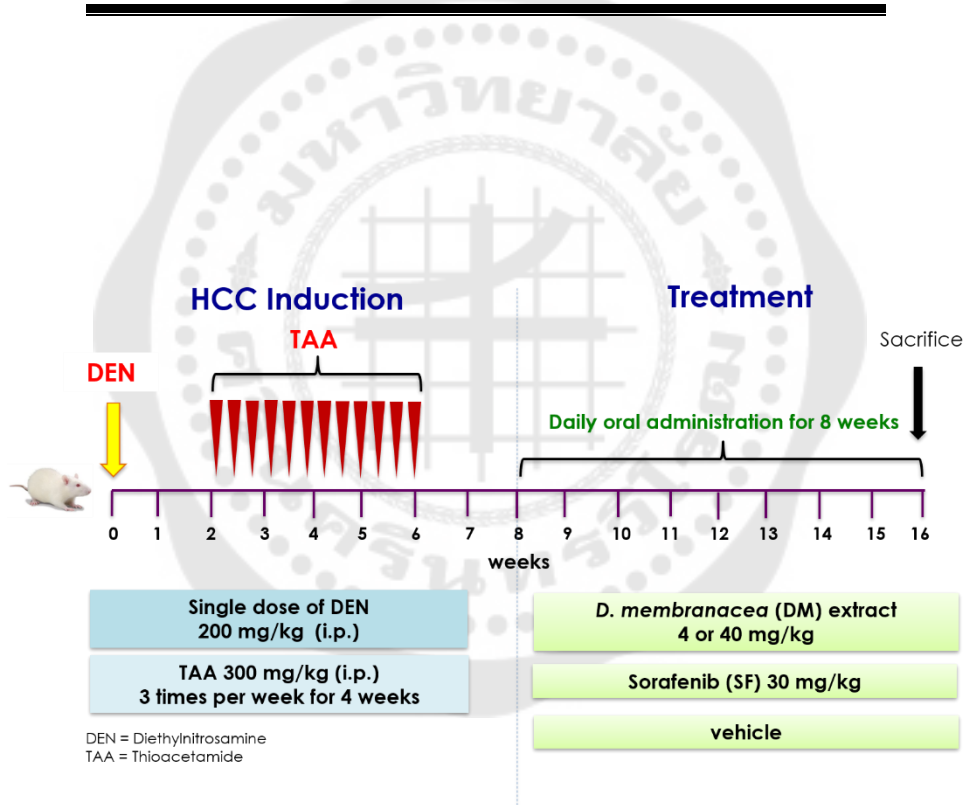


Figure 18 Procedure and timeframe for induction of hepatocellular carcinoma (HCC) and treatment in rat

5. Methods

5.1 Gross examination of the liver

After cut open the abdominal wall, gross examination of the abdominal cavity was carried out to identify gross abnormalities of the organs and photographs were taken. The rat livers were subsequently isolated, dissected, and rinsed in phosphate-buffered saline (PBS). The relative liver weight was calculated as the percentage of liver weight / final body weight.

5.2 Histopathological studies

The liver samples were immediately removed and then rinsed in PBS. The liver tissues were fixed in 4% (v/v) formaldehyde solution and then dehydrated in ascending graded series of ethanol, cleared in xylene and embedded in paraffin. The Liver tissue blocks were then sectioned at 5 micron thick by a microtome. The tissue sections were deparaffinized, rehydrated in descending series of ethanol, and stained with hematoxylin-eosin as well as reticulin (Gordon-Sweet, Bio-Optica, Milano, Italy) methods. The sections were mounted with Permount[®] and scanned with a panoramic digital slide scanner (3DHISTECH Ltd., Budapest, Hungary). For each image, an area of 4,000x2,500 μm (10 mm^2) was randomly selected to locate and calculate the cancer area using the CaseViewer program (v1.3.0.41885) available at <https://www.3dhistech.com/caseviewer>. A total of 30 images of each animal group were sampled, in which three specialists in liver histopathology identified the presence of thick-cell cords or pseudoglandular pattern in hepatic nodules and located the cancer areas (Figure 19).⁽⁴⁹⁾ The mean cancer area in each group was then calculated. To assess the reticulin staining in the liver tissue, both distribution pattern and percentage of stained area were evaluated. Mean percentage of the reticulin-positive areas from 10 mm^2 -randomly area in 30 images of each animal group was accomplished by using Cell Sense Dimensions software (Olympus, Hamburg, Germany).

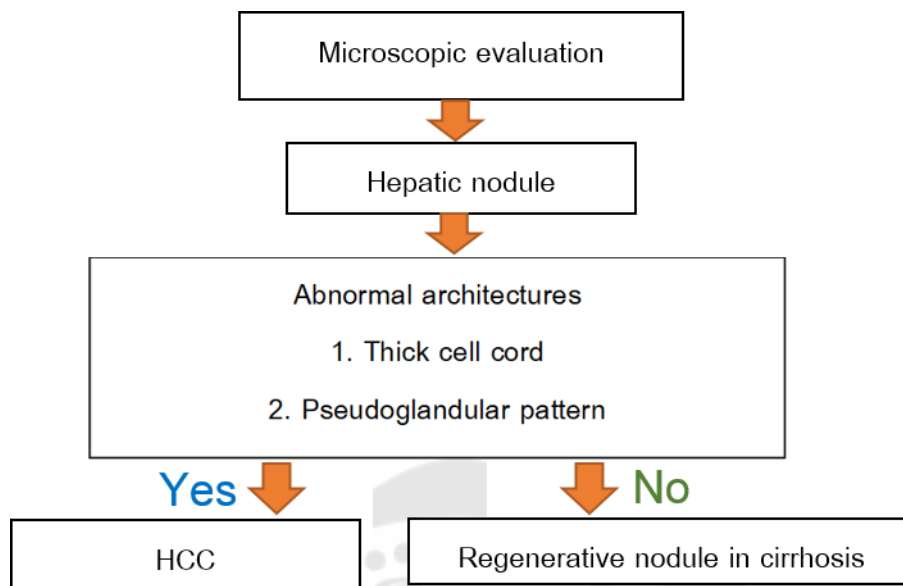


Figure 19 Assessment criteria for cancer area

5.3 Proteomics study

5.3.1 Protein extraction

The 100 mg of frozen liver tissues of each animal group were homogenized with liquid nitrogen and dissolved in 400 μ l of 0.5% SDS then centrifuged at 5,000 rpm for 5 minutes. The supernatant was collected and precipitated twice with 100% cold acetone before incubating at -20°C overnight. After centrifugation at 12,000 rpm for 15 minutes, the supernatant was removed then the pellets were air dried at room temperature. The pellets were dissolved with 300 μ l of 10 mM ammonium bicarbonate and then sonicated in an ultrasonic bath (Elmasonic e100h, USA) at 20°C for 15 minutes. The protein concentrations were measured at 750 nm using the Lowry assay with bovine serum albumin as a protein standard.

5.3.2 Analysis of protein profiles by LC-MS/MS

For in solution digestion, samples solution of 20 $\mu\text{g}/\mu\text{l}$ were incubated with 5 μl of 10 mM dithiothreitol at room temperature for 1 hour. After that, 20 μl of 100 mM iodoacetamide was added then incubated at room temperature in dark for 1 hour. Thereafter, 10 ng of trypsin in 10 mM ammonium bicarbonate was added and stored at

37°C for 3 hours followed by the addition 1 ul of 0.1% formic acid. Finally, all samples were evaluated by LC-MS/MS analysis.

The extracted peptides were subjected to peptide fractionation using reverse-phase high-performance liquid chromatography and the gradient-eluted peptides were analyzed by an HCTultra PTM Discovery System (Bruker Daltonics Ltd., Germany) coupled to an UltiMate 3000 LC System (Dionex Ltd., UK). Peptides were separated on a nanocolumn (PepSwift monolithic column 100 µm i.d. x 50 mm) by using eluents A and B, containing 0.1% formic acid and 80% acetonitrile in water, and 0.1% formic acid, respectively. Peptide separation was achieved with a linear gradient from 10% to 70% solution B for 13 min at a flow rate of 300 nl/min. Including a regeneration step at 90% solution B and an equilibration step at 10% solution B, one run took about 20 min. Peptide fragment mass spectra were acquired in data-dependent AutoMS (2) mode with a scan range of 300-1500 m/z. Three averages and up to 5 precursor ions were selected from the MS scan range of 50-3000 m/z.

The proteins quantitation was analyze by DeCyder MS Differential Analysis software (DeCyderMS, GE Healthcare). Acquired data of LC-MS was converted and using the PepDetect module for automated peptide detection, charge state assignments, and quantitation based on the peptide ions signal intensities in MS mode. From DeCyderMS, the analyzed MS/MS data were added for a database search using the Mascot software. (Matrix Science, London, UK). The identification of protein was analyzed by searching for data against the NCBI database. Database interrogation were taxonomy (*Rattus norvegicus*), enzyme (trypsin), variable modifications (carbamidomethyl oxidation of methionine residues), mass values (monoisotopic), protein mass (unrestricted), peptide mass tolerance (1.2 Da), fragment mass tolerance (± 0.6 Da), peptide charge state (1+, 2+ and 3), and max missed cleavages (3). The maximum value of each group was used to determine the presence or absence of each identified protein.

Data normalization and quantification of the changes in protein abundance between the control and treated samples were performed and visualized using MultiExperiment Viewer (Mev) software version 4.6.1. Briefly, peptide intensities from the LC-MS analyses were transformed and normalized using a mean central tendency procedure. The statistical tests of variance of differences (ANOVA) for these data sets statistically significant proteins ($p < 0.05$) was performed. Gene ontology annotation including biological process, cellular component and molecular function were performed using Panther (<http://www.pantherdb.org/>). The identified proteins were simultaneously submitted to the search tool for interactions of chemicals (STITCH) (<http://string-db.org>) to search for understanding cellular functions, molecular signaling and chemical target relationship.

5.3.3 Analysis of peptide pattern by MALDI-TOF MS

The serum was directly applied onto Nanosep 10K Omega ultrafiltration device (Pall Life Sciences) and the sub-10kDa fraction was removed for protein quantitation by the nanodrop. Serum and Peptide solution was acidified with 0.1 % trifluoroacetic acid and 0.1 Triton X-100 to a final concentration of 0.1 $\mu\text{g}/\mu\text{l}$ and mixed with MALDI matrix solution 10 mg sinapinic acid in 1 ml of 50 % acetonitrile containing 0.1 % trifluoroacetic acid, then the samples were directly spotted on MTP AnchorChip 600/384 (MALDI plate, Bruker GmbH) as dried droplet method at room temperature. The samples were analyzed using Ultraflex III TOF/TOF (Bruker Daltonik, GmbH) in a linear positive mode with a mass range of 5,000–15,000 Da. Five hundred shots were accumulated with a 200-Hz laser for each sample. The mass were listed to show the peptide pattern. MS spectra were analyzed by Flex Analysis 3.0 (Build 92) and ClinProTool software 2.2 (Build 78) (Bruker Daltonik, GmbH) including fingerprint spectra and principal component analysis (PCA) (feature of ClinProTools).

5.4 Real-time PCR

5.4.1 Real-time quantitative PCR

Real-time PCR will be carried out in CFX96 Real-Time PCR Detection System (Bio-Rad, Hercules, CA, USA) using PrimePCRTM SYBR® Green gene assay which is a primer set designs for the detection and quantitation of rat genes in RNA samples those are converted to cDNA. Assay of rat beta-actin gene will be performed as an endogenous control for relative quantification study.

5.4.2 RNA extraction and qualification

Total RNA was extracted from frozen rat liver using the TRIzol reagent (Invitrogen, Carlsbad, CA, USA). Briefly, 50 mg of the liver sample were homogenized with tissue homogenizer (Omni international, USA) for 10 seconds in 1 mL of TRIzol reagent and then incubated at room temperature for 5 minutes before adding 0.2 ml of chloroform, then mixed vigorously by hand for 15 seconds, incubated at room temperature for 3 minutes, and centrifuged at 12,000 g for 15 minutes at 4 °C. After centrifugation, the RNA in the upper aqueous phase was transferred to a fresh tube and then precipitated with 0.5 mL of isopropanol, mixed gently by vortex, and incubated at room temperature for 10 minutes. The pellet of total RNA was collected by centrifugation at 12,000 g for 10 minutes. The supernatant was discarded. The RNA pellet was washed with 1 ml of cold 75% ethanol, and centrifuged at 7,500 g for 5 minutes. Finally, the RNA was dissolved in nuclease-free water and stored at -80 °C to be used later. The RNA concentrations were determined using a NanoDrop® spectrophotometer (Thermo Scientific, Waltham, MA, USA).

5.4.3 Reverse transcription

The reverse transcription was performed using High Capacity cDNA Reverse Transcriptase Kit (Applied Biosystems, USA) according to the manufacturer's instructions. First strand cDNA was synthesized with 2X RT master mix per 20 μ l

reaction. Then 10 μ l of diluted RNA samples (2 μ g of total RNA) were mixed with the 10 μ l RT master mix and run on thermal cycler (Eppendorf Mastercycler® personal; Eppendorf AG, Hamburg, Germany) at 25°C for 10 minutes, 37°C for 120 minutes, 85°C for 5 minutes, and then stored at -20°C until use.

5.4.4 Real time quantitative PCR

Real-time PCR were carried out in CFX96 Real-Time PCR Detection System (Bio-Rad, Hercules, CA, USA), using SsoAdvanced Universal SYBR Green Supermix with designed primers (Table2), and commercial PrimePCR primers (Table3). Rat beta-actin (*Actb*), and hypoxanthine phosphoribosyltransferase 1 (*Hprt1*) mRNA were assayed as an internal control for relative quantification. The thermal cycler protocol was consisted of 2 min activation at 95°C followed by 40 cycles of denaturation at 95°C for 5 sec, and then annealing/extension at 60°C for 30 sec. At the end of each run, a melting curve analysis was performed from 65-95 °C with a heating rate of 0.1°C per sec. Analysis of the mRNA expression levels was performed by Bio-Rad CFX manager™ software version 1.3.1 (Hercules, CA) and quantification of relative mRNA expression was calculated using the $2^{-\Delta\Delta CT}$ (Livak) method of relative quantification.⁽¹⁰³⁾

Table 2 Primers for qPCR

Gene symbol	Protein name	Primer sequence	GenBank accession No
<i>Actb</i>	Beta-actin	F: 5'-GTGGGGCGCCCCAGGCAC R: 5'-CTCCTTAATGTCACGCAC	NM_008047
<i>Flt1</i>	VEGFR1	F: 5'-CTCACAGCCACTCTCATCGT R: 5'-ATACACGGTGCAAGTGAGGA	NM_019306

Table 3 PrimePCR primers designed for SYBR® Green gene expression

Gene symbol	Protein name	Unique Assay ID	GenBank accession No
<i>Actb</i>	Beta-actin	qRnoCID0056984	NM_031144
<i>Hprt1</i>	HPRT1	qRnoCED0057020	NM_012583
<i>Pdgfra</i>	PDGFRA	qRnoCID0003041	NM_012802
<i>Ikbkg</i>	NEMO	qRnoCID0004499	NM_199103
<i>Rps6ka4</i>	MSK2	qRnoCED0005038	NM_001108517
<i>Bik</i>	BIK	qRnoCED0008143	NM_053704
<i>Diablo</i>	DAIBLO	qRnoCED0001128	NM_001008292
<i>Parp1</i>	PARP1	qRnoCID0009491	NM_013063

5.5 Liver function tests

Blood serum collected after a heart puncture were used to assess liver function. The assays included aspartate aminotransferase (AST, alanine aminotransferase (ALT, alkaline phosphatase (ALP), and gamma-glutamyltransferase (GGT) activity, and albumin and total protein concentration. These serum markers were measured in a standard clinical lab (Bangkok R.I.A. Laboratory, Bangkok, Thailand).

5.6 MDA assay

After sacrifice, the liver samples were immediately removed, rinsed with PBS, and stored at -80°C until use. Lipid peroxidation was determined by assaying MDA with thiobarbituric acid (TBA) with a commercial kit (Sigma-Aldrich, St. Louis, MO, USA). Briefly, liver samples of about 20 mg were homogenized and centrifuged at 3,500 rpm for 10 minutes at 4°C. The supernatant was collected, then 0.6 ml of the TBA solution was added to form the MDA-TBA adduct. The absorbance was measured at 532 nm by using a spectrophotometer. The concentration of MDA presence in the samples was determined from a calibration curve.

6. Statistical analysis

All values were represented as mean \pm SD. The data was analyzed using one-way analysis of variance (ANOVA) with Tukey's post hoc test to compare between each group. The significance levels were set at p values less than 0.05.



CHAPTER 4

RESULTS

1. The rat body weight and liver weight ratio

The body weights of the rats decreased upon injection with initiator (DEN) and promoter (TAA), but gradually increased during the last 10 weeks of the experiments. At the end of the experiments, there was no significant difference in the liver-to-body weight ratio between the control, HCC and DM extract-treated groups. The SF-treated group showed the lowest of liver-to-body weight ratio among all six groups and was significantly lower than the HCC groups that were not treated or treated with DM extract (Table 4).

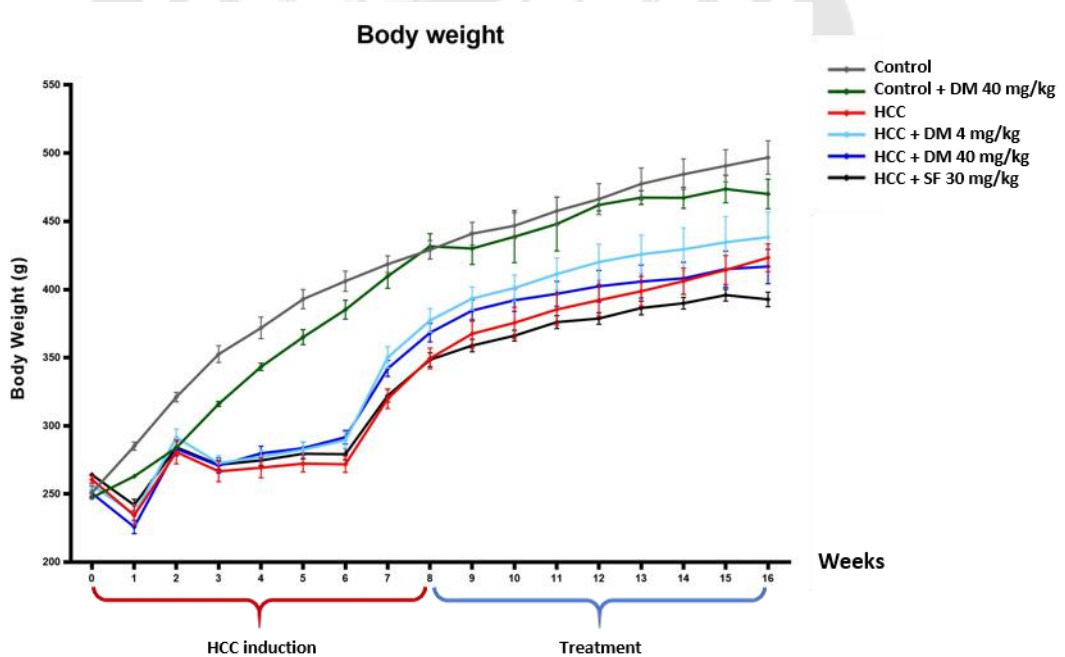


Figure 20 Graph illustrating the body weight from week 0 to week 16

Table 4 The liver weight relative to body weight ratio.

Groups	Body weight (g)	Liver weight (g)	Liver weight/ body weight (%)
Normal control	496.9 ± 12.3	14.38 ± 0.7	2.90 ± 0.16
DM extract 40 mg/kg	455.6 ± 29.8	11.86 ± 0.4	2.70 ± 0.09
HCC control	423.3 ± 10.1	14.05 ± 0.6	3.25 ± 0.09 ^{##}
HCC + DM extract 4 mg/kg	438.4 ± 18.4	14.02 ± 0.7	3.20 ± 0.10 ^{##}
HCC + DM extract 40 mg/kg	416.9 ± 12.6	14.63 ± 0.7	3.26 ± 0.09 ^{##}
HCC + SF 30 mg/kg	392.8 ± 5.4	10.55 ± 0.3	2.68 ± 0.08

The data are presented as the mean ± S.E.M. (N=6). ^{##}*p*<0.01 compared to HCC + sorafenib 30 mg/kg group.

2. Gross structure and histopathology of the rat liver

The gross morphology of livers in the DM-only group was with smooth contour similar to that in the control group. Liver in the HCC groups had clearly visible hepatic nodules (Figure 23). Fewer hepatic nodules were, however, observed in the HCC-bearing rats treated with either DM or sorafenib compared with the non-treated HCC group.

Under microscopy the rat liver sections of the control and DM-only groups showed a normal appearance of hepatocytes with eosinophilic cytoplasm containing numerous mitochondria and rough endoplasmic reticulum stacks. Hepatocytes were organized into cell plates separated by sinusoids radiating from the central vein (Figures 21C, D, G, and H). These findings imply that vehicle and DM extract do not affect liver architecture in rats. The HCC group did show all abnormal histopathological criteria of liver cancer including numerous hepatic nodules (Figures 21K and L), pseudoglandular structures, hepatic cell cords with greater than three cell layers stacking together in thickness, microsteatosis and intracellular hyaline globules (Figures 22A-C). Treatment of HCC rats with DM at doses of 4 and 40 mg/kg or with sorafenib reduced the number of hepatic nodules and gained more normal features of liver histology. (Figures 21M-21X).

The abnormal pattern of reticulin- stained fibers could guarantee the presence of cancer areas in HCC rats., In all HCC-bearing rats induced by DEN and TAA, the abnormal reticulin staining pattern showed a thick layer of reticulin surrounding each hepatic nodule and outlining the hepatic cell plates with more than two layers (Figure ???). . In the control and DM-only groups, in contrast, the reticulin was distributed in between the adjacent hepatic cell plates. (Figure 23). The reticulin-positive areas in all groups of HCC-bearing rats were significantly increased compared with those in the control group ($p < 0.001$). Furthermore, the lesser reticulin areas, which reflected the lesser cancer area, were significantly detected in HCC rats treated with two doses of DM or sorafenib compared with the non-treated HCC rat (Figures 24A and B; $p < 0.001$).

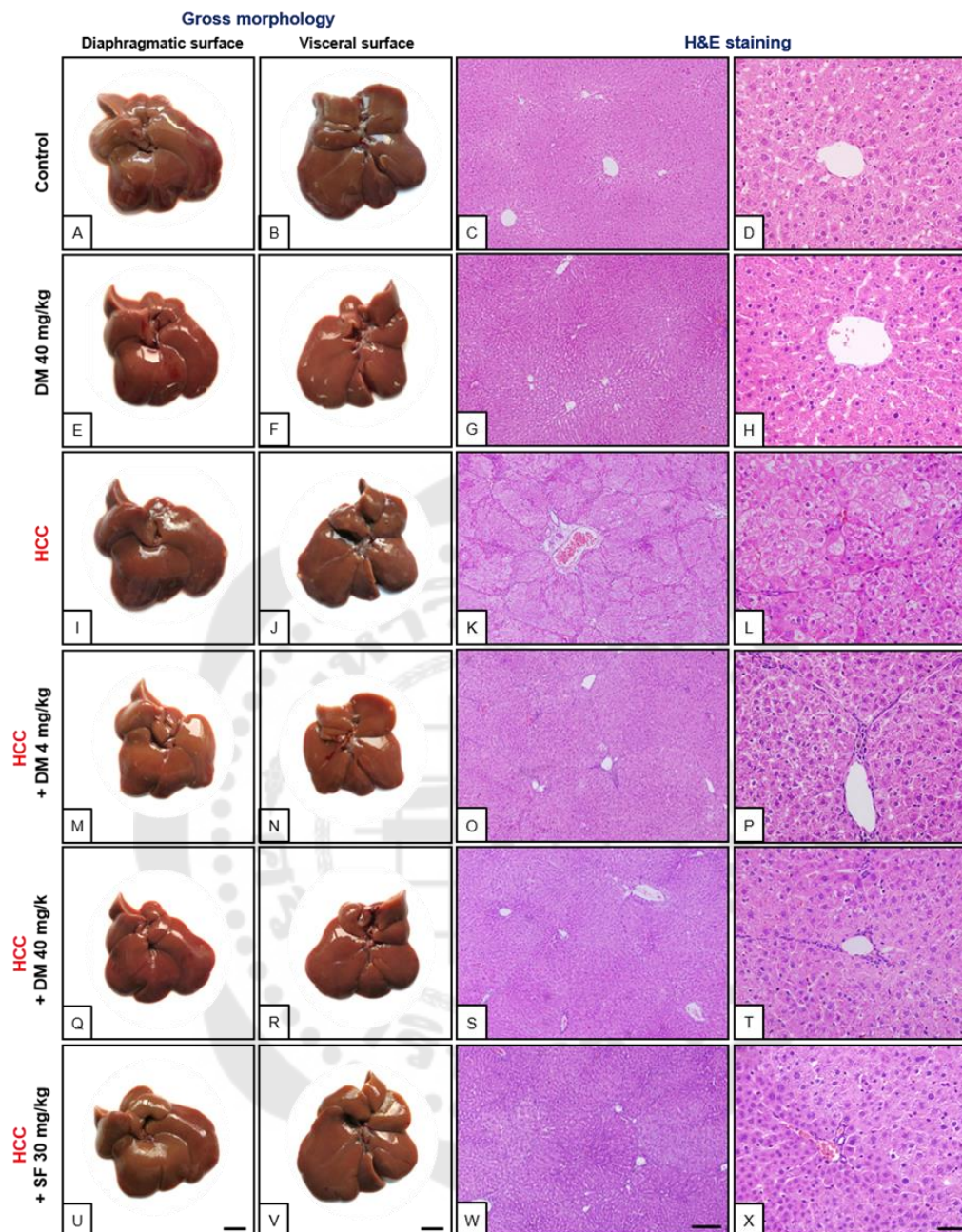


Figure 21 Photograph illustrating the gross examination and histology of the rat livers. Scale bars for both the first and second columns showing the liver gross morphology are of 1 cm. Scale bars for the third and fourth columns revealing the light micrographs of the liver sections are of 200 and 50 μ m, respectively.

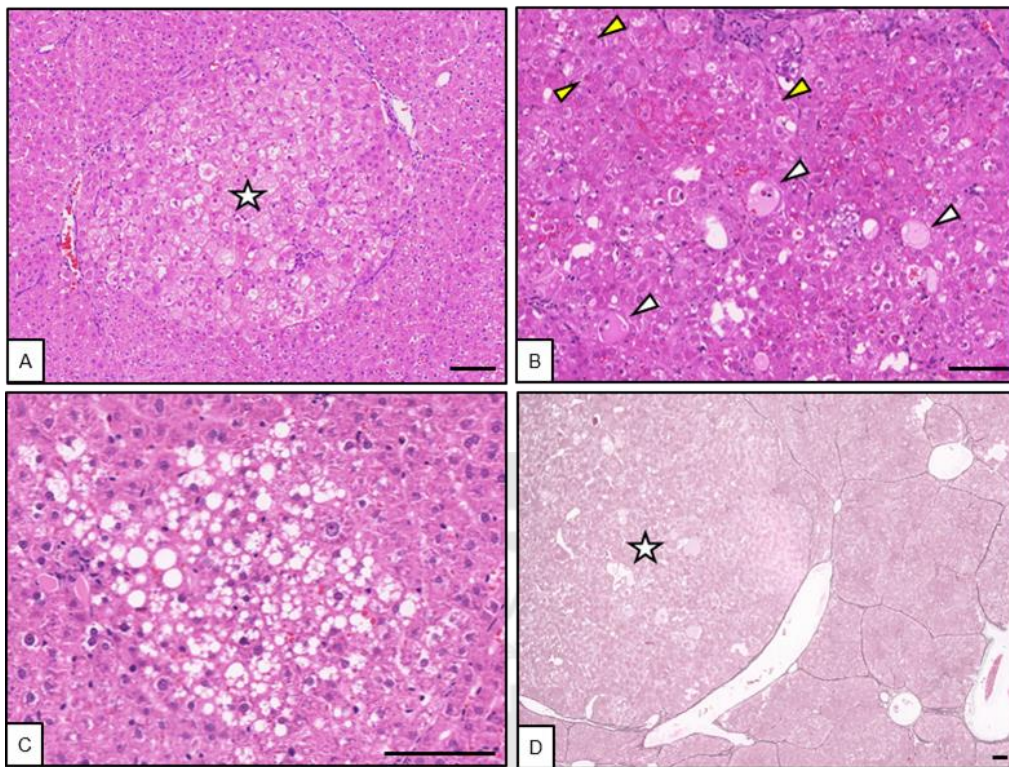


Figure 22 The light micrograph of histopathology in HCC rat.

The HCC features including A) the solid sheath of tumor nest (white star), B) the pseudoglandular pattern (white arrowheads) and hyaline globule (yellow arrowheads), C) the micro-steatosis, and D) the abnormal positive reticulin staining pattern surrounding each hepatic nodule (D). Scale bar in each figure represents 100 μ m.

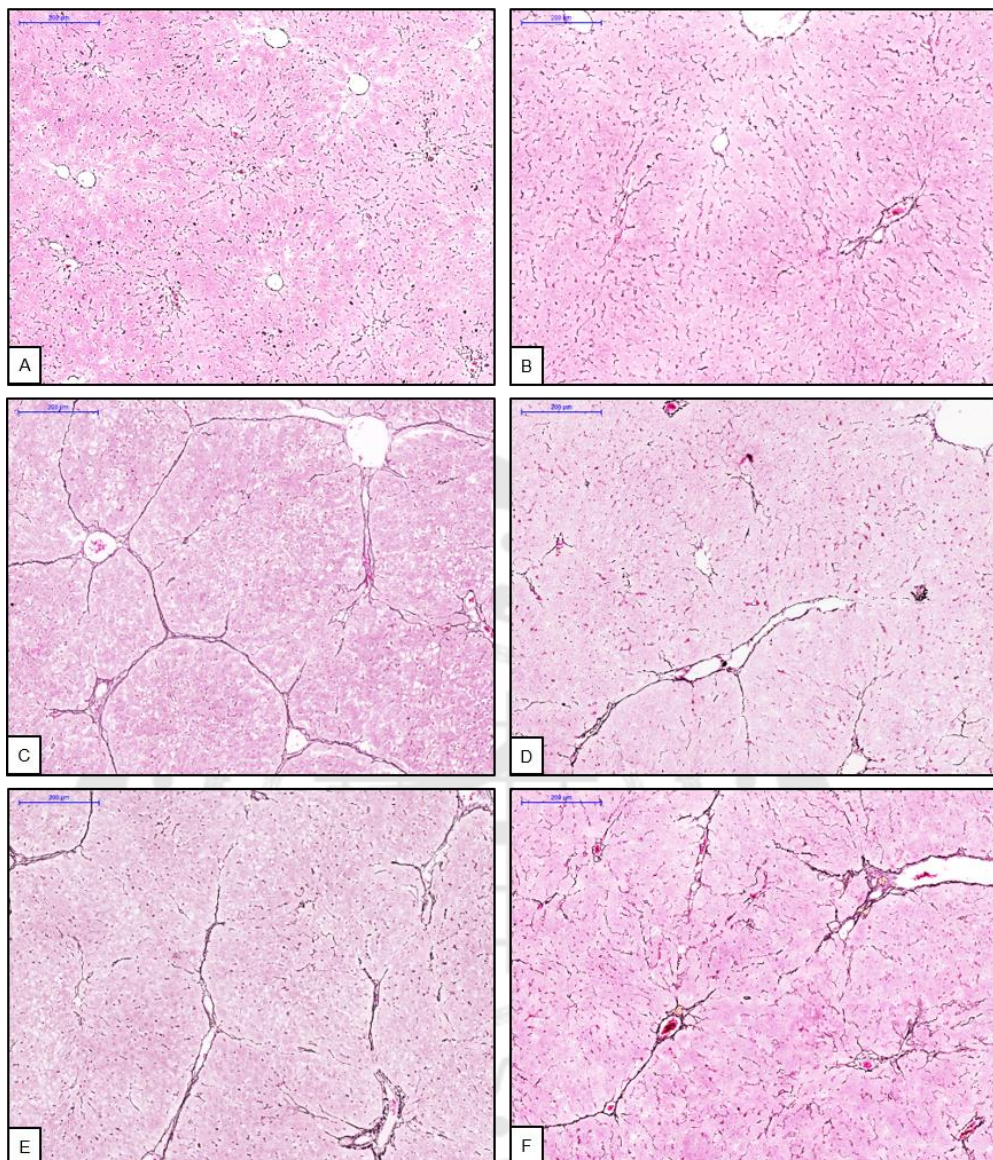


Figure 23 Light micrographs of the liver sections of reticulin staining.

Normal reticulin-stained areas presenting in between the adjacent hepatic cell plates were found in the control (A) and control + DM 40 mg/kg (B) groups. Note the abnormal reticulin pattern in most areas of the non-treated HCC group (C). Areas with normal reticulin scaffold pattern was observed in the HCC + DM 4 mg/kg (D), HCC + DM 40 mg/kg (E), and HCC + sorafenib 30 mg/kg (F) groups. All scale bars presented are of 200 μm .

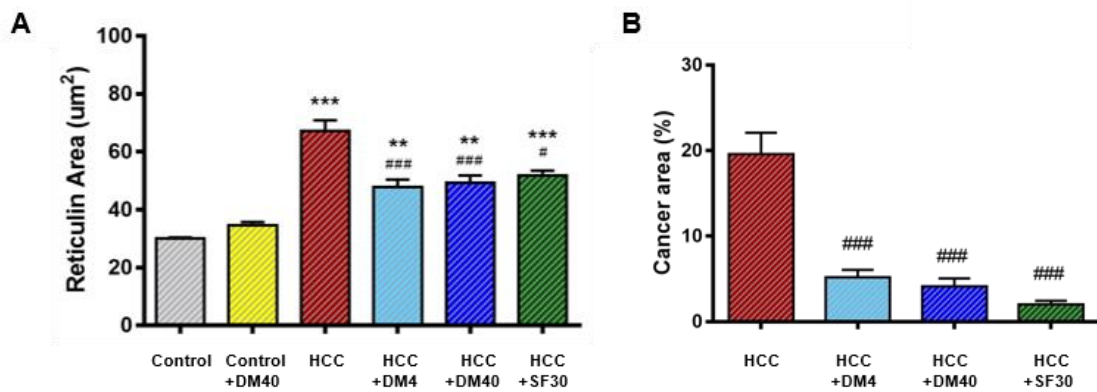


Figure 24 Diagram showing the surface of the reticulin areas per section (A) and relative cancer area (B) in rat liver tissues

(** $p < 0.01$ vs. control group, *** $p < 0.01$ vs. control group, # $p < 0.01$ vs. HCC group, ### $p < 0.001$ vs. HCC group).

3. Protein pathway profiles

Upon blasting the tandem mass spectra against the NCBI database, the 2,471 proteins in liver samples were found to be differentially expressed across the six animal groups. With Panther software only 831 out of 2,471 proteins were known and classified. Of these, only 42 proteins were associated with the proteins involving in the 3 well-established signaling pathways of HCC including proliferation, angiogenesis, and apoptotic pathways.

3.1 The proteins associated with proliferation, angiogenesis, and apoptosis in STITCH database

The data of the proteins were transferred into STITCH 4.0 and matched with sorafenib, reticulin, and compounds isolated from the DM extract. The software STITCH 4.0 could detect the 42 proteins, reticulin, sorafenib drug, and two compounds of the DM; stigmasterol and diosgenin. With STITCH 4.0 software, associations between protein and protein were demonstrated in blue line, and interactions between protein and chemical were in green line. From STITCH analysis, 4 proteins (platelet-derived growth factor receptor alpha (PDGFRA), vascular endothelial growth factor receptor1 (VEGFR1), ribosomal protein S6 kinase alpha-4 (MSK2) had well-defined functions and well-published to up-regulate in HCC, and NF-kappa-B essential modulator (NEMO) was reported to down-regulate in HCC. From the present study the levels of, PDGFRA, VEGFR1 and MSK2 were increased approximately 1.6-, 2.1, and 1.9-fold-change in HCC group compared to control group, respectively. However, NEMO were nondetectable. These proteins can be classified in PI3K/AKT, Ras and MAPK signaling pathways of either cancer-cell proliferation or angiogenesis and associated with sorafenib drug (Figure 25A).

In addition to cell signaling, the apoptotic-enhancing property of DM extract was also investigated. In order to do that, the two apoptotic proteins (BAX, BCL-2) were added in STITCH 4.0 software (Figure 25B). There were only 3 proteins including Bcl-2-interacting killer (BIK), Diablo homolog, mitochondrial-like isoform X1 (DIABLO), and poly [ADP-ribose] polymerase 1 (PARP1) were identified. Those proteins have been reported to be changed in HCC. The present study found that in the HCC group the pro-

apoptotic protein BIK was 0.8-fold downregulated, whereas the PARP1 was 1.5 folds upregulated compared with the control group. However, the DIABLO protein was nondetectable in HCC group suggesting suppression of apoptosis.



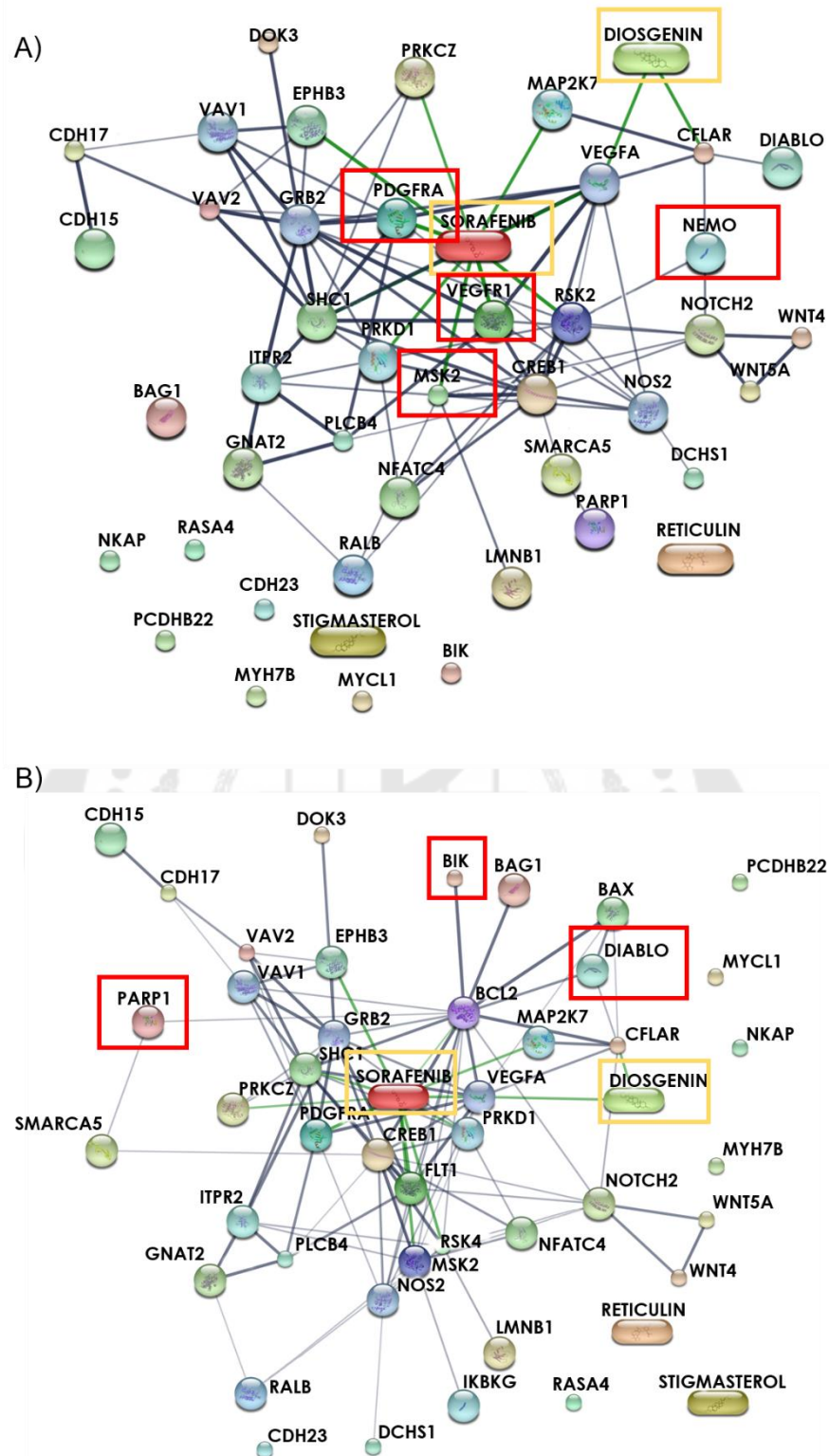


Figure 25 The association network of proteins, chemical, and drug analyzed by using STITCH 4.0.

The proliferation and angiogenesis pathway in (A) and apoptotic pathway in (B)

3.2 The up-and down-regulation proteins in treatment group compared to HCC

The heat map of 7 differentially expressed proteins among the six animal groups was observed (Figure 26). Treatment of HCC with 4 mg/kg DM caused the reduction of VEGFR1 (10.2 folds), MSK2 (1.2 folds), BIK (3.9 folds), and PARP1 (4.4 folds) compared to HCC group. HCC-bearing rats treated with 40 mg/kg DM extract showed a decrease in PDGFRA (5.7 folds), VEGFR1 (1.3 folds), and PARP1 (2.5 folds), whereas an increase in BIK (2.3 folds) compared to HCC group. Treatment of HCC with SF led to a decrease in PDGFRA, VEGFR1, MSK2, and PARP1 at 1.3, 2.4, 2.2, and 1.4-fold-change, respectively and 1.4 folds increase in BIK compared to the HCC group. The log₂ intensity data were shown in Table 5.

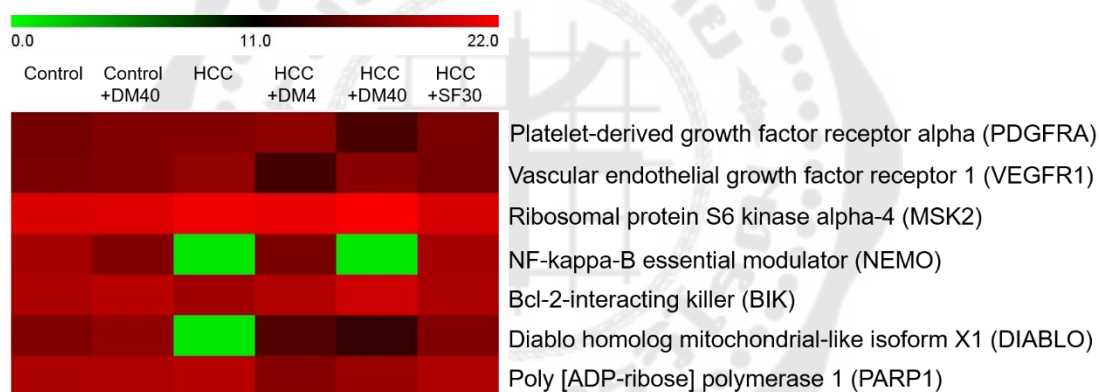


Figure 26 The heat map of 7 differentially expressed of proteins among six groups.

The intensity presented as log₂ values

Table 5 The differentially expressed of proteins among six groups

Protein	Log2 intensity					
	Control	Control +DM4	HCC	HCC +DM4	HCC +DM40	HCC+ SF30
Platelet-derived growth factor receptor alpha precursor (PDGFRA)	16.06	16.62	16.77	17.16	14.25	16.33
Vascular endothelial growth factor receptor 1 (VEGFR1)	16.29	16.54	17.36	14.01	16.97	16.13
Ribosomal protein S6 kinase alpha-4 (MSK2)	20.46	20.60	21.39	21.15	21.87	20.29
NF-kappa-B essential modulator (NEMO)	18.16	16.64	N/A	16.34	N/A	18.24
Bcl-2-interacting killer (BIK)	18.43	19.06	17.93	18.68	19.89	18.37
Diablo homolog mitochondrial-like isoform X1 (DIABLO)	16.59	17.34	N/A	14.57	13.37	16.66
Poly [ADP-ribose] polymerase 1 (PARP1)	18.44	18.54	19.05	16.91	17.70	18.52

3.3 Peptide pattern from MALDI-TOF/MS

The present study demonstrated a potential use of MALDI-TOF MS as a rapid screening method to differentiate peptide patterns of mass signals among six groups of rats. Characteristics of mass signals of 1,000–15,000-Da proteins from liver tissue and 1,000–10,000-Da serum were demonstrated in Figure 27 and 28. The MALDI-TOF/MS showed a slightly different peptide pattern between the 6 groups indicating that the treatment could change the peptide pattern in HCC rats. However, we did not find any dramatically candidate mass signals changed between control and HCC group as a diagnostic peptide biomarker for HCC.



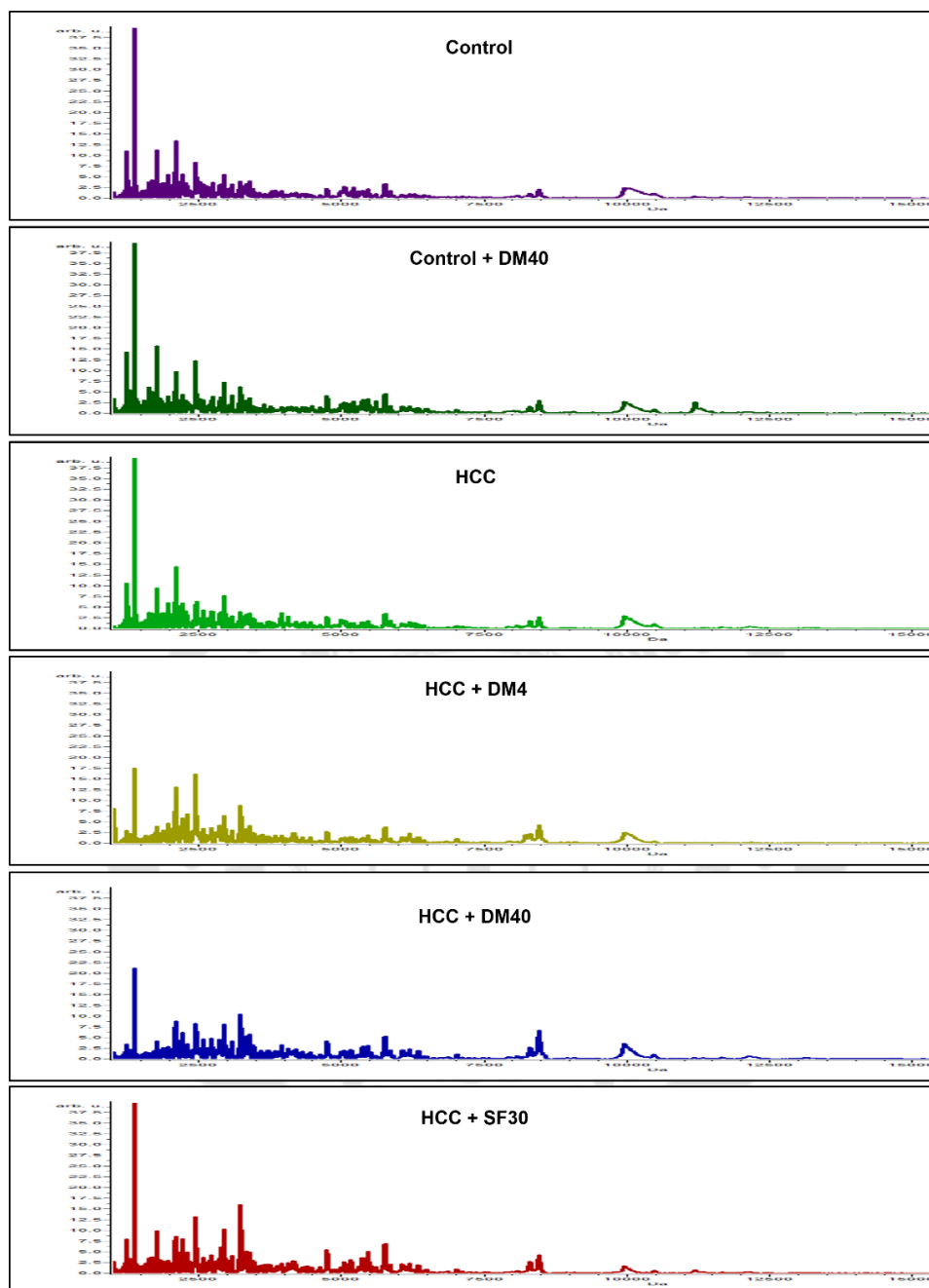


Figure 27 Overview of MALDI-TOF/TOF mass signals of 1,000–15,000 Da from liver tissues of the six animal groups.

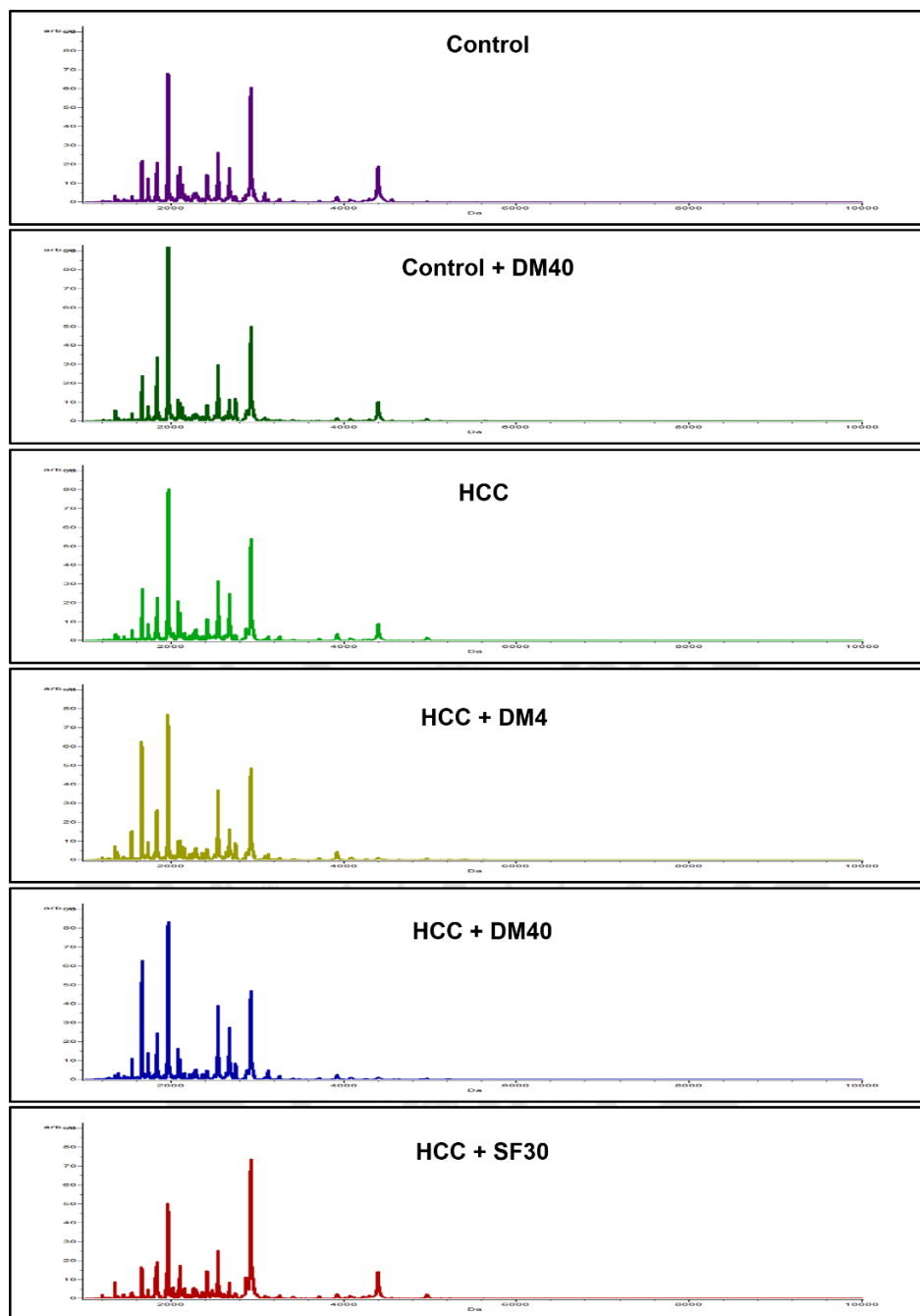


Figure 28 Overview of MALDI-TOF/TOF mass signals of 1,000–10,000 Da from serum of the six animal groups.

4. qPCR analysis

From protein profile results, the qPCR for relating genes was performed to confirm whether the gene expressions were related to protein profile or not. The mRNA relative expression of *Pdgfra*, *Flt1*, *Rps6ka4*, *Parp1* genes was increased while *Ikbkg*, *Bik*, and *Diablo* were decreased in the HCC group compared to the control group. DM 4 mg/kg treatment group showed a decreased in *Bik*, *Diablo*, *Parp1* expression significantly compared to HCC groups. DM 40 mg/kg treatment group showed a significant decreased *Pdgfra*, *Flt1*, *Bik*, *Diablo*, *Parp1* expression compared to HCC group. Both doses of DM extract and SF showed significantly increased in *Ikbkg* *Bik*, and *Diablo* compared to HCC group and significantly decreased *Parp1* expression compared to HCC group (Figure 29). Even though the DM and SF treatment did not show a significant difference in some genes compared to the HCC group, but it showed a promising trend in this study.

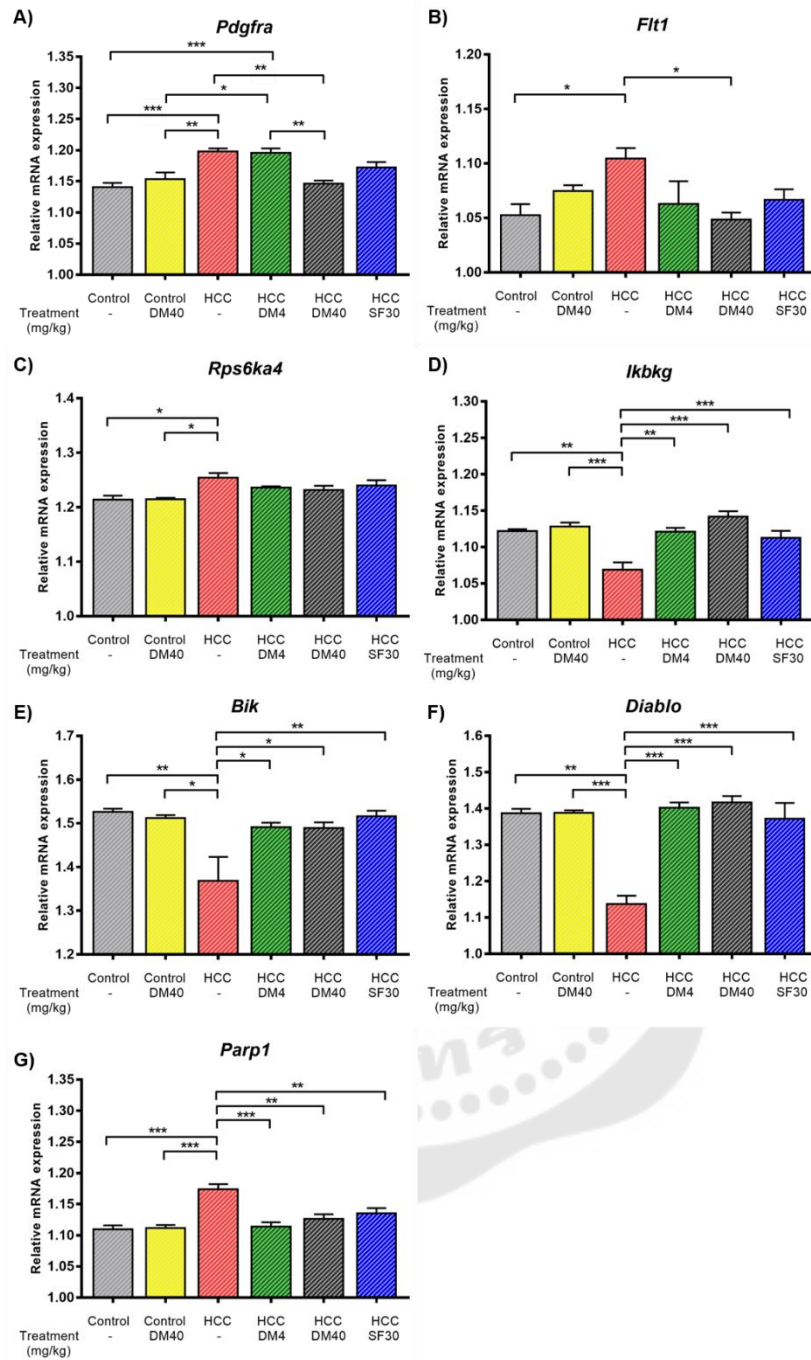


Figure 29 Diagram showing the relative gene expression of *Pdgra*, *Flt1*, *Rps6ka4*, *Bik*, *Diab1o*, and *Parp1* by real-time PCR

(* $p < 0.05$ vs. control group, ** $p < 0.01$ vs. control group, *** $p < 0.01$ vs. control group, # $p < 0.01$ vs. HCC group, ## $p < 0.01$ vs. HCC group, ### $p < 0.001$ vs. HCC group).

5. The liver enzyme and liver function test

5.1 The liver enzyme

All liver enzyme levels in control group were similar to the DM treatment only group. The level of AST and ALT were significantly increased in sorafenib-treated group compared to all other groups ($p < 0.001$). The level of ALP did not change significantly among six groups. GGT level was found in all HCC-induced group but undetectable in normal rats (Figure 30).

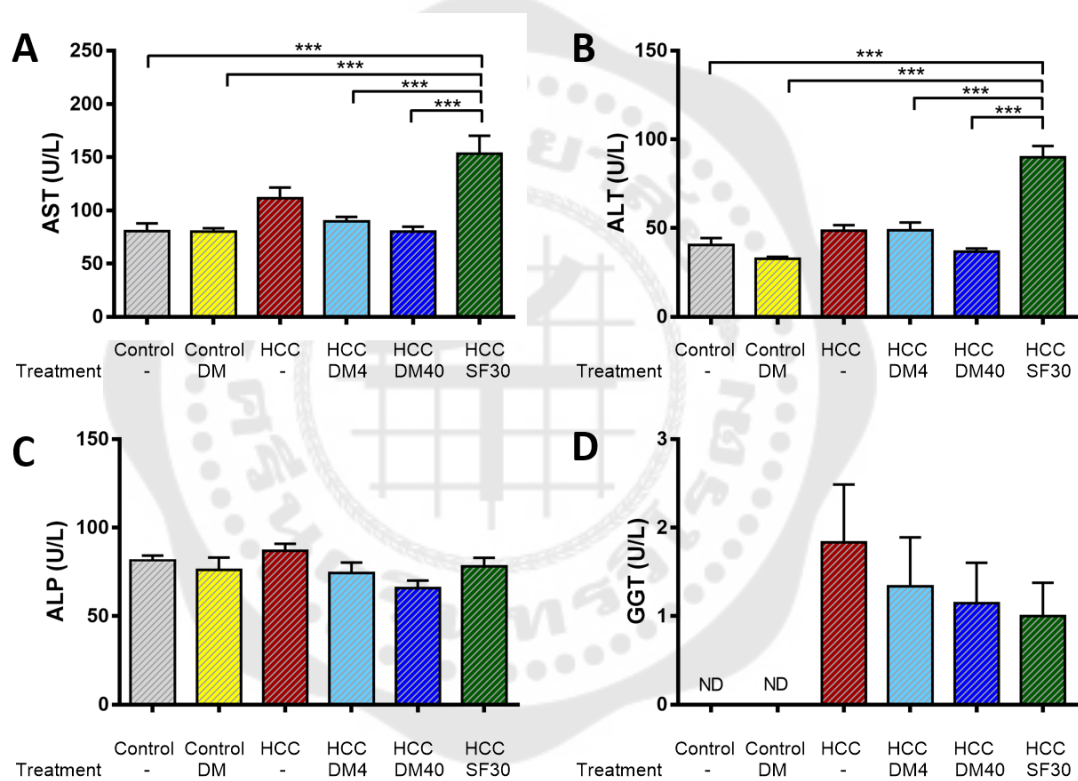


Figure 30 Diagram showing the serum liver enzyme levels. The data are presented as the mean \pm S.E.M. (N=6). A) aspartate aminotransferase (AST), B) alanine aminotransferase (ALT), C) alkaline phosphatase (ALP), D) gamma-glutamyl transferase (GGT) ($*p < 0.05$, $***p < 0.001$, ND = non-detectable).

5.2 The liver function test

The level of albumin was significantly decreased in SF-treated group compared to control group ($p < 0.05$). There was no significant difference in total protein level among six groups of rats (Figure 31).

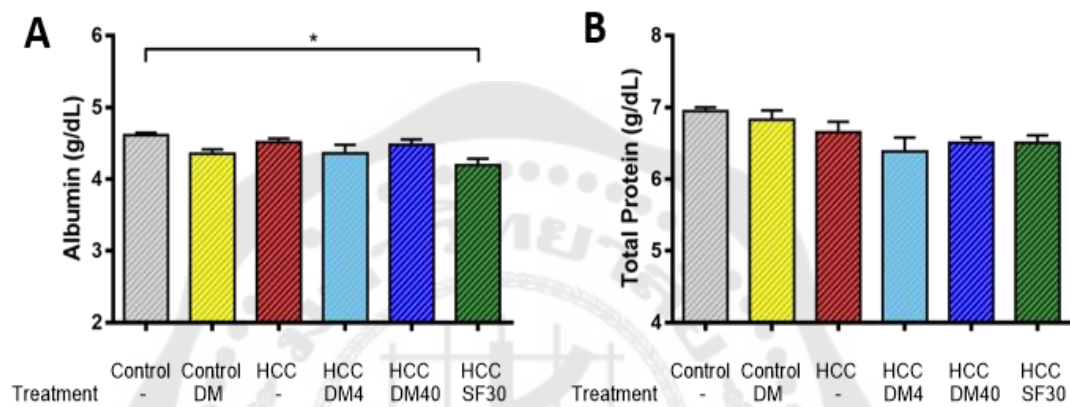


Figure 31 Diagram showing the albumin and total protein levels.

The data are presented as the mean \pm S.E.M. (N=6). A) albumin, and B) Total protein. ($*p < 0.05$)

6. MDA assay

The MDA assay was performed to determine lipid peroxidation. The result showed increased in MDA level in HCC group significantly compared to control group and reduced in DM treatment group ($p < 0.05$) (Figure 32).

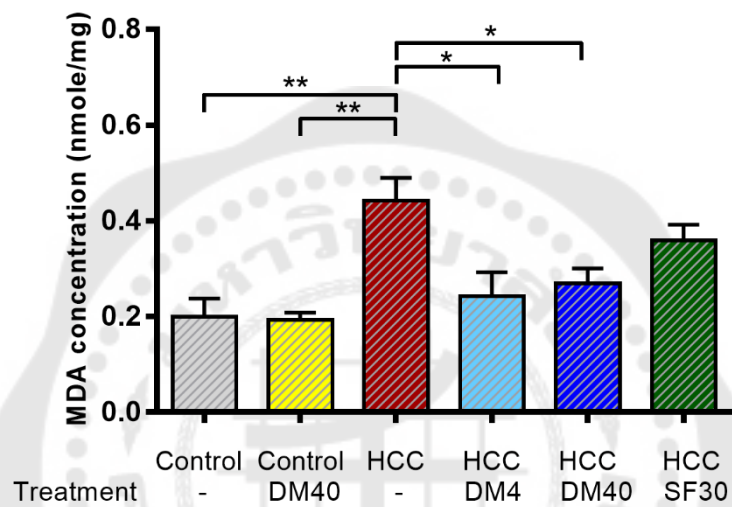


Figure 32 Photograph illustrating the MDA level in the rat liver (** $p < 0.01$ vs. control group, * $p < 0.05$ vs. HCC group,)

CHAPTER 5

DISCUSSION AND CONCLUSION

The histopathological analysis of the effects of DM extract in HCC-bearing rats revealed its potential to reduce the cancer volume and ameliorate its presentation. In HCC-bearing rats, the hepatic nodules had an abnormal reticulin staining pattern. The sorafenib-treated group had the lowest cancer volume, but inflicted more liver injury, as shown by the increased concentration of serum liver enzymes and the lower serum albumin concentration.

Hepatocarcinogenesis is the development of liver cancer due to exposure to a carcinogen that promotes gene damage that, in turn causes hepatocyte transformation. It is a multistep process that includes initiation, promotion, and progression.^(58, 61) In this study, the initiation process, the exposure to the initiator DEN, probably causes DNA mutations in hepatocytes that transform normal cells into cancer cells.^(65, 104, 105) DEN is a widely accepted and commonly used initiator of liver carcinogenesis in rat cancer models.^(60, 106) We used the second toxic agent, TAA, as promoter. This compound promotes inflammation and sustains proliferation of cancer cells specifically in the liver.⁽⁷²⁾ In low dose, TAA induces liver fibrosis and cirrhosis in the rat. Its hepatotoxic response depends on the dose and duration of administration.^(73, 77) Our protocol was adapted from El-Ashmawy et al., in 2014 by increasing dose and treatment duration of rats.⁽¹⁰⁷⁾ This modified protocol results in the development of tumors in all rats. However, rats were severely ill during HCC induction with a dropout rate of 10%. After the cancer progression period, all animals survived.

The visible gross appearance of HCC in the rats was the existence of hepatic nodules at both diaphragmatic and visceral surfaces. However, the microscopic appearance of HCC in the rat liver tissue was investigated and confirmed by the presence of the trabecular pattern (thick cell cord), acinar (pseudoglandular) pattern, solid sheath of tumor, and loss of the reticular network.⁽⁴⁹⁾ In addition, we also observed the intracytoplasmic hyaline globules and micro-steatosis in some HCC rat liver

samples.⁽¹⁰⁸⁻¹¹⁰⁾ The special reticulin staining used in this study is a reliable potential stain to reveal the reticular fibers around the tumor cell nest.⁽¹¹¹⁾ and to confirm the presence of thick hepatic cell cords in the liver tissue. The different patterns of reticulin-positive area between the normal and HCC groups were obvious in this study. Treatment of HCC with DM extract or sorafenib in our experiment clearly showed the lesser extent of reticulin-positive stained area indicating less tumor cell nests. Moreover, DM extract-treated group and sorafenib-treated group also showed the anti-cancer effects by a reduction of hepatic nodules and the reduction of abnormal hepatocytes.

Laboratory liver function tests are useful for the evaluation of liver diseases. Elevated concentrations of liver enzymes, such as AST and ALT, in serum are a response to liver injury.^(112, 113) Many studies report a significant increase in circulating liver enzyme levels in rats with DEN-induced tumors.⁽¹¹⁴⁻¹¹⁶⁾ Our previous study showed that administration of solely TAA three times weekly for eight weeks also increased plasma ALT, AST, and ALP levels and induced severe fibrosis in rat.⁽¹¹⁷⁾ Interestingly, administration of DEN followed by TAA subjection did not elevate circulating liver enzymes significantly, even though many HCC nodules had developed. Our studies, therefore, suggest that elevation of circulating liver enzymes is not a reliable HCC marker.

In the present study, sorafenib induced liver damage, as was clear from the marked elevation in serum AST, ALT activities, and the decreased serum level of albumin. We selected the dosage of sorafenib based on the effective doses commonly used in HCC rat models.^(102, 118, 119) Although Sorafenib-induced hepatotoxicity and severe liver dysfunction rarely occur, sorafenib-induced liver injury in HCC patients is reported.^(120, 121) Laboratory tests showed high circulating concentrations of liver enzymes⁽¹²²⁾ and liver necrosis with inflammatory cell infiltration in HCC patients.⁽¹²³⁾ but sorafenib-treated HCC patients with only a small change in circulating enzyme and albumin levels were reported.^(124, 125) In addition to liver damage people treated with sorafenib incur many other side effects, including fatigue, diarrhea, hand-foot skin

reaction, abdominal pain, nausea, and stomatitis.^(10, 126) Thus, clinicians should be aware of elevated circulating liver enzymes and liver failure in sorafenib-treated patients.^(121, 122)

Our proteomics analysis was undertaken to better understand the working mechanism of the extract. The analysis revealed proteins that are known to be involved in cancer proliferation and angiogenesis, including hepatocarcinogenesis.^(3, 5, 6) The receptors of these factors are all tyrosine kinases (RTKs). Similar to other growth factor receptors, they provide signals essential for survival, proliferation, and migration.⁽¹²⁷⁾ The expression of PDGFRA, VEGFR1 proteins and *Pdgfra*, *Flt1* genes were higher in the HCC than the control group. PDGFRA and VEGFR1 are RTKs.⁽¹²⁸⁾ Growth factors can bind to RTKs leading receptor dimerization then cause the activation of the kinase activity. Following kinase activation, mitogen-activated protein kinase (MAPK) pathway, Raf/ MAPK-ERK kinase (MEK)/extracellular signal-regulated kinase (ERK) pathway were found to have a role in HCC.^(3, 81) The protein MSK2 showed increased expression in HCC group in our study, which suggests more MAPK pathway occurs.

Hence, expression profile analysis showed protein that regulates NF-κB pathway, NF-κB has been shown to play an important role in the development and progression of cancer.⁽¹²⁹⁾ A role for NEMO in hepatocarcinogenesis has recently been suggested by data exclusively derived from animal models, where the selective ablation of NEMO in liver cells causes spontaneous liver tumor development.⁽¹³⁰⁾ Based on these data, a potential tumor suppressive role for NEMO was proposed. We found the up-regulation of NEMO protein in treatment groups suggest that the extract can induce NEMO to act as tumor suppressor gene. Moreover, NEMO has been found to prevent steatohepatitis and HCC.⁽¹³¹⁾

In cell survival and cell death aspects, HCC cells show an imbalance in the expression of pro- and anti-apoptotic proteins, which favors cell survival.⁽¹³²⁾ We were interested in the apoptotic pathway which is one of the potential mechanisms of the effects of DM extract on HCC in rat liver. The *in vitro* results showed that the crude extract selectively inhibited cell growth of all types of cell lines through the induction of G1 cell cycle arrest and apoptosis.⁽⁹⁷⁾ Earlier studies have shown that the number of

apoptotic cells increased to 7-12-fold after treatment with 1-4 $\mu\text{g/mL}$ dioscorealide B, one of the active compounds of the DM extract in cancer cells. In addition, dioscorealide B treatment induced the activation of caspase-7, -8, and -9, increased the expression of the pro-apoptotic protein (BAX), and decreased the anti-apoptotic protein Bcl-2.^(95, 97) The present study supports the induction of apoptotic activity by demonstrating a high expression of the pro-apoptotic BIK and DIABLO proteins. BIK inhibits the combination of BCL2 and BAX, while DIABLO can release the apoptotic factor from the mitochondria into the cytosol, which induces apoptosis. On the other hand, the expression of PARP1 was down-regulated in the DM-treated group. PARP1 plays a critical role in cell proliferation, survival, death, and DNA repair. In agreement, a variety of tumor tissues have shown an elevated content of PARP1 protein.⁽¹³²⁾ Cancers are very often deficient in expression of one or more DNA repair genes. In the apoptotic process, caspase-3 will cleave PARP, which causes DNA fragmentation. Therefore, a high PARP1 content indicates less apoptosis.

The MDA levels suggest that DM extract has antioxidant properties. HCC patients and HCC-bearing animals often have a low expression of antioxidant enzymes and elevated lipid peroxidation levels.⁽¹³³⁻¹³⁵⁾ In 2007, eight compounds that we isolated from DM extract had antioxidant activity, of which the dioscoreanone compound showed the highest antioxidant activity.⁽¹³⁶⁾

In conclusion, the proteomics profiles showed the mechanism of DM extract by inhibiting angiogenesis, proliferation, and promote apoptosis in HCC-induced rat. We recommend the low dose of extract because it shows a similar effect as the high dose. This study suggests that DM extract can be a good candidate for molecular targets drug as SF and has less liver injury than SF.

REFERENCES

1. Park DH, Shin JW, Park SK, Seo JN, Li L, Jang JJ, et al. Diethylnitrosamine (DEN) induces irreversible hepatocellular carcinogenesis through overexpression of G(1)/S-phase regulatory proteins in rat. *Toxicol Lett.* 2009 Dec 15; 191(2-3): 321-6.
2. Whittaker S, Marais R, Zhu AX. The role of signaling pathways in the development and treatment of hepatocellular carcinoma. *Oncogene.* 2010 Sep; 29(36): 4989-5005.
3. Meguro M, Mizuguchi T, Kawamoto M, Hirata K. The molecular pathogenesis and clinical implications of hepatocellular carcinoma. *Int J Hepatol.* 2011; 2011: 818672.
4. Anastas JN, Moon RT. WNT signalling pathways as therapeutic targets in cancer. *Nat Rev Cancer.* 2013 Jan; 13(1): 11-26.
5. Hatano E, Uemoto S. Molecular pathogenesis of hepatocellular carcinoma. *Nihon Shokakibyō Gakkai Zasshi.* 2011 Aug; 108(8): 1347-53.
6. Thorgeirsson SS, Grisham JW. Molecular pathogenesis of human hepatocellular carcinoma. *Nat Genet.* 2002 Aug; 31(4): 339-46.
7. Blanc JF, Lalanne C, Plomion C, Schmitter JM, Bathany K, Gion JM, et al. Proteomic analysis of differentially expressed proteins in hepatocellular carcinoma developed in patients with chronic viral hepatitis C. *Proteomics.* 2005 Sep; 5(14): 3778-89.
8. Kim W, Lim SO, Kim JS, Ryu YH, Byeon JY, Kim HJ, et al. Comparison of proteome between hepatitis B virus- and hepatitis C virus-associated hepatocellular carcinoma. *Clin Cancer Res.* 2003 Nov 15; 9(15): 5493-500.
9. Luk JM, Lam CT, Siu AFM, Lam BY, Ng IOL, Hu MY, et al. Proteomic profiling of hepatocellular carcinoma in Chinese cohort reveals heat-shock proteins (Hsp27, Hsp70, GRP78) up-regulation and their associated prognostic values. *Proteomics.* 2006 Feb; 6(3): 1049-57.
10. Gauthier A, Ho M. Role of sorafenib in the treatment of advanced hepatocellular carcinoma: An update. *Hepatol Res.* 2013 Feb; 43(2): 147-54.
11. Schmieder R, Puehler F, Neuhaus R, Kissel M, Adjei AA, Miner JN, et al. Allosteric

- MEK1/2 Inhibitor Refametinib (BAY 86-9766) in Combination with Sorafenib Exhibits Antitumor Activity in Preclinical Murine and Rat Models of Hepatocellular Carcinoma. *Neoplasia*. 2013 Oct; 15(10): 1147-57.
12. Llovet JM, Bruix J. Molecular targeted therapies in hepatocellular carcinoma. *Hepatology*. 2008 Oct; 48(4): 1312-27.
13. Doudach L, Benbacer L, Meddah B, Faouzi MEA, Hammani K, Mzibri ME, et al. Extract of 1:5 mixture of five Moroccan medicinal plants has cytotoxic effect on some human cancer cell lines. *International Journal of Pharmacy*. 2013; 3(2): 301-7.
14. Itharat A, Thongdeeying P, Ruangnoo S. Isolation and characterization of a new cytotoxic dihydrophenanthrene from *Dioscorea membranacea* rhizomes and its activity against five human cancer cell lines. *J Ethnopharmacol*. 2014 Oct 28; 156: 130-4.
15. Reanmongkol W, Itharat A, Bouking P. Investigation of the anti-inflammatory, analgesic and antipyretic activities of the extracts from the rhizome of *Dioscorea membranacea* Pierre in experimental animals. *Songklanakarin J Sci Technol*. 2007; 29: 49-57.
16. Panthong S, Ruangnoo S, Thongdeeying P, Sriwanthana B, Itharat A. Immunomodulatory activity of *Dioscorea membranacea* Pierre rhizomes and of its main active constituent Dioscorealide B. *BMC Complement Altern Med*. 2014 Oct 16; 14: 403.
17. Itharat A, Houghton PJ, Eno-Amooquaye E, Burke PJ, Sampson JH, Raman A. In vitro cytotoxic activity of Thai medicinal plants used traditionally to treat cancer. *J Ethnopharmacol*. 2004 Jan; 90(1): 33-8.
18. Tewtrakul S, Itharat A. Anti-allergic substances from the rhizomes of *Dioscorea membranacea*. *Bioorg Med Chem*. 2006 Dec 15; 14(24): 8707-11.
19. Tewtrakul S, Itharat A. Nitric oxide inhibitory substances from the rhizomes of *Dioscorea membranacea*. *J Ethnopharmacol*. 2007 Feb 12; 109(3): 412-6.
20. Lim SO, Park SJ, Kim W, Park SG, Kim HJ, Kim YI, et al. Proteome analysis of hepatocellular carcinoma. *Biochem Bioph Res Co*. 2002 Mar 8; 291(4): 1031-7.
21. Geller DA, Goss JA, Tsung A. Chapter 31. Liver. In: Brunicaardi FC, Andersen DK, Billiar TR, Dunn DL, Hunter JG, Matthews JB, et al., editors. *Schwartz's Principles of*

Surgery, 9e. New York, NY: The McGraw-Hill Companies; 2010.

22. Casey G. Diseases of the Liver. *Nurs N Z*. 2016 Dec; 22(11): 20-4.
23. Mitra V, Metcalf J. Metabolic functions of the liver. *Anaesthesia & Intensive Care Medicine*. 2012; 13(2): 54-5.
24. Kennedy PA, Madding GF. Surgical anatomy of the liver. *Surg Clin North Am*. 1977 Apr; 57(2): 233-44.
25. Sutherland F, Harris J. Claude Couinaud: a passion for the liver. *Arch Surg*. 2002 Nov; 137(11): 1305-10.
26. Blumgart L, Hann L. Surgical and Radiologic Anatomy of the Liver, Biliary Tract, and Pancreas. *Blumgart's Surgery of the Liver, Biliary Tract, and Pancreas*. 2012 01/01; 1: 33-4.
27. Townsend CM, Beauchamp RD, Evers BM, Mattox KL. The liver. In: Townsend CM, Beauchamp RD, Evers BM, Mattox KL, editors. *Sabiston textbook of surgery : the biological basis of modern surgical practice*. 10 ed: Elsevier; 2017. p. 1418-81.
28. Martins PNA, Neuhaus P. Surgical anatomy of the liver, hepatic vasculature and bile ducts in the rat. *Liver International*. 2007; 27(3): 384-92.
29. Shi H, Yang G, Zheng T, Wang J, Li L, Liang Y, et al. A preliminary study of ALPPS procedure in a rat model. *Sci Rep*. 2015 Dec 3; 5: 17567.
30. Roy-Chowdhury N, Roy-Chowdhury J. Liver Physiology and Energy Metabolism. In: Feldman M, Friedman L, Brandt L, editors. *Sleisenger and Fordtran's Gastrointestinal and Liver Disease*. 9 ed. Philadelphia: Elsevier Saunders; 2016. p. 1223-42.
31. Paulsen DF. Chapter 16. Glands Associated with the Digestive Tract. *Histology & Cell Biology: Examination & Board Review*, 5e. New York, NY: The McGraw-Hill Companies; 2010.
32. Young B, O'Dowd G, Woodford P. Liver and pancreas. *Wheater's functional histology : a text and colour atlas*. 6 ed. Philadelphia: Churchill Livingstone/Elsevier; 2013.
33. Rogers AB, Dintzis RZ. 13 - Liver and Gallbladder. In: Treuting PM, Dintzis SM, editors. *Comparative Anatomy and Histology*. San Diego: Academic Press; 2012. p. 193-201.

34. Friedman SL. Hepatic stellate cells: protean, multifunctional, and enigmatic cells of the liver. *Physiol Rev.* 2008 Jan; 88(1): 125-72.
35. Kisseleva T, Brenner DA. Hepatic stellate cells and the reversal of fibrosis. *J Gastroenterol Hepatol.* 2006 Oct; 21 Suppl 3: S84-7.
36. Dancygier H. Microscopic Anatomy. In: Dancygier H, editor. *Clinical hepatology : principles and practice of hepatobiliary diseases.* Berlin: Springer; 2010. p. 11-4.
37. Tsutsui H, Nishiguchi S. Importance of Kupffer cells in the development of acute liver injuries in mice. *Int J Mol Sci.* 2014 May 5; 15(5): 7711-30.
38. Tso P, McGill J. The Physiology of the Liver. In: Rhoades RA, Tanner GA, editors. *Medical Physiology.* 2 ed: Lippincott Williams & Wilkins; 2004. p. 514-25.
39. Fiebig T, Boll H, Figueiredo G, Kerl HU, Nittka S, Groden C, et al. Three-Dimensional In Vivo Imaging of the Murine Liver: A Micro-Computed Tomography-Based Anatomical Study. *Plos One.* 2012 Feb 8; 7(2).
40. Paradis V. Histopathology of Hepatocellular Carcinoma. In: Vauthey J-N, Brouquet A, editors. *Multidisciplinary Treatment of Hepatocellular Carcinoma.* Berlin, Heidelberg: Springer; 2013. p. 21-32.
41. Carr BI. Tumors of the Liver and Biliary Tree. In: Kasper D, Fauci A, Hauser S, Longo D, Jameson JL, Loscalzo J, editors. *Harrison's Principles of Internal Medicine, 19e.* New York, NY: McGraw-Hill Education; 2014.
42. Turcotte S, Jarnagin WR. Liver & Portal Venous System. In: Doherty GM, editor. *CURRENT Diagnosis & Treatment: Surgery, 14e.* New York, NY: McGraw-Hill Education; 2015.
43. Kemp WL, Burns DK, Brown TG. Chapter 15. Pathology of the Liver, Gallbladder, and Pancreas. *Pathology: The Big Picture.* New York, NY: The McGraw-Hill Companies; 2008.
44. Bagi CM, Andresen CJ. Models of hepatocellular carcinoma and biomarker strategy. *Cancers (Basel).* 2010 Jul 7; 2(3): 1441-52.
45. Thomas MB, Jaffe D, Choti MM, Belghiti J, Curley S, Fong Y, et al. Hepatocellular carcinoma: consensus recommendations of the National Cancer Institute Clinical Trials

Planning Meeting. *J Clin Oncol*. 2010 Sep 1; 28(25): 3994-4005.

46. Bruix J, Sherman M, American Association for the Study of Liver D. Management of hepatocellular carcinoma: an update. *Hepatology*. 2011 Mar; 53(3): 1020-2.

47. Forner A, Gilibert M, Bruix J, Raoul JL. Treatment of intermediate-stage hepatocellular carcinoma. *Nat Rev Clin Oncol*. 2014 Sep; 11(9): 525-35.

48. Bautista M, Andres D, Cascales M, Morales-Gonzalez JA, Sanchez-Reus MI, Madrigal-Santillan E, et al. Role of Kupffer cells in thioacetamide-induced cell cycle dysfunction. *Molecules*. 2011 Sep 29; 16(10): 8319-31.

49. Schlageter M, Terracciano LM, D'Angelo S, Sorrentino P. Histopathology of hepatocellular carcinoma. *World J Gastroenterol*. 2014 Nov 21; 20(43): 15955-64.

50. Ghosh S, Bhattacharyya S, Rashid K, Sil PC. Curcumin protects rat liver from streptozotocin-induced diabetic pathophysiology by counteracting reactive oxygen species and inhibiting the activation of p53 and MAPKs mediated stress response pathways. *Toxicol Rep*. 2015; 2: 365-76.

51. Nakashima O, Sugihara S, Kage M, Kojiro M. Pathomorphologic characteristics of small hepatocellular carcinoma: a special reference to small hepatocellular carcinoma with indistinct margins. *Hepatology*. 1995 Jul; 22(1): 101-5.

52. Nakashima Y, Nakashima O, Hsia CC, Kojiro M, Tabor E. Vascularization of small hepatocellular carcinomas: correlation with differentiation. *Liver*. 1999 Feb; 19(1): 12-8.

53. Villanueva A, Llovet JM. Targeted therapies for hepatocellular carcinoma. *Gastroenterology*. 2011 May; 140(5): 1410-26.

54. Cheng AL, Kang YK, Chen Z, Tsao CJ, Qin S, Kim JS, et al. Efficacy and safety of sorafenib in patients in the Asia-Pacific region with advanced hepatocellular carcinoma: a phase III randomised, double-blind, placebo-controlled trial. *Lancet Oncol*. 2009 Jan; 10(1): 25-34.

55. Liu L, Cao Y, Chen C, Zhang X, McNabola A, Wilkie D, et al. Sorafenib blocks the RAF/MEK/ERK pathway, inhibits tumor angiogenesis, and induces tumor cell apoptosis in hepatocellular carcinoma model PLC/PRF/5. *Cancer Res*. 2006 Dec 15; 66(24): 11851-8.

56. Wilhelm S, Carter C, Lynch M, Lowinger T, Dumas J, Smith RA, et al. Discovery

and development of sorafenib: a multikinase inhibitor for treating cancer. *Nat Rev Drug Discov.* 2006 Oct; 5(10): 835-44.

57. Wang Y, Gao JC, Zhang D, Zhang J, Ma JJ, Jiang HQ. New insights into the antifibrotic effects of sorafenib on hepatic stellate cells and liver fibrosis. *J Hepatol.* 2010 Jul; 53(1): 132-44.

58. Pitot HC. The molecular biology of carcinogenesis. *Cancer.* 1993 Aug 1; 72(3 Suppl): 962-70.

59. Kaur S, Singh G, Kaur K. Cancer stem cells: an insight and future perspective. *J Cancer Res Ther.* 2014 Oct-Dec; 10(4): 846-52.

60. Asohan K, Krishnan KG, Thirupathi A, Akhilesh U, Sivanandham V. Preventive effect of *Shorea robusta* bark extract against diethylnitrosamine-induced hepatocellular carcinoma in rats. *Int Res J Medical Sci.* 2013 Jan; 1: 2-9.

61. Mukherjee B, Kumar M, Mobaswar C. Chemically Induced Hepatocellular Carcinoma and Stages of Development with Biochemical and Genetic Modulation: A Special Reference to Insulin-Like-Growth Factor II and Raf Gene Signaling. In: Lau WY, editor. *Hepatocellular Carcinoma - Basic Research*: InTech; 2012.

62. Bhattacharya MN, C.K. P. A new experimental model of rat hepatocellular carcinoma. *Experimental Oncology.* 2003 March; 25(1): 55-9.

63. Abdel Salam OM, Mohammed NA, Sleem AA, Farrag AR. The effect of antidepressant drugs on thioacetamide-induced oxidative stress. *Eur Rev Med Pharmacol Sci.* 2013 Mar; 17(6): 735-44.

64. Pitot HC, Dragan Y, Sargent L, Xu YH. Biochemical markers associated with the stages of promotion and progression during hepatocarcinogenesis in the rat. *Environ Health Perspect.* 1991 Jun; 93: 181-9.

65. Becker RA, Shank RC. Kinetics of formation and persistence of ethylguanines in DNA of rats and hamsters treated with diethylnitrosamine. *Cancer Res.* 1985 May; 45(5): 2076-84.

66. Liu X-e, Dewaele S, Vanhooren V, Fan Y-D, Wang L, Van Huisse J, et al. Alteration of N-glycome in diethylnitrosamine-induced hepatocellular carcinoma mice: a non-invasive

monitoring tool for liver cancer. *Liver International*. 2010; 30(8): 1221-8.

67. Ahmed H, Shousha W, El-mezayen H, Ismaiel N, Mahmoud N. In vivo antitumor potential of carvacrol against hepatocellular carcinoma in rat model. *World journal of pharmacy and pharmaceutical sciences*. 2013 Sep; 2: 2367-96.

68. Thangavel P, Vaiyapuri M. Antiproliferative and apoptotic effects of naringin on diethylnitrosamine induced hepatocellular carcinoma in rats. *Biomedicine & Aging Pathology*. 2013 April; 3(2): 59-64.

69. Karin M, Greten FR. NF-kappaB: linking inflammation and immunity to cancer development and progression. *Nat Rev Immunol*. 2005 Oct; 5(10): 749-59.

70. Qi Y, Chen X, Chan CY, Li D, Yuan C, Yu F, et al. Two-dimensional differential gel electrophoresis/analysis of diethylnitrosamine induced rat hepatocellular carcinoma. *Int J Cancer*. 2008 Jun 15; 122(12): 2682-8.

71. Valko M, Rhodes CJ, Moncol J, Izakovic M, Mazur M. Free radicals, metals and antioxidants in oxidative stress-induced cancer. *Chem Biol Interact*. 2006 Mar 10; 160(1): 1-40.

72. Chilakapati J, Shankar K, Korrapati MC, Hill RA, Mehendale HM. Saturation toxicokinetics of thioacetamide: role in initiation of liver injury. *Drug Metab Dispos*. 2005 Dec; 33(12): 1877-85.

73. Munoz Torres E, Paz Bouza JI, Lopez Bravo A, Abad Hernandez MM, Carrascal Marino E. Experimental thioacetamide-induced cirrhosis of the liver. *Histol Histopathol*. 1991 Jan; 6(1): 95-100.

74. Hajovsky H, Hu G, Koen Y, Sarma D, Cui W, Moore DS, et al. Metabolism and toxicity of thioacetamide and thioacetamide S-oxide in rat hepatocytes. *Chem Res Toxicol*. 2012 Sep 17; 25(9): 1955-63.

75. Chilakapati J, Korrapati MC, Hill RA, Warbritton A, Latendresse JR, Mehendale HM. Toxicokinetics and toxicity of thioacetamide sulfoxide: a metabolite of thioacetamide. *Toxicology*. 2007 Feb 12; 230(2-3): 105-16.

76. Kang JS, Wanibuchi H, Morimura K, Wongpoomchai R, Chusiri Y, Gonzalez FJ, et al. Role of CYP2E1 in thioacetamide-induced mouse hepatotoxicity. *Toxicol Appl*

Pharmacol. 2008 May 1; 228(3): 295-300.

77. Koen YM, Sarma D, Hajovsky H, Galeva NA, Williams TD, Staudinger JL, et al. Protein targets of thioacetamide metabolites in rat hepatocytes. *Chem Res Toxicol.* 2013 Apr 15; 26(4): 564-74.

78. Ramaiah SK, Apte U, Mehendale HM. Cytochrome P450E1 induction increases thioacetamide liver injury in diet-restricted rats. *Drug Metab Dispos.* 2001 Aug; 29(8): 1088-95.

79. Alexia C, Fallot G, Lasfer M, Schweizer-Groyer G, Groyer A. An evaluation of the role of insulin-like growth factors (IGF) and of type-I IGF receptor signalling in hepatocarcinogenesis and in the resistance of hepatocarcinoma cells against drug-induced apoptosis. *Biochem Pharmacol.* 2004 Sep 15; 68(6): 1003-15.

80. Roberts LR, Gores GJ. Hepatocellular carcinoma: molecular pathways and new therapeutic targets. *Semin Liver Dis.* 2005; 25(2): 212-25.

81. Abou-Alfa GK, Schwartz L, Ricci S, Amadori D, Santoro A, Figer A, et al. Phase II study of sorafenib in patients with advanced hepatocellular carcinoma. *J Clin Oncol.* 2006 Sep 10; 24(26): 4293-300.

82. Kumar M, Zhao X, Wang XW. Molecular carcinogenesis of hepatocellular carcinoma and intrahepatic cholangiocarcinoma: one step closer to personalized medicine? *Cell Biosci.* 2011 Jan 24; 1(1): 5.

83. Heindryckx F, Colle I, Van Vlierberghe H. Experimental mouse models for hepatocellular carcinoma research. *Int J Exp Pathol.* 2009 Aug; 90(4): 367-86.

84. Fabregat I. Dysregulation of apoptosis in hepatocellular carcinoma cells. *World J Gastroenterol.* 2009 Feb 7; 15(5): 513-20.

85. Fabregat I, Roncero C, Fernandez M. Survival and apoptosis: a dysregulated balance in liver cancer. *Liver Int.* 2007 Mar; 27(2): 155-62.

86. Elmore S. Apoptosis: a review of programmed cell death. *Toxicol Pathol.* 2007 Jun; 35(4): 495-516.

87. Hu W, Kavanagh JJ. Anticancer therapy targeting the apoptotic pathway. *Lancet Oncol.* 2003 Dec; 4(12): 721-9.

88. Saraste A, Pulkki K. Morphologic and biochemical hallmarks of apoptosis. *Cardiovasc Res.* 2000 Feb; 45(3): 528-37.
89. Poon TC, Johnson PJ. Proteome analysis and its impact on the discovery of serological tumor markers. *Clin Chim Acta.* 2001 Nov; 313(1-2): 231-9.
90. Chignard N, Beretta L. Proteomics for hepatocellular carcinoma marker discovery. *Gastroenterology.* 2004 Nov; 127(5 Suppl 1): S120-5.
91. Seow TK, Liang RC, Leow CK, Chung MC. Hepatocellular carcinoma: from bedside to proteomics. *Proteomics.* 2001 Oct; 1(10): 1249-63.
92. Rodrigo MA, Zitka O, Krizkova S, Moulick A, Adam V, Kizek R. MALDI-TOF MS as evolving cancer diagnostic tool: a review. *J Pharm Biomed Anal.* 2014 Jul; 95: 245-55.
93. Itharat A, Plubrukarn A, Kongsaree P, Bui T, Keawpradub N, Houghton PJ. Dioscorealides and dioscoreanone, novel cytotoxic naphthofuranoxepins, and 1,4-phenanthraquinone from *Dioscorea membranacea* Pierre. *Org Lett.* 2003 Aug 7; 5(16): 2879-82.
94. Maneenoon K. Medicinal plants of the genus *Dioscorea* L. used in traditional Thai medicine prescriptions. *KKU Science Journal.* 2013; 41(4): 797-807.
95. Saekoo J, Dechsukum C, Graidist P, Itharat A. Cytotoxic effect and its mechanism of dioscorealide B from *Dioscorea membranacea* against breast cancer cells. *J Med Assoc Thai.* 2010 Dec; 93 Suppl 7: S277-82.
96. Rithichai P, Itharat A, Jirakiattikul Y, Ruangnoo S. Growth of *Dioscorea membranacea* Pierre ex Prain & Burkill and dioscorealide B content at different harvest times. *Pharmacologyonline.* 2013 Jan; 1: 225-9.
97. Aree K, Panunto W, Tanuchit S, Itharat A, Hansakul P. Cellular mechanisms of anticancer effects of *Dioscorea membranacea* Pierre. *Thammasat Medical Journal.* 2011; 11(2): 210-20.
98. Thongdeeying P, editor. Inhibitory effect on LPS-induced PGE2 release in RAW264.7 cells of compounds from *Dioscorea membranacea*. Proceedings of the 1st Conference on Graduate Student Network of Thailand (GS-NETT 2012); 2012 Dec 18; Thammasat university, Pathumthani.

99. Mollica JQ, Cara DC, D'Auriol M, Oliveira VB, Cesar IC, Brandão MGL. Anti-inflammatory activity of American yam *Dioscorea trifida* L.f. in food allergy induced by ovalbumin in mice. *Journal of Functional Foods*. 2013 Oct; 5(4): 1975-84.
100. Seemakhan S. In vitro anti-inflammatory activity of some medicinal plants from ban ang-ed official community forest, chanthaburi province. Burapha University; 2015.
101. Tewtrakul S, Itharat A, Rattanasuwan P. Anti-HIV-1 protease- and HIV-1 integrase activities of Thai medicinal plants known as Hua-Khao-Yen. *J Ethnopharmacol*. 2006 Apr 21; 105(1-2): 312-5.
102. Gu FM, Li QL, Gao Q, Jiang JH, Huang XY, Pan JF, et al. Sorafenib inhibits growth and metastasis of hepatocellular carcinoma by blocking STAT3. *World J Gastroenterol*. 2011 Sep 14; 17(34): 3922-32.
103. Livak KJ, Schmittgen TD. Analysis of relative gene expression data using real-time quantitative PCR and the 2(-Delta Delta C(T)) Method. *Methods*. 2001 Dec; 25(4): 402-8.
104. Verna L, Whysner J, Williams GM. N-nitrosodiethylamine mechanistic data and risk assessment: bioactivation, DNA-adduct formation, mutagenicity, and tumor initiation. *Pharmacol Ther*. 1996 Jan; 71(1-2): 57-81.
105. Liu JG, Zhao HJ, Liu YJ, Liu YW, Wang XL. Effect of two selenium sources on hepatocarcinogenesis and several angiogenic cytokines in diethylnitrosamine-induced hepatocarcinoma rats. *J Trace Elem Med Biol*. 2012 Oct; 26(4): 255-61.
106. Ha WS, Kim CK, Song SH, Kang CB. Study on mechanism of multistep hepatotumorigenesis in rat: development of hepatotumorigenesis. *J Vet Sci*. 2001 Apr; 2(1): 53-8.
107. El-Ashmawy NE, El-Bahrawy HA, Shamloula MM, El-Feky OA. Biochemical/metabolic changes associated with hepatocellular carcinoma development in mice. *Tumour Biol*. 2014 Jun; 35(6): 5459-66.
108. Cohen C. Intracytoplasmic hyaline globules in hepatocellular carcinomas. *Cancer*. 1976 Apr; 37(4): 1754-8.
109. Chelliah AR, Radhi JM. Hepatocellular Carcinoma with Prominent Intracytoplasmic Inclusions: A Report of Two Cases. *Case Reports Hepatol*. 2016; 2016: 2032714.

110. Ismail MH. Glypican-3-Expressing Hepatocellular Carcinoma in a Non-Cirrhotic Patient with Nonalcoholic Steatohepatitis: Case Report and Literature Review. *Gastroenterology Res.* 2010 Oct; 3(5): 223-8.
111. Hong H, Patonay B, Finley J. Unusual reticulin staining pattern in well-differentiated hepatocellular carcinoma. *Diagn Pathol.* 2011 Feb 22; 6: 15.
112. Gowda S, Desai PB, Hull VV, Math AA, Vernekar SN, Kulkarni SS. A review on laboratory liver function tests. *Pan Afr Med J.* 2009 Nov 22; 3: 17.
113. Kim WR, Flamm SL, Di Bisceglie AM, Bodenheimer HC. Serum activity of alanine aminotransferase (ALT) as an indicator of health and disease. *Hepatology.* 2008; 47(4): 1363-70.
114. Cui H, Han F, Zhang L, Wang L, Kumar M. Gamma linolenic acid regulates PHD2 mediated hypoxia and mitochondrial apoptosis in DEN induced hepatocellular carcinoma. *Drug Des Devel Ther.* 2018; 12: 4241-52.
115. Alzahrani FA, El-Magd MA, Abdelfattah-Hassan A, Saleh AA, Saadeldin IM, El-Shetry ES, et al. Potential Effect of Exosomes Derived from Cancer Stem Cells and MSCs on Progression of DEN-Induced HCC in Rats. *Stem Cells Int.* 2018; 2018: 8058979.
116. El-Magd MA, Mohamed Y, El-Shetry ES, Elsayed SA, Abo Gazia M, Abdel-Aleem GA, et al. Melatonin maximizes the therapeutic potential of non-preconditioned MSCs in a DEN-induced rat model of HCC. *Biomed Pharmacother.* 2019 Jun; 114: 108732.
117. Rodniem S, Tiya V, Nilbu-Nga C, Poonkhum R, Pongmayteegul S, Pradidarcheep W. Protective effect of alpha-mangostin on thioacetamide-induced liver fibrosis in rats as revealed by morpho-functional analysis. *Histol Histopathol.* 2019 Apr; 34(4): 419-30.
118. Li QL, Gu FM, Wang Z, Jiang JH, Yao LQ, Tan CJ, et al. Activation of PI3K/AKT and MAPK pathway through a PDGFRbeta-dependent feedback loop is involved in rapamycin resistance in hepatocellular carcinoma. *Plos One.* 2012 Mar; 7(3): e33379.
119. Kiroplatis K, Fouzas I, Katsiki E, Patsiaoura K, Daoudaki M, Komninou A, et al. The effect of sorafenib on liver regeneration and angiogenesis after partial hepatectomy in rats. *Hippokratia.* 2015 Jul-Sep; 19(3): 249-55.
120. Van Hootegem A, Verslype C, Van Steenberghe W. Sorafenib-induced liver failure:

a case report and review of the literature. *Case Reports Hepatol.* 2011; 2011: 941395.

121. Kuroda D, Hayashi H, Nitta H, Imai K, Abe S, Hashimoto D, et al. Successful treatment for sorafenib-induced liver dysfunction: a report of case with liver biopsy. *Surg Case Rep.* 2016 Dec; 2(1): 4.

122. Wang QL, Li XJ, Yao ZC, Zhang P, Xu SL, Huang H, et al. Sorafenib-induced acute-on-chronic liver failure in a patient with hepatocellular carcinoma after transarterial chemoembolization and radiofrequency ablation: A case report. *Mol Clin Oncol.* 2017 Oct; 7(4): 693-5.

123. Fisher K, Vuppalanchi R, Saxena R. Drug-Induced Liver Injury. *Arch Pathol Lab Med.* 2015 Jul; 139(7): 876-87.

124. Llovet JM, Ricci S, Mazzaferro V, Hilgard P, Gane E, Blanc JF, et al. Sorafenib in advanced hepatocellular carcinoma. *N Engl J Med.* 2008 Jul 24; 359(4): 378-90.

125. Raoul JL, Bruix J, Greten TF, Sherman M, Mazzaferro V, Hilgard P, et al. Relationship between baseline hepatic status and outcome, and effect of sorafenib on liver function: SHARP trial subanalyses. *J Hepatol.* 2012 May; 56(5): 1080-8.

126. Cho JY, Paik YH, Lim HY, Kim YG, Lim HK, Min YW, et al. Clinical parameters predictive of outcomes in sorafenib-treated patients with advanced hepatocellular carcinoma. *Liver Int.* 2013 Jul; 33(6): 950-7.

127. Hofer E, Schweighofer B. Signal transduction induced in endothelial cells by growth factor receptors involved in angiogenesis. *Thromb Haemost.* 2007 Mar; 97(3): 355-63.

128. Demoulin JB, Essagher A. PDGF receptor signaling networks in normal and cancer cells. *Cytokine Growth Factor Rev.* 2014 Jun; 25(3): 273-83.

129. Park MH, Hong JT. Roles of NF-kappaB in Cancer and Inflammatory Diseases and Their Therapeutic Approaches. *Cells.* 2016 Mar 29; 5(2).

130. Aigelsreiter A, Haybaeck J, Schauer S, Kiesslich T, Bettermann K, Griessbacher A, et al. NEMO expression in human hepatocellular carcinoma and its association with clinical outcome. *Hum Pathol.* 2012 Jul; 43(7): 1012-9.

131. Kondylis V, Polykratis A, Ehlken H, Ochoa-Callejero L, Straub BK, Krishna-

- Subramanian S, et al. NEMO Prevents Steatohepatitis and Hepatocellular Carcinoma by Inhibiting RIPK1 Kinase Activity-Mediated Hepatocyte Apoptosis. *Cancer Cell*. 2015 Nov 9; 28(5): 582-98.
132. Wang L, Liang C, Li F, Guan D, Wu X, Fu X, et al. PARP1 in Carcinomas and PARP1 Inhibitors as Antineoplastic Drugs. *Int J Mol Sci*. 2017 Oct 8; 18(10): 2111.
133. Jungst C, Cheng B, Gehrke R, Schmitz V, Nischalke HD, Ramakers J, et al. Oxidative damage is increased in human liver tissue adjacent to hepatocellular carcinoma. *Hepatology*. 2004 Jun; 39(6): 1663-72.
134. Hussain SP, Schwank J, Staib F, Wang XW, Harris CC. TP53 mutations and hepatocellular carcinoma: insights into the etiology and pathogenesis of liver cancer. *Oncogene*. 2007 Apr 2; 26(15): 2166-76.
135. Amin A, Hamza AA, Bajbouj K, Ashraf SS, Daoud S. Saffron: a potential candidate for a novel anticancer drug against hepatocellular carcinoma. *Hepatology*. 2011 Sep 2; 54(3): 857-67.
136. Itharat A, Plubrukan A, Kaewpradub N, Chuchom T, Ratanasuwan P, Houghton PJ. Selective Cytotoxicity and Antioxidant Effects of Compounds from *Dioscorea membranacea* Rhizomes. *Natural Product Communications*. 2007 Jun; 2(6): 1934578X0700200605.

VITA

NAME Vichununt Kerdput

DATE OF BIRTH 14 June 1991

PLACE OF BIRTH Bangkok, Thailand

INSTITUTIONS ATTENDED 2012 B.Sc. (Biology), Faculty of Science, Srinakharinwirot University
2019 Ph.D. (Biomedical Science), Faculty of Medicine, Srinakharinwirot University

HOME ADDRESS 2/1 soi Lat Phrao 48/1 Wangthonglang, Bangkok 10310, Thailand

